The Aging Heart: Mechanisms of Arrhythmogenesis and Sudden Cardiac Death

By

Kevin Ronald Murphy

BS, Providence College, 2012

AM, Brown University, 2014

Submitted in Partial Fulfillment of the Requirements for the Degree of Doctor of Philosophy in the Division of Biology and Medicine at Brown University

Providence, Rhode Island

May 2018

This dissertation by Kevin Ronald Murphy is accepted in its present form by the Division of Biology and Medicine as satisfying the dissertation requirement for the degree of Doctor of Philosophy.

Date _____ _____

Gideon Koren, MD, Advisor

Recommended to the Graduate Council

Date _____ _____

John Sedivy,PhD, Reader

Date _____ _____

David Rand, PhD, Reader

Date _____ _____

Marc Tatar, PhD, Reader

Date _____ _____

Shey-Shing Sheu, PhD, External Reader
Thomas Jefferson University

Approved by the Graduate Council

Date _____ _____

Andrew G. Campbell, PhD
Dean of the Graduate School

Kevin R. Murphy

1 Nicholas Drive
Franklin, MA 02038
774.571.8511 (Cell)

Brown University, Providence, RI
Email: kevin_murphy@brown.edu
LinkedIn: linkedin.com/in/kmurph37

Education

2012-2017 (Expected)
Brown University, Providence, Rhode Island
Department of Molecular Biology, Cell Biology, and Biochemistry
Track: Molecular Biology of Aging
Doctor of Philosophy
Cardiovascular Research Center (CVRC)
Thesis Advisor: Dr. Gideon Koren, MD

2014
Brown University, Providence, Rhode Island
Master of Art, Molecular Biology, Cell Biology, and Biochemistry

2008-2012
Providence College, Providence, Rhode Island
Bachelor of Science, Biology

Research Experience & Training

2012-2017 Graduate Student, PhD Candidate
Project: "The Aging Heart: Mechanisms of Arrhythmogenesis and Sudden Cardiac Death"
Principle Investigator: Gideon Koren, MD
Director, Cardiovascular Research Center (CVRC)
Professor of Medicine
Brown University and Rhode Island Hospital

2008-2012 Undergraduate Research Student and Lab Manager
Project: "BAX Inhibitor Links the ER and Programmed Cell Death in Yeast"
Principle Investigator: Nicanor Austriaco, OP, PhD
Associate Professor of Biology
Providence College

2011 Undergraduate Research Fellow
Principle Investigator: Leonard P. Guarente, PhD
Professor of Biology, Director of Glenn Aging Research Center
Massachusetts Institute of Technology

2010 Undergraduate Research Fellow
Principle Investigator: Klaas Van Wijk, PhD
Professor of Plant Biology
Cornell University and Boyce Thompson Institute

Leadership Roles

1. **Co-Founder/Owner, 509 Photography MA**
   Founded in 2013. Responsible for building an online presence, marketing, and customer service

2. **Front End Supervisor, CVS Pharmacy**
   Held role for three years. Managed a team of 6-10 employees per shift. Responsible for fulfillment of day-to-day store operations.

Technical Skills Acquired

The Koren Laboratory [March 2013-Present]: Molecular Biology, Brown University
Cardiac biology, cellular and molecular biology, and translational physiology, Brown University
System(s): Young and Aged Rabbits, Primary Cell Culture, Transgenic Mice, HEK and HL-1 Cell Lines
Techniques: Rabbit cardiac myocyte and fibroblast isolation (Langendorff), large mammalian husbandry, *in vivo* cardiac telemetry, primary cell culture, establishing stable cells lines (HEK and HL-1), confocal calcium imaging, live cell fluorescence microscopy, transmission electron microscopy, adenovirus gene transfer, RT-qPCR, western blots, immunohistochemistry/fluorescence

The Austriaco Laboratory [2008-2012]: Cellular and Molecular Biology, Providence College
System(s): *Saccharomyces cerevisiae*
Techniques: Reading scientific papers, developing research plans, yeast & bacterial cell culture, cellular transformation, luciferase based cellular assays, caspase activity/viability assays, molecular cloning, PCR, nucleic acid electrophoresis, fluorescence & confocal microscopy

The Guarente Laboratory [Summer 2011]: Molecular Biology, M.I.T.
Systems(s): Young and Aged Mice, HEK cell lines
Techniques: Animal husbandry, molecular cloning, cellular transfection, mammalian cell culture

The Van Wijk Laboratory [Summer 2010]: Biochemistry, Cornell University
System(s): *Arabidopsis thaliana*
Techniques: Yeast two hybrid interaction assay, Arabidopsis growth and maintenance, western blots

Publications

1. Morrissey PJ*, **Murphy KR***, et al. A Novel Method of Standardized Myocardial Infarction in Aged Rabbits. American Journal of Physiology - Heart and Circulatory Physiology (2017) *co-first authors
2. Kim TY, Terentyeva R, Roder KH, Li W, Liu M, Greener I, Hamilton S, Polina I, **Murphy KR**, Clements RT, Dudley SC Jr, Koren G, Choi BR, Terentyev D. SK channel enhancers attenuate Ca2+-dependent arrhythmia in hypertrophic hearts by regulating mito-ROS-dependent oxidation and activity of RyR. Cardiovascular research. (2017)
3. **Murphy KR**, Cooper LL, Lu YC, O-Uchi J, Terentyev D, Koren G. Diminished Autophagy Contributes to Aberrant Ca2+ Homeostasis and Arrhythmogenesis in Aging Rabbit Hearts. (*Under Review, Aging Cell)*

Scientific Presentations

Murphy, K., Cooper, LL., Lu, Y., Terentyev, D., Koren, G., "The Role of Autophagy in Cardiomyocyte Arrhythmogenesis"
Experimental Biology 2017, Chicago, IL, April 22-26th, 2017. (Platform & Poster)
Annual Lifespan Corporation Research Symposium, Providence RI, October 31st, 2017. (Poster)
***Award for "Second Place Translational Science" ***
Annual Lifespan Corporation Research Symposium, Providence RI,
***Award for "Third Place Translational Science" ***

Murphy, K., Cooper, LL., Lu, Y., Terentyev, D., Koren, G., "The Role of Autophagy in Cardiomyocyte Arrhythmogenesis"
60th Annual Meeting of the Biophysical Society, Los Angeles, CA, March 1st, 2016. (Poster)

Murphy, K., Cooper, LL., Lu, Y., Terentyev, D., Koren, G., "Myocardial Infarction in the Aging Heart: The Role of Myofibroblast Senescence in Arrhythmogenesis"
Molecular Biology of Aging Retreat, Brown University, Providence, RI. September 17th, 2016. (Platform & Poster)

Murphy, K., Selinski, C., Swan, B., Sullivan, J., N. Austriaco, OP, "Investigating the Role of Calcium in BAX-induced Cell Death in the Yeast, Saccharomyces cerevisiae."
65th Eastern Colleges Science Conference, Sacred Heart, NY, April 2, 2011. (Poster)
Award for "Excellent Poster Presentation

Murphy, K., Selinski, C., Swan, B., Sullivan, J., N. Austriaco, OP, "Investigating the Role of Calcium in BAX-induced Cell Death in the Yeast, Saccharomyces cerevisiae."
5th BioNES Conference, Roger Williams University, Bristol, RI, December 4, 2010. (Poster)
***Award for "Significant Research Contribution" ***

Honors & Societies

2017-Present	Member of the American Physiological Society
2015-Present	Member of the Biophysical Society
2012	Providence College Biology's "Albertus Magnus Award" Award given to a senior biology student who best exemplifies excellence in moving forward in science.
2011	Providence College Dean's List (Spring and Fall Semesters) Attained a semester GPA of 3.92 or higher.
2009-2012	President, Providence College Chapter of Sigma Xi - Scientific Research Honor Society Currently organizing club events such as scientific journal discussions, and community service.
2011	Providence College Student Leader of the Month, November 2011 Nominated by faculty and students for "outstanding contributions to the college."
2009-2012	Member of Providence College Biology Society

Teaching Experience

2016-Present	Undergraduate Student Research Mentor Design and plan experiments for undergraduate honors thesis work, teaching reading and integration of scientific papers, teaching basic principles of data and statistical analysis.
2013	Teaching Assistant, Brown University Instructor of lab sections, designing, planning, preparing, and teaching methods and logic of experiments. BIOL 0470: Genetics
2009-2011	Teaching Assistant, Providence College Department of Biology Aid in laboratory planning and preparation, modifying and coordinating experiments, and helping students for the weekly teaching laboratory. BIO307: Genetics Laboratory BIO410: Microbial Physiology Laboratory BIO103: General Biology Laboratory

Student Mentorship

5/2016-9/2017 Yueming Cao (Brown Undergraduate, Class of 2018)

Last Updated: December 2017

Dedication

This dissertation is dedicated to Father Nicanor Austriaco, OP, PhD. I met you many years ago after just starting my freshman year at Providence College. I had a question in general biology lab about a microbial petri dish and was sent to your office to better understand why I found an unexpected phenotype. After an extensive conversation, you offered me a position in your laboratory. You were the first to teach me how to think as a scientist. We designed my first experiments together. It was in your lab that I, in your words, “caught the research bug.” Your guidance (and persistence) kept me on track to get summer fellowships each year and join the Providence Area Aging Research meetings. Through the years, the interest in the biology of human aging and disease that you instilled in me came to the forefront of my scientific focus.

Thank you for seeing the potential in me as a young scientist. We’ve had many great memories working late hours in the lab and attending conferences, even as far away as Italy. I look back on my experience in the Austriaco Lab and realize just how valuable the time in your lab was for my formation as a young scientist and a young adult. I poured the passion and responsibility I found in my four years with you into the work presented here.

One evening, you and I were standing in my research bay in Hickey Hall Laboratory 181 after you said evening mass. You gave me some perspective I will never forget: no matter what I do in life, science or otherwise, do it the very best I can… In the end, I will stand and be judged on what I’ve accomplished, the amount of honesty

I do it with, and how passionately I was able to commit myself to truth. In the toughest of days, I've kept that advice close to my heart and my work.

I'm extremely proud be a part the Austriaco Lab's pedigree. I'll always fondly remember our time in lab together. I am forever grateful for your mentorship, guidance, and friendship. I look forward to sharing with you developments in my scientific career, as well as the personal milestones surely ahead.

Thank you for everything, Father Nic.

Acknowledgements

Thank you to my advisor, Dr. Gideon Koren, for accepting me into the Cardiovascular Research Center (CVRC) at Brown University during my first year in graduate school. His great patience in enhancing my scientific training and professionalism has certainly benefited me as a scientist. His mentorship has shaped my performance, from my daily lab routine to my interactions with the scientific community. I am very proud to come from the CVRC, and will never forget where and how I was trained.

I have been fortunate to have additional mentors and friends at the CVRC. I would like to thank Dr. Dmitry Terentyev for working long hours to teach me the rigors of physiology and cardiac calcium handling. Upon reflection, I appreciate the lessons I've learned about asking the appropriate scientific questions, formulating my scientific stories, and, most importantly, staying focused on the goals I needed to achieve. I would like to thank my friends I have shared a research bay with: Mr. Jacob Moller and Dr. Shanna Hamilton. Despite the difficulty and frustration of research, we always managed to laugh and push forward. Next, Ms. Rada Terentyieva, Ms. Michelle King, Mr. Patrick Morrissey, Dr. Jin O-Uchi, Dr. Bongsook Jhun, Dr. Celinda Kofron, Dr. Nelly Valkov, Ms. Kara Ford, Mr. Amen Okundaye, and Mr. Brett Baggett have always lent a helping hand (or spare reagent). Moreover, I appreciate your friendship and conversations about science and life. I look forward to visiting soon to enjoy a cup of coffee with you all.

The Koren Lab staff has supported me for over the years throughout my PhD. Ms. Yichun Lu was particularly supportive in not only her constant encouragement, but for her endless efforts in preparing cells for the work presented in this dissertation. Dr. Karni

Moshal and Dr. Karim Roder offered their expertise whenever I needed a helping hand. The surgical team, including Ms. Lorraine Schofield, Dr. Jean Daley, Mr. Patrick Morrissey, and Dr. Nilufer Turan, taught me about cardiac biology on the organ level. I appreciate the long days required to generate surgical models.

I would also like to thank my undergraduate mentee, Ms. Yueming Cao. I appreciate your hard work and wish you the most success in your future after Brown. A large portion of our project happened thanks to her tireless efforts. Thank you! And thank you to the rest of the CVRC including Dr. Ulrike Mende, Dr. Bum Rak Choi, Dr. Tae Yun Kim, Dr. Karup Arunachalam, Ms. Dongqin Yang, Dr. Sam Dudley, Ms. Mary Ann Machado, and all others.

During my time at Brown University I have been supported by a wonderful committee including Dr. John Sedivy, Dr. David Rand, and Dr. Mark Tatar. The MCB department has facilitated many aspects of my time at Brown, largely in part due to a wonderful administrative staff including Ms. Elaine Butler and Ms. Ashley Walker. I appreciate all the time spent ensuring my career at Brown stayed on track and was productive.

When I joined graduate school, I started first semester becoming friends with Dr. Bethany Biron-Girard, Ms. Courtney Anderson, and Ms. Lauren Watts. We attended class together, enjoyed many evenings out in Providence, and met for luncheons at the hospital when we could get away from the bench. Families have started, relationships progressed, and our careers to move forward through our years of friendship. I look forward to staying in touch as we all move onto the next steps in life.

I would like to thank my collaborators at the Lifespan Biostatistics Core, Dr. Jason Machan and Dr. Alison Chambers. Their assistance in analyzing complex data was invaluable. I would like to thank Dr. Derek Merck for his innovative thoughts in analyzing mitochondria in electron micrographs. Lastly, I would like to thank Ms. Paula Weston and Mr. Paul Monfils for their extensive knowledge in histological methodologies. Their input was critical for completing the work presented here, and their attention to detail and methodical approach to solving problems will have a long-lasting impression on me.

Before coming to Brown, I would like to thank the wonderful mentors I met at Providence College: Fr. Nicanor Austriaco, Dr. Brett Pellock, and Dr. Yinsheng Wan. I will always remember my time in Hickey Hall, and look forward to coming back to visit often. Your guidance in science and personally have made a great impact on my life. Thank you very much for your time and friendship.

I would like to thank Ms. Jessica Galvez for her support and encouragement during the time spent earning PhD. I have been extremely lucky to have a clinician-in-training at my side at this point in my career, asking questions about what my work will mean to the field of cardiology and future patients. Thank you for always challenging me to look beyond the bench and see the bigger picture.

Lastly, I have a wonderful family that has been a large source of support through my education. I would like to thank my sister, Ms. Laura Murphy. It was a wonderful gift to work with you in lab for a summer in the surgery lab. Thank you to my parents, Linda and Leo. You have always believed in me and pushed me to the best I can be. It has been a very long road and you both have sacrificed so much for me. Thank you, for all

you have done, are doing, and will continue to do for me. I had wonderful grandparents who always believed in me. Thank you, Grandma and Poppy. Thank you, Nana. You gave me more than I deserved. I am incredibly proud of this work and thank you for teaching me to value my education.

This dissertation is based upon work supported by NIH grants R01-HL110791 (to G. Koren), R21-AG049608 (to J. Sedivy and G. Koren), R01-HL121796 (to D. Terentyev), and by T32AG041688 (to J. Sedivy).

Thank you, all!

Table of Contents

List of Figures and Tables

Chapter 1: Introduction and Specific Aims

Abbreviations and Keywords:

LV	Left Ventricle
MI	Myocardial Infarction
LAD	Left anterior descending (artery)
SCD	Sudden Cardiac Death
CVD	Cardiovascular Disease
RyR	Ryanodine Receptor
SR	Sarcoplasmic Reticulum
mito-ROS	Mitochondria Derived Reactive Oxygen Species
VT	Ventricular Tachycardia
VF	Ventricular Fibrillation
SCW	Spontaneous Calcium Wave
mTOR	Mammalian Target of Rapamycin
RZ	Remote Zone
IBZ	Infarct Border Zone
SASP	Senescence Associated Secretory Phenotype
MMP	Matrix Metalloproteinase
TIMP	Tissue Inhibitor of Metalloproteinases

1.1 Biology of Cardiac Aging

1.1A Epidemiology of Cardiac Aging

Changes in cardiovascular structure and function are impacted by age and have long been recognized to lead to increased morbidity and mortality as humans age. Indeed, age is the single most important predicting factor to a person's cardiac health, and the prevalence of cardiovascular disease (CVD) is >70% above the age of 65 [1]. With a growing aging population, by the year 2030 the burden of healthcare cost responsible for treating cardiovascular disease will triple to $818 billion [1]. The major changes that occur in the aged human heart can be grouped to functional, structural, and molecular. These changes affect the heart at the cellular, tissue and organ scales.

1.1B Functional Changes During Cardiovascular Aging:

The heart is responsible for the circulation of blood throughout the body. There are two phases that defines its function: systole and diastole. Systole is the pumping phase where about 60% of the total blood in the heart is pumped out [2]. Diastole is the phase following systole where the heart fills with blood. In a resting state, the heart's systolic function does not change with age [3], while the resting diastolic dysfunction increases progressively during aging [4]. The rate at which the left ventricle (LV) fills during diastole changes with age, switching from early diastole (rapid filling wave) to late diastole (atrial contraction). This delayed filling is largely due to structural changes in the myocardium leading to decreased compliance [5]. Another contributing factor is the impaired relaxation of the myocardium in the aging heart [6]. Investigation using echocardiography revealed

decreased E/A ratio, a measurement quantifying peak flow velocity of blood in early diastole over peak velocity of blood flow in late diastole [3]. As the heart becomes stiffer and diastolic dysfunction increases the functional reserve of the heart under stimulation decreases [7, 8]. Although there are no changes at rest, during sympathetic stimulation systolic function is blunted due to decreased reserve and myocardial stiffness.

The maximal heart rate is notably decreased during aging further decreasing cardiac output under stress [9, 10]. Controlling this process are the sinoatrial node, and the conduction system including the atrioventricular node, the His bundle and the Purkinje network which are all remodeled during aging. The sinoatrial node is the biologic pacemaker of the heart [11]. The atrioventricular node [12] is important in propagating electrical impulse between the atrium and the ventricle where the His bundle and the Purkinje network are critical for timely spread of signaling across the ventricular myocardium [13]. Aging hearts have reduced numbers of pacemaker myocytes in the sinoatrial node [9, 14]. In addition, the atrioventricular node, the His bundle and the Purkinje fibers are also remodeled significantly displaying a significant increase in fibrosis as well as decreased network complexity [15]. Commonly, the remodeling of the conduction system slows the propagation of electrical impulse leading to bradycardia, or conduction block [16]. These changes together with electrical remodeling of aged cardiomyocytes can lead to the formation of ectopic beats [17] (early after depolarizations or delayed after depolarizations) that could be propagated to the entire heart and lead to malignant arrhythmias and sudden cardiac death (SCD).

1.1C Structural Changes During Cardiovascular Aging

The human heart undergoes structural changes during aging. Fibrosis is implicated in myocardial stiffness and diastolic dysfunction [18]. Possible mechanisms for increased fibrosis during aging include cardiomyocyte death, as the heart replaces lost myocytes with fibroblasts. The infiltration of fibroblasts to the aged myocardium results in increased interstitial fibrosis [19]. This phenomenon is associated with an increase in the cell size of surviving cardiomyocytes [20].

The extracellular matrix is critical for support of myocardial function as it serves as a scaffolding mechanism to maintain proper 3D geometry of the heart. The extracellular matrix is regulated by both the synthesis and degradation of its different components. For example, collagen content increases [21] with age, as determined from autopsies from healthy young and aged humans. Furthermore, the shifts in collagen types and cross-linked states have been shown to contribute to LV stiffness and cardiac dysfunction [19, 22]. The extracellular matrix is remodeled by multiple matrix metalloproteinases (MMPs) that degrades the matrix. This class of enzymes is controlled by tissue inhibitors of metalloproteinases (TIMPs) [23]. Increased circulating MMPs and TIMPs have been correlated with diastolic dysfunction in humans [24]. In summary, changes in fibroblast numbers, collagen production, with dysregulated MMPs and TIMPs result in less compliant myocardium and lead to stiffer myocardium, and diastolic dysfunction as discussed in **Section 1.1B**.

In addition, aging is also associated with an increase in peri-vascular fibrosis. This fibrosis can contribute to increased vascular stiffness of the conduit vessels reflected in increased pulse wave velocity [25, 26]. The stiffening of these arteries results in larger

amplitude and faster pulse wave and in an increase in the amplitude of the reflected wave which in turn increases the hemodynamic load on the heart [4, 27]. Moreover, the increased amplitude of the pulse pressure damages organs such as brain and kidneys [28, 29].

We showed that the aging rabbit heart simulates the functional and structural changes that occur in the aging human heart including increased fibrosis and collagen content, abnormal diastolic function, impaired electrical conduction, stiffer myocardium, stiffer aorta, and reduced threshold for induction of malignant arrhythmias [30]. Thus, the aged rabbit heart is an appropriate model to study cardiac aging and dysfunction (**Chapter 4**).

1.1D Molecular Changes in Aged Cardiac Myocytes

Cardiac aging is associated with marked changes at the single cell scale which underlie the phenotypes mentioned in the ***Sections above.*** Notably, cells display reduced myocyte shortening with prolonged relaxation after contraction [31]. Aging is also associated with electrical remodeling including prolongation of the APD, modified expression of ion channels and transporters, altered calcium homeostasis [32, 33], as well as differential expression of proteins that control conduction such as Cx43 [34]. Mechanisms controlling the functional and electrical dysfunction during aging are still poorly understood.

1.1E Aging and Cardiac Mitochondria

The mitochondria are subcellular organelles that contain the electron transport chain and carry out oxidative phosphorylation making them a critical source of energy for the cardiac myocyte. Mitochondria exist in a vast network regulated by fission and fusion [35]. To that end, the regulation of mitochondria biogenesis and degradation via mitophagy is critical to the function of the normal heart. Healthy, fully functional parts are reintegrated into the mitochondria network while damaged parts are recycled [36]. Age-related down-regulation of mitophagy may result in accumulation of damaged or impaired mitochondria in the aging heart [37]. Hence, mitophagy serves a protective role in eliminating defective mitochondria [38, 39].

The accumulation of defective mitochondria is associated with increased production of reactive oxygen species (mito-ROS) that participate in promiscuous chemistry. mito-ROS can present a redox burden through massive generation of free radicals from the electron transport chain (mainly produced in complex I and III) [40] and from the tricarboxylic acid cycle (mainly produced from α-ketoglutarate dehydrogenase) [41]. The cell has mitochondria-targeted endogenous ROS-scavenging enzymes such as superoxide dismutase (MnSOD), catalase [42], and peroxidases [43]. Even with the endogenous system to scavenge the harmful mito-ROS, proteins and other biologic material can be post translationally modified and directly oxidized [44]. As ROS are short-lived molecules and highly reactive [45], this property has put forth the notion that ROS will most likely act in local compartments [46, 47]. Therefore, designed therapies should act locally to avoid disrupting signaling processes elsewhere in other cellular compartments [48].

In post mitotic cells like aged cardiac myocytes, the biogenesis of mitochondria and the turnover of dysfunctional mitochondria is critical for proper maintenance of cardiomyocyte excitation, contractile function, and calcium homeostasis. The failure to remove damaged mitochondria through autophagy or the mitochondrial specific form, mitophagy, can result in the accumulation of dysfunctional organelles [37, 49]. Dysfunction manifests through increased redox burden, depolarized mitochondria membrane potential, and decreased ATP production [50]. Indeed, aged cardiac myocytes produce more mitochondrial reactive oxygen species (mito-ROS) [51, 52].

Dr. Koren's laboratory previously published that mito-ROS participates in the direct oxidation of the sarcoplasmic reticulum (SR) calcium release channel, ryanodine receptor. Oxidation of ryanodine receptor results in the leak of calcium from the SR which in turn leads to the generation of pro-arrhythmic spontaneous calcium waves [53]. The mechanisms underlying increased mito-ROS and the connection to arrhythmogenesis remain elusive. In this work, we targeted cellular processes that maintain and modify mitochondria to reduce the oxidative stress and aberrant calcium release.

1.2 Cardiac Autophagy Decreases with Age

1.2A Autophagy Dysregulation During Aging

Autophagy is a cellular process that degrades unnecessary or dysfunctional cellular components using lysosomes [54]. This basic process is conserved from yeast to worms to humans. There are three main forms of autophagy: macroautophagy, microautophagy, and chaperone-mediated autophagy. The work presented in this thesis

focuses on macroautophagy which is a basic, self-degradative, catabolic process capable of processing macromolecules, organelles, and invading pathogens [55]. Here, the cell forms a *de novo*, double membrane around substrates, such as organelles, forming an autophagosome [54]. A particular form of macroautophagy, mitophagy, recycles damaged mitochondria [56]. In the energy-demanding heart, maintaining a fully functioning population of mitochondria is imperative.

Autophagy is accepted to decrease during aging [57] in a variety of tissues including the heart. Indeed, decline in autophagy is linked to several pathological states including underlying atrial arrhythmias [58, 59]. Autophagy also plays a protective role in response to nutrient starvation, and genetically overexpressing autophagy factors in HL-1 cardiac myocytes subjected to ischemia/reperfusion treatment were protective [60]. [61, 62]

Despite a lack of in-depth understanding of the response of autophagy to injury and stress cues, autophagy is critical for the maintenance of cardiac tissue throughout the entire life cycle. Autophagy is regulated by several different factors transcriptionally and post-transcriptionally. For instance, reactive oxygen species are signaling molecules in the cell that directly regulate ATG4 [63]. Calcium through CaMKII has the ability to induce autophagy [64]. In addition to these molecules the endogenous mammalian target of rapamycin (mTOR) system is a potent regulator and inhibitor of autophagy. In this thesis, we will target and inhibit mTOR as a therapeutic approach to enhance autophagy to control mito-ROS production and reduce age-related, pro-arrhythmic spontaneous calcium release.

1.2C Cardiac Myocyte Calcium Cycling During Aging

Aging is associated with a 5-40-fold increase in the incidence of sudden cardiac death between early adulthood and age 65 [65]. While increased fibrosis provides the proper substrate for maintaining arrhythmia, abnormal calcium homeostasis can provide the potential trigger to initiate the arrhythmias. Aging alters calcium homeostasis through a variety of mechanisms; the type 2 ryanodine receptor (RyR) calcium channel on the sarcoplasmic reticulum (SR) is a major regulator of calcium homeostasis. During action potential calcium flows through the RyR from the SR and raises calcium concentration in the cytosol initiating CM contraction [66]. Indeed, abnormally high RyR activity underlying enhanced calcium leak from the SR can result in calcium-induced arrhythmias. This phenomenon is present in a variety of diseases such as heart failure and myocardial infarction [67]. The generation of aberrant spontaneous calcium waves (SCWs) results in membrane potential depolarization, linking spontaneous calcium waves to arrhythmogenesis [68].

RyR opening and calcium leak is affected by redox modifications [53]. In fact, in cardiac myocytes from aged hearts the RyR is oxidized by mitochondrial reactive oxygen species (mito-ROS). The RyR contains sulfhydryl groups of cysteine residues that are prone to oxidation [69]. Indeed, this channel/ROS interaction is among the most well-studied to date in redox mediation of calcium channels and transporters. Channel oxidation results in calcium leak from the SR, increasing cytosolic calcium leading to the formation of pro-arrhythmic spontaneous calcium waves [53]. In **Chapter 3** we uncover a basic mechanism underlying mito-ROS generation that participate in the oxidation of RyRs.

1.3 Aging and Cellular Senescence

1.3A Molecular Control of Cellular Senescence

Cellular senescence is a process that changes the phenotype of cells that usually can divide by inducing irreversible arrest of cell growth and proliferation. It is primarily caused by genomic stress such as DNA damage (mediated by the P53/P21 pathway) [70, 71], oncogenesis, or ROS (mediated in part by the p16 pathway) [72]. In addition to growth arrest, senescent cells display a multi-component senescent-associated secretory phenotype (SASP) that includes the secretion of growth factors, chemokines, cytokines, and matrix remodeling proteins [73]. Of note, senescent cells are resistant to apoptosis [73-76]. The SASP allows a senescent cell to recruit inflammatory cells that remove them and allow tissue recovery.

1.3B The Beneficial Effects of Clearing Senescent Cells

Senescence has a beneficial effect during wound healing. Fibroblast senescence in cutaneous injury response limits the extent of fibrosis during tissue repair [77]. The same outcome was observed in acute liver injury senescence where senescent satellite cells reduced fibrosis through immune response in acute tissue damage [78]. Yet, persistent presence of senescent cells may eventually lead to tissue dysfunction through a chronic inflammatory and remodeling response [73, 79, 80]. For instance, after dermal abrasion the chronic persistence of senescent cells leads to dermal thinning [81].

Senescent cells accumulate in different organs such as skin [82], liver during aging [78, 83]. Several studies tested the theory that chronic or persistent accumulation of senescent cells in a tissue will lead to dysfunction and therefore have investigated the beneficial effects of removing or clearing these senescent cells [84]. Baker *et al.* showed that using the INK-ATTAK mouse model to selectively clear senescent, p16-positive cells *in vivo* both increased lifespan and tissue level health after intervention in a progeroid mouse background [85, 86]. The pharmacologic clearance of senescent cells from mice with non-alcoholic fatty liver disease resulted in a drastic reduction in steatosis and improvement in health [87]. These results underline the therapeutic potential of targeting senescence cells. Because senescent cells have the potential to modify the surrounding tissue via SASP, clearance of senescent cells may have beneficial effects in reducing deleterious effects in various other diseases as well.

1.3C The Senescence-Associated Secretory Phenotype

Senescent cells also exhibit a pro-inflammatory phenotype termed the senescence-associated secretory phenotype (SASP) [80]. The features of the SASP include growth factors, cytokines, chemokines, matrix remodeling enzymes, and more [74, 75]. The SASP can modify the surrounding tissue microenvironment through paracrine effects. Despite the deleterious effects senescent cells have on the surrounding tissue during wound healing, no studies to date have carefully quantified the senescence response in the aged heart post-myocardial infarction (MI).

1.3D Detecting Senescent Cells

The detection of senescent cells requires the identification of several factors or characteristics: such as senescence-associated β-galactosidase (SA-βGal)-positive cells, expression of senescence-controlling genes, and even the presence of SASP. Several biomarkers of senescence have been identified, including the widely accepted SA-β-gal assay [88, 89], telomere dysfunction-induced foci (TIF) assay [90], and increased p16 or p21 expression [91]. Recently Biran *et al*. developed a quantitative approach to assessing cellular senescence using flow cytometry that allows for dual SA-βGal and immunofluorescence staining on a single-cell level. Using current staining protocols, these investigators developed a high-throughput single cell approach for a variety of tissues. They validated their approach using cells dissociated from multiple tissue types from young and aged mice [92]. Other groups have developed novel applications of Sudan Black B dye in identifying protein aggregates characteristic of aged tissues. Georgakopoulou *et al* reported that lipofuscin staining was an excellent marker of senescent cells pH that is specific and pH independent [93]. In the past year another universal biomarker has been commercially developed to easily and quickly detect senescent cells in tissue based on a modified Sudan Black B chemical structure known as SenTraGor [94]. This is an antibody-enhanced method to detect senescent cells with high specificity and sensitivity. SenTraGor targets lipofuscin-containing senescent cells [93]. These methodologies can detect senescent cells *in vitro* or *ex vivo*.

1.3E Previous Reports of Cellular Senescence in the Heart

Our group has conducted experiments to detect senescent cells in young and aged cardiac tissue. In steady state, healthy myocardium we did not detect senescent cardiomyocytes in aged hearts (data not shown). Zhu *et al.* reported in 2013 that cellular senescence occurs post-MI in the border and scar zones [95]. However, they performed these experiments in young mice. Next, in 2016 a series of genetic experiments in a TAC model of hypertrophy showed induction of perivascular senescence of cardiac myofibroblasts [96]. These cells stained positive to α-smooth muscle actin (αSMA) positive, several markers of DNA damage response as well as markers of senescence. This combination of positive makers indicates that myofibroblasts are senescing near the zone of injury in these models. Again, experiments were performed in young animals. Thus, the field lacks an in-depth analysis of senescence of myofibroblasts in aged cardiac tissue in response to pathophysiological injury [76]. In **Chapter 4** we characterized the senescence response in infarcted young and aged rabbits to uncover novel mechanisms underlying the senescence response after injury in the aging heart.

1.4 The Rabbit as a Model System for Cardiac Aging

The rabbit action potential closely resembles the human action potential [97, 98]. In contrast, rodents exhibit a shortened action potential with different morphology compared to humans [99, 100]. In addition to action potential morphology, rabbit cardiac myocytes derive about 70% of cytosolic calcium from the sarcoplasmic reticulum, like humans. In both cases the sodium calcium exchanger is responsible for calcium efflux [101] whereas in rodents, most calcium comes from the sarcoplasmic reticulum [102].

New Zealand White rabbits are the model our laboratory uses. Previously published literature showed that the lifespan of a New Zealand White rabbit to be about 5-7 years, with a 50% mortality rate above the age of 4 years [103]. Therefore, we utilized two groups of animals for the work presented in this dissertation: young rabbits (6-10 months old) and aged rabbits (4-6 years old). These groups allow for experimentation in age appropriate models. These aged rabbits are equivalent to 50-70 year old humans [103].

The rabbit provides a useful model for ischemic disease like MI because of similarities to the human heart in terms of structure and function. Further, the rabbit heart exhibits a different response to ischemia (when compared with rodents) that more closely recapitulates the human heart [104]. The coronary anatomy of the rabbit heart (like the human) is complex and variable [105, 106]. To that end, Podesser *et al.* showed that the rabbit coronary anatomy exists in multiple configurations such as bifurcation and trifurcation. The authors acknowledge that due to the drastic differences in perfusion of blood to specific areas that “defined ischemic area is difficult to reproduce under these anatomical conditions” [107, 108]. Indeed, inducing MI in the rabbit heart by blind ligation

of the circumflex artery yielded inconsistent and unreproducible results [109, 110]. Thus, there is a great need to standardize the experimental infarct in the rabbit heart and to further characterize the coronary anatomy in aged rabbits. In **Chapter 2** we established a methodology to overcome these issues and create a standardized MI in young and aged rabbits.

1.4A Characterization of the Aged Rabbit Heart

In 2012 Cooper *et al.* established an age appropriate model of cardiac aging using rabbit [30]. *In vivo* imaging and hemodynamic studies showed that the aged rabbit heart revealed several functional differences compared to young hearts. First, upon investigation of left ventricular function, aged hearts displayed increased end systolic and diastolic pressure volume relations indicating a stiffer myocardium. Resting echocardiography studies revealed increased thickness of the septum, with no changes in ejection fraction, fractional shortening, or left ventricular diameters in systole and diastole. These studies also showed increased pulse wave in aged rabbits as compared to young rabbits indicating stiffening of the aorta, a phenomenon also observed in human aging [25, 27, 111].

Aging rabbit hearts harbor defects in several aspects of electrical conduction. The aged hearts display a slower heart beat at baseline and during β-adrenergic stimulation. The majority of rabbits exhibited changes in QRS duration and right bundle branch block. Indeed, magnetic resonance imaging (MRI) of fixed rabbit hearts revealed changes in Purkinje fiber orientation during aging [30]. Indeed, the geometry of the fiber network lost

complexity with age as well as fiber thickness. Together, these results indicate a deterioration of the Purkinje fiber network that underlies the previously described conduction abnormalities. Using high resolution optical mapping, no difference in action potential duration between young and aged rabbits was observed. However, aged hearts did display increased anisotropic conduction, with decreased transverse conduction velocity. Ventricular fibrillation (VF) could be experimentally induced in most aged hearts by ramp pacing whereas only a small number of young hearts were inducible.

Accompanying histological analysis of ventricular tissue from aged hearts uncovered an important structural change during aging. Their analysis revealed increased interstitial fibrosis in aged hearts using picrosirius red staining [30, 112]. Aged rabbit hearts contained increased interstitial fibrosis measured by total fibrosis excluding peri-epicardial, valve, and vascular staining. Increased fibrosis is likely one contributing factor for the incidence of VF during aging. Indeed, fibrosis is an important, pro-arrhythmic substrate for sustaining arrhythmia [113, 114].

The Koren laboratory has utilized myocytes from young and aged rabbits (defined in **Section 1.4**) to uncover key alterations and underlying mechanisms of age-related shortened refractoriness of calcium release from the calcium handling RyRs. Aged rabbit myocytes exhibit a slight reduction in SR calcium content, along with decreased calcium spark (RyR-mediated spontaneous localized calcium release events) amplitude but no change in spark frequency [53]. These data suggest that RyRs are leaky in the aged rabbit myocyte. Hyperactive RyRs are recognized to underlie calcium mediated arrhythmogenesis [115, 116]. The refractoriness of RyR-mediated spontaneous calcium

release was also decreased in aged rabbit cardiac myocytes, measured by the latency from last field pace to wave formation.

Post-translational modification of RyRs, such as phosphorylation or oxidation, are known to underlie increased RyR activity [69, 117]. In aged rabbit cardiac myocytes, no changes in the phosphorylation status of calcium handling proteins were detected. Direct measurement of RyR oxidation using the monobromobimane assay [118] revealed a significant increase in RYR oxidation with age. Further studies into the source of ROS showed that cardiac myocytes produce excess mito-ROS capable of oxidizing RyR during aging. The application of the specific mito-ROS scavenger, MitoTEMPO [119], reduced the instance of spontaneous calcium waves (SCWs) and increased the refractoriness restoring calcium cycling parameters to young controls. These results implicate a role of mitochondria dysfunction, mito-ROS production, and oxidized RYR in underlying aberrant calcium release and pro-arrhythmic cellular behavior during aging [53]. However, the exact mechanisms responsible for decreased mitochondrial function and/or increased mito-ROS production that participate in aberrant RyR-mediated calcium handling are not well understood.

1.5 Hypotheses and Specific Aims

1.5A Rationale and Overall Hypothesis

The incidence of sudden cardiac death increases 5-40–fold in humans over 65 years compared to younger individuals [120, 121]. The mechanisms controlling the pro-arrhythmic changes that occur to the aging heart on the organ and cellular levels remain elusive. Thus, it is critical to discover novel pathways that will lead to create triggers that

initiate arrhythmias as well as the substrate that will maintain them and will thereby lead to persistent ventricular arrhythmias and sudden cardiac death (SCD). To that end, it is essential to use a large animal model that will enable us to investigate the mechanisms of SCD to better understand and eventually prevent SCD in humans. Given that ischemic disease is associated with SCD in over 65% of the cases [120, 121], we thought to develop a reproducible model of minimally invasive MI in aged rabbits. Given the role of mito-ROS in aging and injury [122-125] we decided to investigate the mechanisms that lead to increase mito-ROS production, such as decreased autophagy and altered mitochondrial maintenance in the heart as these can lead to arrhythmogenesis directly through changing calcium homeostasis. In addition, cellular senescence of myofibroblasts may modify wound repair and contribute to a chronic and pro-inflammatory phenotype during aging enhancing the propensity for arrhythmogenesis [126].

1.5B Specific Aim 1

Rationale: This aim directly addresses a current problem in modeling cardiac injury in aged hearts. Previous methods of myocardial infarction in rabbits relied on coronary artery ligation. The ligation surgical method provided poor visualization of the coronary anatomy and did not allow the surgeon to precisely ligate arteries that would lead to a consistent size and location of scar between animals. Coronary anatomy is variable and unique for each heart. This aim intends to create and validate an atlas from analyzing coronary angiography of a cohort of over 100 rabbits to increase reproducibility between surgeries.

This chapter summarizes our published work in February of 2017 as an original innovative methodology in American Journal of Physiology Heart and Circulation [127].

This Aim will test the hypothesis that variation in coronary anatomy of individual animals leads to the reduction in reproducibility of infarction procedures. Therefore, site-specific targeting of the pro-thrombotic coil should reduce variation between surgeries regardless of anatomy configuration of the aged (or young) hearts.

Specific Aim 1: To create a coronary anatomy atlas of the structures present in young and aged rabbits. (A) Collect and analyze coronary angiography to determine the configurations of the anatomy. (B) Create a rubric for coil implantation to generate standardized location and size for infarction regardless of anatomy or any other factor. (C) Validate the surgical rubric using historical and functional experimental methods.

1.5C Specific Aim 2

Rationale: It is generally accepted that autophagy is decreased in aging tissues. Autophagy is a cellular process critical for recycling dysfunctional cellular components including organelles like mitochondria. Here we investigate age-related decreased autophagy and the increased production of mito-ROS that oxidize the calcium-handling RyR leading to pro-arrhythmic spontaneous calcium release. These malignant changes may underlie the formation of fatal arrhythmia that can propagate across the aging, fibrotic heart leading to sudden cardiac death.

*In collaboration with the Terentyev Lab, this chapter summarizes data **in submission** as an original research article to the journal Aging Cell.*

In this chapter, we test the hypotheses that aging at the cellular level leads to diminished autophagy flux which leads to increased mito-ROS that promote pro-arrhythmic spontaneous calcium release, and that promoting autophagy will restore mitochondrial function in primary aged myocytes and reduce the instance of pro-arrhythmic spontaneous calcium release.

Specific Aim 2: To characterize structural changes in the mitochondria of aging cardiac myocytes and their regulatory factors, and to quantify changes in autophagy during aging in the cardiac myocyte. To inhibit or enhance autophagy in healthy and aged cardiac myocytes and measure the effect on ROS, mitochondria, and spontaneous pro-arrhythmic calcium release.

1.5D Specific Aim 3

Rationale: The accumulation of senescent cells is a feature of aging tissues and has been shown to have negative effects on many tissues such as liver, spleen, brain etc. Senescent myofibroblasts play an important role in wound healing. However, they may modify the risk for arrhythmogenesis in two ways: (1) modify the scar to provide substrate for re-entrant arrhythmia primarily through matrix remodeling or (2) by exhibiting an altered SASP that would trigger abnorm7al myocyte excitability.

In collaboration with the Choi Lab, this chapter summarizes unpublished data and tests the hypothesis that delayed and persistent senescence response in aged infarcted hearts leads to electrical remodeling that reduce the threshold for arrhythmogenesis.

Here, we will test the hypothesis that post-MI senescence of cardiac myofibroblasts is modified by aging and leads to an arrhythmogenic phenotype post-MI.

Specific Aim 3: To quantify the kinetics of cellular senescence of cardiac myofibroblasts and fibrosis in young and aged rabbit hearts post MI histologically and biochemically. To characterize the senescence-associated secretory phenotype (SASP) in samples isolated from infarcted young and aged rabbit hearts.

1.6 References

1. Yazdanyar A, Newman AB: **The burden of cardiovascular disease in the elderly: morbidity, mortality, and costs**. *Clin Geriatr Med* 2009, **25**(4):563-577, vii.
2. Cain PA, Ahl R, Hedstrom E, Ugander M, Allansdotter-Johnsson A, Friberg P, Arheden H: **Age and gender specific normal values of left ventricular mass, volume and function for gradient echo magnetic resonance imaging: a cross sectional study**. *BMC Med Imaging* 2009, **9**:2.
3. Strait JB, Lakatta EG: **Aging-associated cardiovascular changes and their relationship to heart failure**. *Heart Fail Clin* 2012, **8**(1):143-164.
4. Lakatta EG: **Age-associated cardiovascular changes in health: impact on cardiovascular disease in older persons**. *Heart Fail Rev* 2002, **7**(1):29-49.
5. Villari B, Campbell SE, Hess OM, Mall G, Vassalli G, Weber KT, Krayenbuehl HP: **Influence of collagen network on left ventricular systolic and diastolic function in aortic valve disease**. *J Am Coll Cardiol* 1993, **22**(5):1477-1484.
6. Akasheva DU, Plokhova EV, Tkacheva ON, Strazhesko ID, Dudinskaya EN, Kruglikova AS, Pykhtina VS, Brailova NV, Pokshubina IA, Sharashkina NV *et al*: **Age-Related Left Ventricular Changes and Their Association with Leukocyte Telomere Length in Healthy People**. *PLoS One* 2015, **10**(8):e0135883.
7. Howden EJ, Carrick-Ranson G, Sarma S, Hieda M, Fujimoto N, Levine BD: **Effects of Sedentary Aging and Lifelong Exercise on Left Ventricular Systolic Function**. *Med Sci Sports Exerc* 2017.

8. Sun JP, Popovic ZB, Greenberg NL, Xu XF, Asher CR, Stewart WJ, Thomas JD: **Noninvasive quantification of regional myocardial function using Doppler-derived velocity, displacement, strain rate, and strain in healthy volunteers: effects of aging**. *J Am Soc Echocardiogr* 2004, **17**(2):132-138.

9. Larson ED, St Clair JR, Sumner WA, Bannister RA, Proenza C: **Depressed pacemaker activity of sinoatrial node myocytes contributes to the age-dependent decline in maximum heart rate**. *Proc Natl Acad Sci U S A* 2013, **110**(44):18011-18016.

10. Hagberg JM, Allen WK, Seals DR, Hurley BF, Ehsani AA, Holloszy JO: **A hemodynamic comparison of young and older endurance athletes during exercise**. *J Appl Physiol (1985)* 1985, **58**(6):2041-2046.

11. Larsson HP: **How is the heart rate regulated in the sinoatrial node? Another piece to the puzzle**. *J Gen Physiol* 2010, **136**(3):237-241.

12. D'Este D, Bertaglia E, Zanocco A, Reimers B, Pascotto P: **Electrophysiological properties of the atrioventricular node and ageing: evidence of a lower incidence of dual nodal pathways in the elderly**. *Europace* 2001, **3**(3):216-220.

13. Sanchez-Quintana D, Yen Ho S: **[Anatomy of cardiac nodes and atrioventricular specialized conduction system]**. *Rev Esp Cardiol* 2003, **56**(11):1085-1092.

14. Yaniv Y, Ahmet I, Tsutsui K, Behar J, Moen JM, Okamoto Y, Guiriba TR, Liu J, Bychkov R, Lakatta EG: **Deterioration of autonomic neuronal receptor signaling and mechanisms intrinsic to heart pacemaker cells contribute to**

age-associated alterations in heart rate variability in vivo. *Aging Cell* 2016, **15**(4):716-724.

15. Klausner SC, Schwartz AB: **The aging heart**. *Clin Geriatr Med* 1985, **1**(1):119-141.

16. Agruss NS, Rosin EY, Adolph RJ, Fowler NO: **Significance of chronic sinus bradycardia in elderly people**. *Circulation* 1972, **46**(5):924-930.

17. Fleg JL, Kennedy HL: **Cardiac arrhythmias in a healthy elderly population: detection by 24-hour ambulatory electrocardiography**. *Chest* 1982, **81**(3):302-307.

18. Burlew BS: **Diastolic dysfunction in the elderly--the interstitial issue**. *Am J Geriatr Cardiol* 2004, **13**(1):29-38.

19. Biernacka A, Frangogiannis NG: **Aging and Cardiac Fibrosis**. *Aging Dis* 2011, **2**(2):158-173.

20. Olivetti G, Melissari M, Capasso JM, Anversa P: **Cardiomyopathy of the aging human heart. Myocyte loss and reactive cellular hypertrophy**. *Circ Res* 1991, **68**(6):1560-1568.

21. Gazoti Debessa CR, Mesiano Maifrino LB, Rodrigues de Souza R: **Age related changes of the collagen network of the human heart**. *Mech Ageing Dev* 2001, **122**(10):1049-1058.

22. Bradshaw AD: **The role of SPARC in extracellular matrix assembly**. *J Cell Commun Signal* 2009, **3**(3-4):239-246.

23. Nagase H, Visse R, Murphy G: **Structure and function of matrix metalloproteinases and TIMPs**. *Cardiovasc Res* 2006, **69**(3):562-573.

24. Bonnema DD, Webb CS, Pennington WR, Stroud RE, Leonardi AE, Clark LL, McClure CD, Finklea L, Spinale FG, Zile MR: **Effects of age on plasma matrix metalloproteinases (MMPs) and tissue inhibitor of metalloproteinases (TIMPs)**. *J Card Fail* 2007, **13**(7):530-540.

25. Mitchell GF, Guo CY, Benjamin EJ, Larson MG, Keyes MJ, Vita JA, Vasan RS, Levy D: **Cross-sectional correlates of increased aortic stiffness in the community: the Framingham Heart Study**. *Circulation* 2007, **115**(20):2628-2636.

26. Lakatta EG: **Arterial and cardiac aging: major shareholders in cardiovascular disease enterprises: Part III: cellular and molecular clues to heart and arterial aging**. *Circulation* 2003, **107**(3):490-497.

27. McEniery CM, Yasmin, Hall IR, Qasem A, Wilkinson IB, Cockcroft JR, Investigators A: **Normal vascular aging: differential effects on wave reflection and aortic pulse wave velocity: the Anglo-Cardiff Collaborative Trial (ACCT)**. *J Am Coll Cardiol* 2005, **46**(9):1753-1760.

28. Lockhart CJ, Hamilton PK, Quinn CE, McVeigh GE: **End-organ dysfunction and cardiovascular outcomes: the role of the microcirculation**. *Clin Sci (Lond)* 2009, **116**(3):175-190.

29. Mitchell GF: **Effects of central arterial aging on the structure and function of the peripheral vasculature: implications for end-organ damage**. *J Appl Physiol (1985)* 2008, **105**(5):1652-1660.

30. Cooper LL, Odening KE, Hwang MS, Chaves L, Schofield L, Taylor CA, Gemignani AS, Mitchell GF, Forder JR, Choi BR *et al*: **Electromechanical and structural**

alterations in the aging rabbit heart and aorta. *Am J Physiol Heart Circ Physiol* 2012, **302**(8):H1625-1635.

31. Weisser-Thomas J, Nguyen Q, Schuettel M, Thomas D, Dreiner U, Grohe C, Meyer R: **Age and hypertrophy related changes in contractile post-rest behavior and action potential properties in isolated rat myocytes**. *Age (Dordr)* 2007, **29**(4):205-217.

32. Zahn JM, Sonu R, Vogel H, Crane E, Mazan-Mamczarz K, Rabkin R, Davis RW, Becker KG, Owen AB, Kim SK: **Transcriptional profiling of aging in human muscle reveals a common aging signature**. *PLoS Genet* 2006, **2**(7):e115.

33. Nattel S, Maguy A, Le Bouter S, Yeh YH: **Arrhythmogenic ion-channel remodeling in the heart: heart failure, myocardial infarction, and atrial fibrillation**. *Physiol Rev* 2007, **87**(2):425-456.

34. Jones SA, Lancaster MK, Boyett MR: **Ageing-related changes of connexins and conduction within the sinoatrial node**. *J Physiol* 2004, **560**(Pt 2):429-437.

35. Zhou J, Chong SY, Lim A, Singh BK, Sinha RA, Salmon AB, Yen PM: **Changes in macroautophagy, chaperone-mediated autophagy, and mitochondrial metabolism in murine skeletal and cardiac muscle during aging**. *Aging (Albany NY)* 2017, **9**(2):583-599.

36. Ashrafi G, Schwarz TL: **The pathways of mitophagy for quality control and clearance of mitochondria**. *Cell Death Differ* 2013, **20**(1):31-42.

37. Hoshino A, Mita Y, Okawa Y, Ariyoshi M, Iwai-Kanai E, Ueyama T, Ikeda K, Ogata T, Matoba S: **Cytosolic p53 inhibits Parkin-mediated mitophagy and promotes mitochondrial dysfunction in the mouse heart**. *Nat Commun* 2013, **4**:2308.

38. Ikeda Y, Shirakabe A, Maejima Y, Zhai P, Sciarretta S, Toli J, Nomura M, Mihara K, Egashira K, Ohishi M *et al*: **Endogenous Drp1 mediates mitochondrial autophagy and protects the heart against energy stress**. *Circ Res* 2015, **116**(2):264-278.

39. Shirakabe A, Zhai P, Ikeda Y, Saito T, Maejima Y, Hsu CP, Nomura M, Egashira K, Levine B, Sadoshima J: **Drp1-Dependent Mitochondrial Autophagy Plays a Protective Role Against Pressure Overload-Induced Mitochondrial Dysfunction and Heart Failure**. *Circulation* 2016, **133**(13):1249-1263.

40. Quinlan CL, Perevoshchikova IV, Hey-Mogensen M, Orr AL, Brand MD: **Sites of reactive oxygen species generation by mitochondria oxidizing different substrates**. *Redox Biol* 2013, **1**:304-312.

41. Tretter L, Adam-Vizi V: **Generation of reactive oxygen species in the reaction catalyzed by alpha-ketoglutarate dehydrogenase**. *J Neurosci* 2004, **24**(36):7771-7778.

42. Dai DF, Santana LF, Vermulst M, Tomazela DM, Emond MJ, MacCoss MJ, Gollahon K, Martin GM, Loeb LA, Ladiges WC *et al*: **Overexpression of catalase targeted to mitochondria attenuates murine cardiac aging**. *Circulation* 2009, **119**(21):2789-2797.

43. Li X, Fang P, Mai J, Choi ET, Wang H, Yang XF: **Targeting mitochondrial reactive oxygen species as novel therapy for inflammatory diseases and cancers**. *J Hematol Oncol* 2013, **6**:19.

44. Maharjan S, Oku M, Tsuda M, Hoseki J, Sakai Y: **Mitochondrial impairment triggers cytosolic oxidative stress and cell death following proteasome inhibition**. *Sci Rep* 2014, **4**:5896.

45. Dickinson BC, Chang CJ: **Chemistry and biology of reactive oxygen species in signaling or stress responses**. *Nat Chem Biol* 2011, **7**(8):504-511.

46. Zhang L, Li Y, Xing D, Gao C: **Characterization of mitochondrial dynamics and subcellular localization of ROS reveal that HsfA2 alleviates oxidative damage caused by heat stress in Arabidopsis**. *J Exp Bot* 2009, **60**(7):2073-2091.

47. Maron BA, Michel T: **Subcellular localization of oxidants and redox modulation of endothelial nitric oxide synthase**. *Circ J* 2012, **76**(11):2497-2512.

48. Valko M, Leibfritz D, Moncol J, Cronin MT, Mazur M, Telser J: **Free radicals and antioxidants in normal physiological functions and human disease**. *Int J Biochem Cell Biol* 2007, **39**(1):44-84.

49. Shaik A, Schiavi A, Ventura N: **Mitochondrial autophagy promotes healthy aging**. *Cell Cycle* 2016, **15**(14):1805-1806.

50. Sohal RS, Sohal BH: **Hydrogen peroxide release by mitochondria increases during aging**. *Mech Ageing Dev* 1991, **57**(2):187-202.

51. Ikeda Y, Sciarretta S, Nagarajan N, Rubattu S, Volpe M, Frati G, Sadoshima J: **New insights into the role of mitochondrial dynamics and autophagy during oxidative stress and aging in the heart**. *Oxid Med Cell Longev* 2014, **2014**:210934.

52. Wohlgemuth SE, Calvani R, Marzetti E: **The interplay between autophagy and mitochondrial dysfunction in oxidative stress-induced cardiac aging and pathology**. *J Mol Cell Cardiol* 2014, **71**:62-70.

53. Cooper LL, Li W, Lu Y, Centracchio J, Terentyeva R, Koren G, Terentyev D: **Redox modification of ryanodine receptors by mitochondria-derived reactive oxygen species contributes to aberrant Ca2+ handling in ageing rabbit hearts**. *J Physiol* 2013, **591**(23):5895-5911.

54. Ravikumar B, Sarkar S, Davies JE, Futter M, Garcia-Arencibia M, Green-Thompson ZW, Jimenez-Sanchez M, Korolchuk VI, Lichtenberg M, Luo S *et al*: **Regulation of mammalian autophagy in physiology and pathophysiology**. *Physiol Rev* 2010, **90**(4):1383-1435.

55. Nemchenko A, Chiong M, Turer A, Lavandero S, Hill JA: **Autophagy as a therapeutic target in cardiovascular disease**. *J Mol Cell Cardiol* 2011, **51**(4):584-593.

56. Lemasters JJ: **Selective mitochondrial autophagy, or mitophagy, as a targeted defense against oxidative stress, mitochondrial dysfunction, and aging**. *Rejuvenation Res* 2005, **8**(1):3-5.

57. Martinez-Lopez N, Athonvarangkul D, Singh R: **Autophagy and aging**. *Adv Exp Med Biol* 2015, **847**:73-87.

58. Garcia L, Verdejo HE, Kuzmicic J, Zalaquett R, Gonzalez S, Lavandero S, Corbalan R: **Impaired cardiac autophagy in patients developing postoperative atrial fibrillation**. *J Thorac Cardiovasc Surg* 2012, **143**(2):451-459.

59. Wiersma M, Meijering RAM, Qi XY, Zhang D, Liu T, Hoogstra-Berends F, Sibon OCM, Henning RH, Nattel S, Brundel B: **Endoplasmic Reticulum Stress Is Associated With Autophagy and Cardiomyocyte Remodeling in Experimental and Human Atrial Fibrillation**. *J Am Heart Assoc* 2017, **6**(10).

60. Hamacher-Brady A, Brady NR, Gottlieb RA: **Enhancing macroautophagy protects against ischemia/reperfusion injury in cardiac myocytes**. *J Biol Chem* 2006, **281**(40):29776-29787.

61. Shimizu S, Kanaseki T, Mizushima N, Mizuta T, Arakawa-Kobayashi S, Thompson CB, Tsujimoto Y: **Role of Bcl-2 family proteins in a non-apoptotic programmed cell death dependent on autophagy genes**. *Nat Cell Biol* 2004, **6**(12):1221-1228.

62. Nezis IP, Shravage BV, Sagona AP, Lamark T, Bjorkoy G, Johansen T, Rusten TE, Brech A, Baehrecke EH, Stenmark H: **Autophagic degradation of dBruce controls DNA fragmentation in nurse cells during late Drosophila melanogaster oogenesis**. *J Cell Biol* 2010, **190**(4):523-531.

63. Scherz-Shouval R, Shvets E, Fass E, Shorer H, Gil L, Elazar Z: **Reactive oxygen species are essential for autophagy and specifically regulate the activity of Atg4**. *EMBO J* 2007, **26**(7):1749-1760.

64. Rizzuto R, Pozzan T: **Microdomains of intracellular Ca2+: molecular determinants and functional consequences**. *Physiol Rev* 2006, **86**(1):369-408.

65. Zipes DP, Wellens HJ: **Sudden cardiac death**. *Circulation* 1998, **98**(21):2334-2351.

66. Cheng H, Lederer WJ, Cannell MB: **Calcium sparks: elementary events underlying excitation-contraction coupling in heart muscle**. *Science* 1993, **262**(5134):740-744.

67. Plummer BN, Cutler MJ, Wan X, Laurita KR: **Spontaneous calcium oscillations during diastole in the whole heart: the influence of ryanodine reception function and gap junction coupling**. *Am J Physiol Heart Circ Physiol* 2011, **300**(5):H1822-1828.

68. Orchard CH, Houser SR, Kort AA, Bahinski A, Capogrossi MC, Lakatta EG: **Acidosis facilitates spontaneous sarcoplasmic reticulum Ca2+ release in rat myocardium**. *J Gen Physiol* 1987, **90**(1):145-165.

69. Zima AV, Blatter LA: **Redox regulation of cardiac calcium channels and transporters**. *Cardiovasc Res* 2006, **71**(2):310-321.

70. Qian Y, Chen X: **Senescence regulation by the p53 protein family**. *Methods Mol Biol* 2013, **965**:37-61.

71. Campisi J: **Cancer, aging and cellular senescence**. *In Vivo* 2000, **14**(1):183-188.

72. Rayess H, Wang MB, Srivatsan ES: **Cellular senescence and tumor suppressor gene p16**. *Int J Cancer* 2012, **130**(8):1715-1725.

73. Coppe JP, Patil CK, Rodier F, Sun Y, Munoz DP, Goldstein J, Nelson PS, Desprez PY, Campisi J: **Senescence-associated secretory phenotypes reveal cell-nonautonomous functions of oncogenic RAS and the p53 tumor suppressor**. *PLoS Biol* 2008, **6**(12):2853-2868.

74. Coppe JP, Desprez PY, Krtolica A, Campisi J: **The senescence-associated secretory phenotype: the dark side of tumor suppression**. *Annu Rev Pathol* 2010, **5**:99-118.

75. Rodier F, Coppe JP, Patil CK, Hoeijmakers WA, Munoz DP, Raza SR, Freund A, Campeau E, Davalos AR, Campisi J: **Persistent DNA damage signalling triggers senescence-associated inflammatory cytokine secretion**. *Nat Cell Biol* 2009, **11**(8):973-979.

76. Tchkonia T, Zhu Y, van Deursen J, Campisi J, Kirkland JL: **Cellular senescence and the senescent secretory phenotype: therapeutic opportunities**. *J Clin Invest* 2013, **123**(3):966-972.

77. Jun JI, Lau LF: **The matricellular protein CCN1 induces fibroblast senescence and restricts fibrosis in cutaneous wound healing**. *Nat Cell Biol* 2010, **12**(7):676-685.

78. Krizhanovsky V, Yon M, Dickins RA, Hearn S, Simon J, Miething C, Yee H, Zender L, Lowe SW: **Senescence of activated stellate cells limits liver fibrosis**. *Cell* 2008, **134**(4):657-667.

79. Freund A, Orjalo AV, Desprez PY, Campisi J: **Inflammatory networks during cellular senescence: causes and consequences**. *Trends Mol Med* 2010, **16**(5):238-246.

80. Kuilman T, Peeper DS: **Senescence-messaging secretome: SMS-ing cellular stress**. *Nat Rev Cancer* 2009, **9**(2):81-94.

81. Velarde MC, Flynn JM, Day NU, Melov S, Campisi J: **Mitochondrial oxidative stress caused by Sod2 deficiency promotes cellular senescence and aging phenotypes in the skin**. *Aging (Albany NY)* 2012, **4**(1):3-12.

82. Herbig U, Ferreira M, Condel L, Carey D, Sedivy JM: **Cellular senescence in aging primates**. *Science* 2006, **311**(5765):1257.

83. Kang TW, Yevsa T, Woller N, Hoenicke L, Wuestefeld T, Dauch D, Hohmeyer A, Gereke M, Rudalska R, Potapova A *et al*: **Senescence surveillance of pre-malignant hepatocytes limits liver cancer development**. *Nature* 2011, **479**(7374):547-551.

84. Campisi J: **Senescent cells, tumor suppression, and organismal aging: good citizens, bad neighbors**. *Cell* 2005, **120**(4):513-522.

85. Baker DJ, Wijshake T, Tchkonia T, LeBrasseur NK, Childs BG, van de Sluis B, Kirkland JL, van Deursen JM: **Clearance of p16Ink4a-positive senescent cells delays ageing-associated disorders**. *Nature* 2011, **479**(7372):232-236.

86. Baker DJ, Childs BG, Durik M, Wijers ME, Sieben CJ, Zhong J, Saltness RA, Jeganathan KB, Verzosa GC, Pezeshki A *et al*: **Naturally occurring p16(Ink4a)-positive cells shorten healthy lifespan**. *Nature* 2016, **530**(7589):184-189.

87. Ogrodnik M, Miwa S, Tchkonia T, Tiniakos D, Wilson CL, Lahat A, Day CP, Burt A, Palmer A, Anstee QM *et al*: **Cellular senescence drives age-dependent hepatic steatosis**. *Nat Commun* 2017, **8**:15691.

88. Dimri GP, Lee X, Basile G, Acosta M, Scott G, Roskelley C, Medrano EE, Linskens M, Rubelj I, Pereira-Smith O *et al*: **A biomarker that identifies senescent human**

cells in culture and in aging skin in vivo. *Proc Natl Acad Sci U S A* 1995, **92**(20):9363-9367.

89. Itahana K, Campisi J, Dimri GP: **Methods to detect biomarkers of cellular senescence: the senescence-associated beta-galactosidase assay**. *Methods Mol Biol* 2007, **371**:21-31.

90. Jeyapalan JC, Ferreira M, Sedivy JM, Herbig U: **Accumulation of senescent cells in mitotic tissue of aging primates**. *Mech Ageing Dev* 2007, **128**(1):36-44.

91. Capparelli C, Chiavarina B, Whitaker-Menezes D, Pestell TG, Pestell RG, Hulit J, Ando S, Howell A, Martinez-Outschoorn UE, Sotgia F *et al*: **CDK inhibitors (p16/p19/p21) induce senescence and autophagy in cancer-associated fibroblasts, "fueling" tumor growth via paracrine interactions, without an increase in neo-angiogenesis**. *Cell Cycle* 2012, **11**(19):3599-3610.

92. Biran A, Zada L, Abou Karam P, Vadai E, Roitman L, Ovadya Y, Porat Z, Krizhanovsky V: **Quantitative identification of senescent cells in aging and disease**. *Aging Cell* 2017, **16**(4):661-671.

93. Georgakopoulou EA, Tsimaratou K, Evangelou K, Fernandez Marcos PJ, Zoumpourlis V, Trougakos IP, Kletsas D, Bartek J, Serrano M, Gorgoulis VG: **Specific lipofuscin staining as a novel biomarker to detect replicative and stress-induced senescence. A method applicable in cryo-preserved and archival tissues**. *Aging (Albany NY)* 2013, **5**(1):37-50.

94. Evangelou K, Lougiakis N, Rizou SV, Kotsinas A, Kletsas D, Munoz-Espin D, Kastrinakis NG, Pouli N, Marakos P, Townsend P *et al*: **Robust, universal**

biomarker assay to detect senescent cells in biological specimens. *Aging Cell* 2017, **16**(1):192-197.

95. Zhu F, Li Y, Zhang J, Piao C, Liu T, Li HH, Du J: **Senescent cardiac fibroblast is critical for cardiac fibrosis after myocardial infarction**. *PLoS One* 2013, **8**(9):e74535.

96. Meyer K, Hodwin B, Ramanujam D, Engelhardt S, Sarikas A: **Essential Role for Premature Senescence of Myofibroblasts in Myocardial Fibrosis**. *J Am Coll Cardiol* 2016, **67**(17):2018-2028.

97. Goldhaber JI, Xie LH, Duong T, Motter C, Khuu K, Weiss JN: **Action potential duration restitution and alternans in rabbit ventricular myocytes: the key role of intracellular calcium cycling**. *Circ Res* 2005, **96**(4):459-466.

98. Puglisi JL, Yuan W, Bassani JW, Bers DM: **Ca(2+) influx through Ca(2+) channels in rabbit ventricular myocytes during action potential clamp: influence of temperature**. *Circ Res* 1999, **85**(6):e7-e16.

99. Varro A, Lathrop DA, Hester SB, Nanasi PP, Papp JG: **Ionic currents and action potentials in rabbit, rat, and guinea pig ventricular myocytes**. *Basic Res Cardiol* 1993, **88**(2):93-102.

100. Knollmann BC, Schober T, Petersen AO, Sirenko SG, Franz MR: **Action potential characterization in intact mouse heart: steady-state cycle length dependence and electrical restitution**. *Am J Physiol Heart Circ Physiol* 2007, **292**(1):H614-621.

101. Ottolia M, Torres N, Bridge JH, Philipson KD, Goldhaber JI: **Na/Ca exchange and contraction of the heart**. *J Mol Cell Cardiol* 2013, **61**:28-33.

102. Hasenfuss G: **Animal models of human cardiovascular disease, heart failure and hypertrophy**. *Cardiovasc Res* 1998, **39**(1):60-76.

103. von Holst D, Hutzelmeyer H, Kaetzke P, Khaschei M, Schonheiter R: **Social rank, stress, fitness, and life expectancy in wild rabbits**. *Naturwissenschaften* 1999, **86**(8):388-393.

104. Harken AH, Simson MB, Haselgrove J, Wetstein L, Harden WR, 3rd, Barlow CH: **Early ischemia after complete coronary ligation in the rabbit, dog, pig, and monkey**. *The American journal of physiology* 1981, **241**(2):H202-210.

105. Burton RA, Schneider JE, Bishop MJ, Hales PW, Bollensdorff C, Robson MD, Wong KC, Morris J, Quinn TA, Kohl P: **Microscopic magnetic resonance imaging reveals high prevalence of third coronary artery in human and rabbit heart**. *Europace* 2012, **14 Suppl 5**:v73-v81.

106. Day SB, Johnson JA: **The distribution of the coronary arteries of the rabbit**. *Anat Rec* 1958, **132**(4):633-643.

107. Podesser B, Wollenek G, Seitelberger R, Siegel H, Wolner E, Firbas W, Tschabitscher M: **Epicardial branches of the coronary arteries and their distribution in the rabbit heart: the rabbit heart as a model of regional ischemia**. *Anat Rec* 1997, **247**(4):521-527.

108. Baptista CA, DiDio LJ, Prates JC: **Types of division of the left coronary artery and the ramus diagonalis of the human heart**. *Jpn Heart J* 1991, **32**(3):323-335.

109. Hu N, Straub CM, Garzarelli AA, Sabey KH, Yockman JW, Bull DA: **Ligation of the left circumflex coronary artery with subsequent MRI and histopathology in rabbits**. *J Am Assoc Lab Anim Sci* 2010, **49**(6):838-844.

110. Isorni MA, Casanova A, Piquet J, Bellamy V, Pignon C, Puymirat E, Menasche P: **Comparative Analysis of Methods to Induce Myocardial Infarction in a Closed-Chest Rabbit Model**. *Biomed Res Int* 2015, **2015**:893051.

111. Steppan J, Barodka V, Berkowitz DE, Nyhan D: **Vascular stiffness and increased pulse pressure in the aging cardiovascular system**. *Cardiol Res Pract* 2011, **2011**:263585.

112. Orlandi A, Francesconi A, Marcellini M, Ferlosio A, Spagnoli LG: **Role of ageing and coronary atherosclerosis in the development of cardiac fibrosis in the rabbit**. *Cardiovasc Res* 2004, **64**(3):544-552.

113. Morita N, Mandel WJ, Kobayashi Y, Karagueuzian HS: **Cardiac fibrosis as a determinant of ventricular tachyarrhythmias**. *J Arrhythm* 2014, **30**(6):389-394.

114. Kazbanov IV, ten Tusscher KH, Panfilov AV: **Effects of Heterogeneous Diffuse Fibrosis on Arrhythmia Dynamics and Mechanism**. *Sci Rep* 2016, **6**:20835.

115. Zima AV, Bovo E, Mazurek SR, Rochira JA, Li W, Terentyev D: **Ca handling during excitation-contraction coupling in heart failure**. *Pflugers Archiv : European journal of physiology* 2014, **466**(6):1129-1137.

116. Belevych AE, Terentyev D, Terentyeva R, Ho HT, Gyorke I, Bonilla IM, Carnes CA, Billman GE, Gyorke S: **Shortened Ca2+ signaling refractoriness underlies cellular arrhythmogenesis in a postinfarction model of sudden cardiac death**. *Circ Res* 2012, **110**(4):569-577.

117. Bito V, Heinzel FR, Biesmans L, Antoons G, Sipido KR: **Crosstalk between L-type Ca2+ channels and the sarcoplasmic reticulum: alterations during cardiac remodelling**. *Cardiovasc Res* 2008, **77**(2):315-324.

118. Terentyev D, Gyorke I, Belevych AE, Terentyeva R, Sridhar A, Nishijima Y, de Blanco EC, Khanna S, Sen CK, Cardounel AJ *et al*: **Redox modification of ryanodine receptors contributes to sarcoplasmic reticulum Ca2+ leak in chronic heart failure**. *Circ Res* 2008, **103**(12):1466-1472.

119. Murphy MP, Smith RA: **Targeting antioxidants to mitochondria by conjugation to lipophilic cations**. *Annu Rev Pharmacol Toxicol* 2007, **47**:629-656.

120. Zheng ZJ, Croft JB, Giles WH, Mensah GA: **Sudden cardiac death in the United States, 1989 to 1998**. *Circulation* 2001, **104**(18):2158-2163.

121. Podrid PJ, Myerburg RJ: **Epidemiology and stratification of risk for sudden cardiac death**. *Clin Cardiol* 2005, **28**(11 Suppl 1):I3-11.

122. Dai DF, Chiao YA, Marcinek DJ, Szeto HH, Rabinovitch PS: **Mitochondrial oxidative stress in aging and healthspan**. *Longevity & healthspan* 2014, **3**:6.

123. Essick EE, Sam F: **Oxidative stress and autophagy in cardiac disease, neurological disorders, aging and cancer**. *Oxid Med Cell Longev* 2010, **3**(3):168-177.

124. Sabharwal SS, Schumacker PT: **Mitochondrial ROS in cancer: initiators, amplifiers or an Achilles' heel?** *Nat Rev Cancer* 2014, **14**(11):709-721.

125. Shadel GS, Horvath TL: **Mitochondrial ROS signaling in organismal homeostasis**. *Cell* 2015, **163**(3):560-569.

126. Cao DJ, Gillette TG, Hill JA: **Cardiomyocyte autophagy: remodeling, repairing, and reconstructing the heart**. *Curr Hypertens Rep* 2009, **11**(6):406-411.

127. Morrissey PJ, Murphy KR, Daley JM, Schofield L, Turan NN, Arunachalam K, Abbott JD, Koren G: **A novel method of standardized myocardial infarction in aged rabbits**. *Am J Physiol Heart Circ Physiol* 2017, **312**(5):H959-H967.

Chapter 2: A Novel Method of Standardized Myocardial Infarction in Aged Rabbits

This chapter has been published*: Am J Physiol - Heart C*, 2017. May 1;312(5):H959-H967

The author contributed to this manuscript by performing histology and staining, ECG collection, and assisted writing the manuscript as well as creating the figures. PJM, JMD, and LS performed the surgeries. PJM worked with the author to design experiments, create figures, and write the manuscript.

Patrick J. Morrissey[1]*, **Kevin R. Murphy[1,2]***, Jean M. Daley[1], Lorraine Schofield[1], Nilufer N. Turan[1], Karuppiah Arunachalam[1,3], J. Dawn Abbott[1], and Gideon Koren[1]

*Co-First Authors

[1]Cardiovascular Research Center, Division of Cardiology, Rhode Island Hospital, Warren Alpert Medical School of Brown University, Providence RI

[2]Department of Molecular Biology, Cellular Biology and Biochemistry, Brown University, Providence RI

[3]Department of Internal Medicine, Rhode Island Hospital, Warren Alpert Medical School of Brown University, Providence RI

Running Title: A Novel Method of Standardized Myocardial Infarction in Aged Rabbits

Total number of words: 4610 words

To whom all correspondence should be addressed:

Gideon Koren, M.D.

Cardiovascular Research Center

Division of Cardiology, Rhode Island Hospital

Alpert Medical School of Brown University

Providence, RI 02903

Phone: (401) 444-6129

Fax: (401) 444-9203

E-mail: Gideon_Koren@brown.edu

2.1 Abstract

The incidence of both myocardial infarction (MI) and sudden cardiac death (SCD) increases with age. Here we describe the development of a minimally invasive large animal model of MI that can be applied to young or aged animals. We demonstrate that rabbit coronary anatomy is highly variable, more so than described in previous literature. In this work we categorize the coronary pattern of 37 young and 64 aged rabbits. Aged rabbits had a higher degree of branching from the left main coronary artery. Standardizing the model across age cohorts required a new approach, targeting an area of myocardium rather than a specific vessel. Here we present a method for achieving a reproducible infarct size, one that has yielded a consistent scar encompassing ~30% of the apical left ventricular free wall. The model's consistency has allowed for more valid comparisons of MI sequelae between age cohorts.

Key Words*:* Myocardial Infarction, Ventricular Fibrillation, Arrhythmia, Aging, Coronary angiography, Coronary anatomy,

List of Abbreviations*:* MI: Myocardial Infarction, SCD: Sudden Cardiac Death, LM: Left Main Coronary Artery, LAD: Left Anterior Descending, OM Obtuse Marginal, LCX, Left Circumflex, LV: Left ventricle, RV: Right ventricle,

New & Noteworthy: This manuscript describes the coronary angiographic imaging of young and aged rabbits. We developed and improved a novel minimally invasive approach for coil embolization that targets a specific area of myocardium and has yielded a consistent scar encompassing ~30% the left ventricular free wall of young and aged rabbit hearts.

2.2 Introduction

Sudden cardiac death (SCD) is a major public health issue responsible for approximately 1 in 5 deaths in industrialized countries [1, 2]. The risk of SCD increases tenfold for people over the age of 65 [1, 2]. Nearly half of SCD victims show healed myocardial infarctions (MI) at autopsy [3]. The mechanisms that make MI more deadly in the aging heart are largely unknown [4]. To probe these mechanisms, age-appropriate models of cardiac disease are necessary. One such model is the aged rabbit.

The rabbit has similar action potential morphology and cardiomyocyte calcium homeostasis as humans [5, 6]. Accordingly, the rabbit heart has long been used as a model for studying myocardial ischemia and infarction [7-11]. In all models of cardiac disease, understanding coronary anatomy is crucial to standardize surgical techniques and increase animal-to-animal reproducibility. The rabbit heart, like other mammalian hearts, displays a high degree of coronary anatomy variability [12].

Current infarction models rely on ligation or occlusion of the same artery in each surgical case, regardless of coronary anatomy [13-16]. In rabbits, the most commonly ligated vessels are the left anterior descending (LAD) and the left circumflex (LCX) [7, 17, 18]. Experience with coronary angiography reveals that these vessels vary greatly in length and diameter between hearts. As the literature suggests, targeting one specific vessel, whether it be LAD or LCX, leads to highly unpredictable infarctions [19]. We have identified no ischemia or infarct studies to date that have accounted for the complexity of coronary anatomy and no surgical solution has directly addressed this problem.

The literature on rabbit coronary anatomy suggests a simple dichotomy - half of all hearts exhibit bifurcation and half exhibit trifurcation of the left main (LM) coronary artery

[12, 20]. This is an oversimplification that fails to account for other common variants. We have observed right coronary dominance in both young and aged rabbits, as well as quadrifurcation of the LM in aged rabbits. Thus, coronary variability makes the one-size-fits-all infarct methodology susceptible to unpredictable outcomes [19].

Using our knowledge of rabbit coronary anatomy, and optimizing our infarction procedure accordingly, we have developed a novel methodology to target an area of myocardium in each rabbit as opposed to a specific artery. This technique standardizes the size and location of the infarction between rabbits. This level of model consistency allows for direct comparisons between study groups, without adjustment for infarct size, across a wide array of assays on the organ, tissue, and cellular levels. The most reproducible area to target in the rabbit heart is the apical, anterolateral left ventricular wall. This area is almost always served by a single vessel with relatively little anastomosis. We provide a rubric for creating a reproducible infarct of 30% of the LV free wall.

2.3 Methods

This investigation conformed to the current Guide for Care and Use of Laboratory Animals published by the National Institutes of Health (NIH Publication No. 85–23, revised 1996), as well as the standards recently delineated by the American Physiological Society (Guiding Principles for Research Involving Animals and Human Beings), and was approved by the Institutional Animal Care and Use Committee at Rhode Island Hospital. Adult female rabbits (3.5–5.5 kg) ages 6–12 mo were used for young group, and ages 4.0-5.5 yo were used for aged group [21]. The prophylactic drug regimen includes 3 days of oral amiodarone, 400 mg given twice daily 6 to 8 hours apart prior and 400 mg the day

following the experimental MI. Rabbits were anesthetized with intramuscular ketamine/xylazine (25 mg/kg/3.75 mg/kg) and buprenorphine (0.03 mg/kg), intubated, and ventilated with isoflurane (1–2%, FiO_2 0.5). Blood pressure and peripheral oxygen saturation were measured continuously. A continuous 12-lead ECG was recorded during the induction of myocardial infarction. Procedurally, a bolus of intravenous amiodarone (5 mg/kg) is given during a 20 minute period before and again 40 minutes after coronary coil placement, with a continuous infusion (12.5 mcg/kg/min) between the boluses. Additionally, premature ventricular contractions (PVC's) are suppresed with intravenous lidocaine using a bolus of 1 mg/kg and an 40 mcg/kg/min infusion.

Echocardiography

Transthoracic echocardiography was performed in sedated animals at baseline (pre-MI) and 3 weeks post-MI. Two-dimensional echo images (Hewlett Packard 5500) were obtained with a 7.5-mHz probe, and long axis and short axis views were performed mimicking those used in human echocardiography. Analysis included dimensions of the LV, fractional shortening and LV ejection fraction (calculated using simple Quinone's method) and was performed by an experienced echocardiographer. Functional outcomes were compared between bifurcated and trifurcated cohorts.

Coronary Angiography

Coronary angiography was performed by injection of contrast (OmniPaque, 3.5 mg/mL, GE Healthcare) through a 4-Fr guide catheter proximal to the ostia of the left and right main coronary arteries. Direct insertion into the main coronaries is not possible as a

4-Fr catheter is needed for optimal contrast levels and the ostia are smaller in diameter than the catheter. Cine acquistions were taken from the left anterior oblique (+35°), anterior posterior (0°), right anterior oblique (-35°) and right anterior oblique caudal view (-35° and 30° tilt). Angiograms were reviewed using Encompass software (Heartlab, Inc., Agfa HealthCare; Westerly, RI) to determine configuration of the coronary anatomy (Table 1).

Myocardial Infarction and Coil Placement

Our minimally-invasive endovascular site-specific infarct methodology has been previously described [15]. In brief, a neck incision was performed to isolate the right carotid and a 4-Fr guide catheter was advanced to the ostia of the desired coronary artery. The coronary anatomy was defined by angiography and coil location was decided upon. Coil placement was most often performed in the right anterior oblique view for optimal visualization of the left ventricular free wall. A 0.014-in guidewire was advanced into the selected coronary to the coil deployment site and a 2.5-fr microcatheter was advanced over the wire. The guidewire was removed and an 0.018” platinum coil, cut to a length of 2mm, was advanced through the micro-catheter. A standardized algorithm was used to determine location of coil placement (Table 2).

Histochemistry

Left ventricular (LV) free wall tissues from young and aged rabbits three weeks post-MI were embedded in OTC tissue freezing medium and cryosectioned at 10μM intervals. To assess scar size, Hematoxylin and Eosin, Masson’s Trichome, and Sirius Red staining were performed. Histopathology images were collected using a Nikon

TE2000 microscope with Retiga EXi camera. A previously published ImageJ macro was used to analyze blue, fibrosis area in the uncompressed image files acquired [22].

2.4 Results

We have created an angiographic atlas that includes coronary artery anatomy from 37 young (<1yr) and 64 aged (>4yrs) New Zealand White female rabbits. The average age of the young animals was 10 months and for the aged animals, 4.6 years. The New Zealand White rabbit exhibits a wide range of coronary anatomy, but the variability is not sex-dependent. Comparison of anatomical configurations between 28 young male and 37 young female rabbits reveals no difference (data not shown). No aged male rabbits were studied.

The LM coronary artery supplies the posterior descending artery (PDA) in 84% (32/38) of cases where we have studied both the left and right main coronary arteries. The LM can bifurcate into two, three or four arteries. We refer to each case respectively as: bifurcation, trifurcation or quadrifurcation (Table 1). In bifurcated rabbits, the LM divides into the LAD and LCX arteries. In these cases, the first obtuse marginal artery (OM1) is the dominant vessel in the left coronary system, perfusing the entire inferior lateral wall of the LV. In some bifurcated cases, the OM1 also perfuses the septum and anterior right ventricle (Figure 1). In trifurcated rabbits, the LM divides into the LAD, Ramus and LCX (Figure 2). The ramus stretches from the LM to the apex, directly perfusing the inferior anterolateral LV. The circumflex perfuses the posterior aspect of the LV as well as the right ventricle (RV). Quadrifurcated rabbits present with two ramus

arteries with one perfusing the inferior anterior LV, while the other perfuses the posterolateral wall of the LV and the posterior RV (Figure 3).

In general, the LAD is a relatively minor artery in the rabbit, perfusing the superior anterior aspect of the heart. The LAD does not have prominent diagonal branches and therefore is not a major contributor to the perfusion of the left ventricular wall. The LAD does exhibit a single prominent septal branch (Figure 2).

The LCX perfuses the posterior LV, as well as the posterolateral RV. The LCX artery varies in size and prominence from rabbit to rabbit. In general, if the origin of the OM1 is proximal to the mid-segment of the LV, the LCX is prominent and shows two or more branches. If the origin of the OM1 is distal to the mid-segment of the LV, the artery is minor and does not have branches.

Thirty young animals exhibit bifurcation of the LM, while only 7 exhibit trifurcation (Table 1). This result is significantly different than previously published results [12]. Thirty-four aged animals exhibit bifurcation, while 27 show trifurcation. Additionally, 3 aged animals exhibit quadrifurcation of the LM. The coronary anatomy of the aged rabbit has not been previously described. We find that the anatomy of our aged animals is significantly different than our young animals (two-tailed, 2x3 fisher's exact contingency table $p<0.05$).

Bifurcation and Trifurcation (Table 2)

Eighty-one percent (30/37) of our young rabbits exhibit bifurcation of the LM. The OM1 exhibits proximal branching in 7 (23%) bifurcated young rabbits and distal branching in 23 (77%).

Fifty-three percent (34/64) of aged rabbits exhibit bifurcation of the LM. The OM1 exhibits proximal branching in 11 (32%) cases and distal branching in 23 (68%) cases.

Trifurcation (Figure 3)

Nineteen percent (7/37) of young rabbits exhibit trifurcation of the LM. One (14%) rabbit exhibits proximal branching of the ramus and 6 (86%) exhibit distal branching of the ramus.

Forty-two percent (27/64) of aged rabbits exhibit trifurcation of the LM. In these rabbits, the ramus exhibits proximal branching in 11 (41%) cases and distal branching in 16 (59%) cases.

Quadrifurcation in Aged Rabbits (Figure 4)

Three (5%) of our 64 aged rabbits exhibit quadrifurcation of the LM. All of these rabbits exhibit distal branching of the ramus (Table 1). These rabbits have an LAD, Ramus 1, Ramus 2 and a LCX. The LAD and LCX are usually normal in these rabbits. Ramus 1 extends to the apex and perfuses the anterior inferior portion of the left ventricle. Ramus 2 is a more lateral artery perfusing the lateral and posterior left ventricle.

The Right Coronary Artery

We have studied the right and left coronary systems in 38 rabbits and the right is relatively diminutive in 32 (84%) of these rabbits. We do find, however, that the right coronary artery uniformly stretches to at least the midpoint of the heart. This is contradictory to previous studies [12]. The right coronary perfuses the lateral wall of the RV. Three of 19 young rabbits exhibit right dominance and 3 of 19 aged rabbits exhibit right dominance. Right dominance has never before been documented in rabbits. Right dominant rabbits have right marginal and posterior descending arteries. The LCX is diminutive in these rabbits and the OM1 is unaffected. In general, the RCA is more developed in the aged rabbit heart.

The Third Coronary Artery

We find that the majority of rabbits have a third coronary artery, which originates at a minuscule ostium within millimeters of the RCA. This result matches similar studies of the RCA [23].

The Standardized Infarct

Standardizing the size and location of the infarct in an experimental model is necessary for comparisons between groups. In the rabbit heart, the supply of blood to the inferior, anterolateral portion of the LV is not redundant. In bifurcated, trifurcated and quadrifurcated rabbits there is a single vessel that supplies this region, encompassing 30% of the left ventricle. We targeted this region via an endovascular coil embolization technique in 31 young and 61 aged rabbits using target locations defined in Table 2 [15]. 81% (25/31) of young and 72% (44/61) of the aged rabbits survived the procedure

(p=NS). The remaining rabbits included in the construction of our coronary atlas were unsuitable for infarction due to the size of coronary artery being small or instance of vasospasm that would not allow the advancement of the catheter system to the target location. For these animals, angiography was collected and the animal was excluded from the infarction cohort. Figure 5A illustrates a typical case in a bifurcated heart, whereas Figure 5D illustrates a typical trifurcated heart. We have also included relevant leads and gross histology (Fig 5B, 5E and 5C, 5F, respectively) to illustrate the similarity of MI despite anatomical differences. By using coronary angiography to identify the arterial supply to the anterolateral LV, we were able to achieve consistent size and location of the infarct. Specific target locations are illustrated in Figure 6. To quantify the reproducibility of the scar size we calculated percentage of the LV free wall infarcted using two methodologies: Figure 7A quantifies the size of the scar in 8 young and 9 aged rabbits using photos of the dissected LV free wall. Figure 7B quantifies the scar size in histologic studies done in five young and eight aged rabbits (the rest of the infarcted young and aged hearts were devoted to other ongoing functional and molecular studies). Despite the variations in coronary anatomy, two-tailed tests reveal no difference in infarct size between young and aged infarcted hearts (p=NS), regardless of coronary anatomy (Figure 7). The presence of scar was confirmed in histology studies performed in serial frozen sections. Figure 7D shows the heart stained with H&E stain. Figure 7E is a serial section stained with Massons Trichrome fibrosis staining. Lastly, Figure 7F is a serial section stained with Sirius Red collagen stain, imaged with polarized light to visualize the birefringence of collagen fibers.

Echocardiography results were analyzed before and after MI in both bifurcated (n=7) and trifurcated rabbits (n=5) (Table 3). Significantly lower Left Ventricular Fractional Shortening (LVFS) and Left Ventricular Ejection Fraction (LVEF) were observed in all rabbits 3 weeks after performing MI as compared to the pre-MI values ($p<0.05$). Importantly, after MI, there were no significant differences found in Left Ventricular Internal Diameter (LVID) at end-diastole and end systole, LVEF and LVFS between bifurcated and trifurcated rabbits either before or after the MI (p=ns).

2.5 Discussion

Our understanding of rabbit coronary anatomy has enabled us to develop a method of site-specific occlusion that yields a highly reproducible infarct model. Using echocardiography, we report no difference in functional outcomes between anatomy cohorts. Both bi- and trifurcated hearts display the same degree of reduction in LVEF and LVFS three weeks after MI.

Angiographic data demonstrate that the standard experimental technique of induced MI in rabbits, LCX ligation, is unsuitable to create a reproducible infarct model. The coronary anatomy of the rabbit varies considerably from case to case. Not only does the left coronary system display different and complex branching patterns, but the right coronary varies in size and importance.

The LCX artery ligation model cannot produce a consistent infarct for several reasons. First, the LCX varies greatly in size from animal to animal. In most animals, the OM1 is the dominant artery in the left coronary system and the LCX proper is relatively

minor. In some cases, however, the LCX is a dominant artery. Ligating or occluding this type of artery almost always results in peri-procedural death. Finally, the occasional occurrence of right coronary dominance is a confounding variable. In right coronary dominant cases, the LCX is miniscule after branching from the OM1. We find that in right dominant cases, occluding the LCX proximal to the origin of the OM1 is fatal and occluding it distal to the OM1 does not result in infarcts of sufficient size. For these reasons, right dominant rabbits are best infarcted by targeting the OM1.

The LAD or LCX ligation model makes physiological assays, such as high-resolution optical mapping of the epicardial surface, impossible due to fibrosis and surgical artifact. Moreover, the LAD is a minor vessel in the rabbit. In our experience, occlusion of this vessel does not guarantee a transmural infarction. Furthermore, since the LAD perfuses the septum, the infarction is more complicated, encompassing the septum and anterior, superior LV. This complicated infarction lessens the investigators ability to use optical mapping to view the entire infarction. For these reasons, we have chosen to target an area of myocardium rather than a specific vessel.

The variability of coronary anatomy between young and aged rabbits does not inhibit reproducibility. Our main challenge in creating a reproducible model was comparing rabbits with different anatomies, i.e. bifurcated versus trifurcated and quadrifurcated. That aged rabbits tend to have more collateral blood supply has not affected our model because we are targeting an area that does not experience blood supply redundancies in either age cohort. Similarly, and for the same reasons, quadrifurcation in aged rabbits does not seem to be confounding variable.

One of the striking differences in epicardial branching patterns between age cohorts is the presence of quadrifurcation in the aged cohort exclusively. The origins of this difference are not clear. Does the second ramus artery result from angiogenesis over time or is it present throughout the animal's lifetime? The latter is certainly possible as angiography is apt to miss a very small progenitor artery. As for the former, to our knowledge angiogenesis of this kind has not been previously documented. We believe a long-term study involving multiple angiographic time points across the animal's lifetime would be necessary to answer this intriguing question.

As shown by others, the use of perioperative amiodarone has reduced our incidence of SCD in the first 48 hours post-MI. Indeed, several studies show that amiodarone treatment results in decreased incidence of tachyarrhythmias and VF after MI in rats [24], sheep [25], and pigs [26]. Amiodarone may, however, modify ventricular remodeling through reducing matrix remodeling [27]. In rats, administration of amiodarone over four weeks post-MI prevents the upregulation of MMP2 in the left ventricle and preserves fractional shortening compared to vehicle control [28]. Importantly, long term administration of amiodarone in pigs post-MI was not associated with increased ventricular fibrosis and there was no significant elevation of BNP or MMP-9 when compared to vehicle control [26]. In humans, a small study of eight patients after coronary artery bypass grafting surgery showed increased proinflammatory activity via increased fibrinogen, but without increased mortality [29]. This study reports that plasma levels of TNF-α, IL-6, IL-10, and monocyte chemoattractant protein 1 all changed over time, but amiodarone treatment did not significantly change the expression of these factors

between amiodarone vs. placebo group. Given our relatively short dosing duration, we do not expect a substantial effect on the long-term outcomes of our study.

Though we have chosen the method of endovascular embolization, we believe our findings should also benefit those employing open-chest infarction methodology. The open-chest method can be specific enough to differentiate between bifurcation and trifurcation of the LMCA [30]. We posit that open-chest operators would be able to use our atlas not only to predict what LMCA branching to expect but also the branching of more distal epicardial vessels. In this light, employing our infarction rubric is feasible. Additionally, since our methodology does not involve re-perfusion, it is possible that an open-chest method could translate our anatomic findings and infarction rubric to the field of myocardial re-perfusion.

Here we present an age appropriate model of myocardial infarction in the rabbit. By targeting a specific area of the myocardium with minimally invasive coil embolization we achieve infarcts in the same location with similar size and similar functional outcomes. We believe this approach solves the long-lasting reproducibility problem associated with coronary artery ligation. This new methodology allows investigators to objectively assess interventions to reduce infarct size, regardless of anatomical configuration.

2.6 Acknowledgements

Sources of Funding

The research conducted in this publication was supported by the National Institute on Aging award number 1R21AG049608-01.

Acknowledgements

We would like to thank Dr. Malcolm Kirk for his valuable insights and recommendations in creating the antiarrhythmic drug regimen.

Conflicts of Interest

None.

2.7 Figures and Table

Figure 2.1: Bifurcation of the Left Main Coronary Anatomy

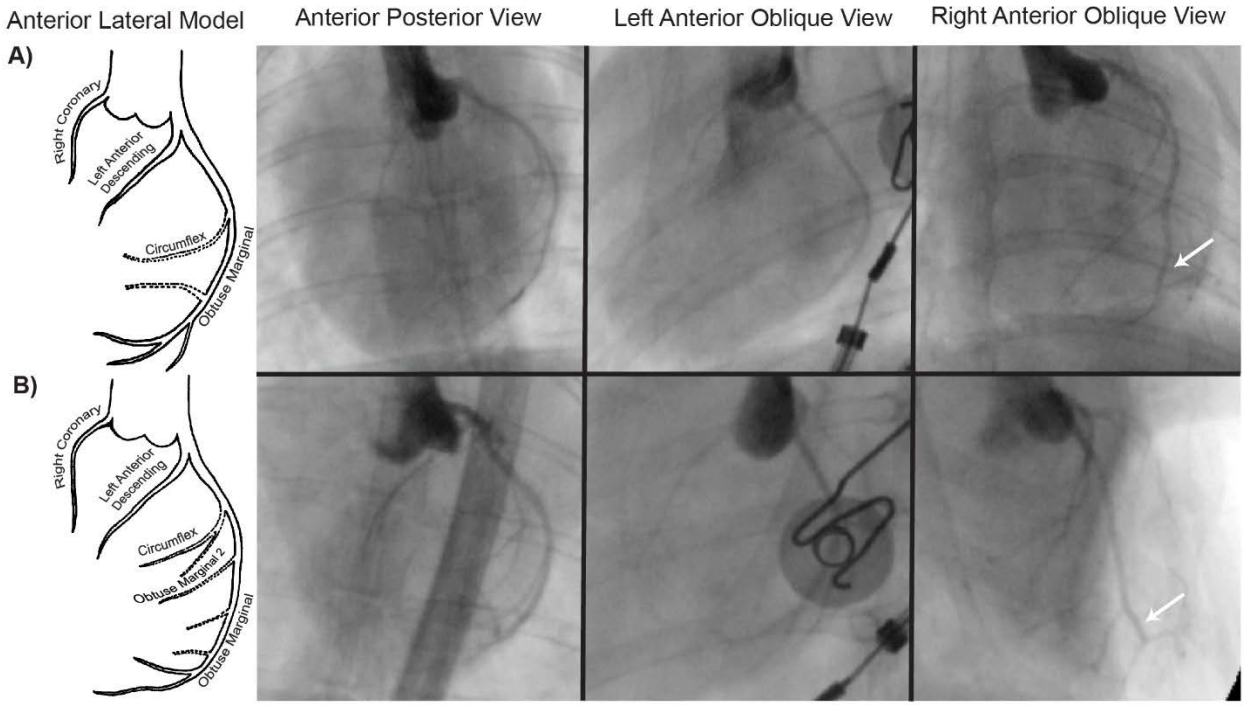

A) Young rabbit displaying proximal origin of OM1 with a minor circumflex artery. The major bifurcation of the OM1 is proximal. The LAD is minor. **B)** Aged rabbit displaying proximal origin of the OM1 from the circumflex. The circumflex is well-developed with significant branching. The OM1 shows proximal branching with a more substantial anterior branch. The posterolateral and posterior perfusion has many collaterals. White arrow denotes coil target location. *PJM performed the angiography, KRM assisted in the design of this experiment.*

Figure 2.2: Trifurcation of the Left Main Coronary Anatomy

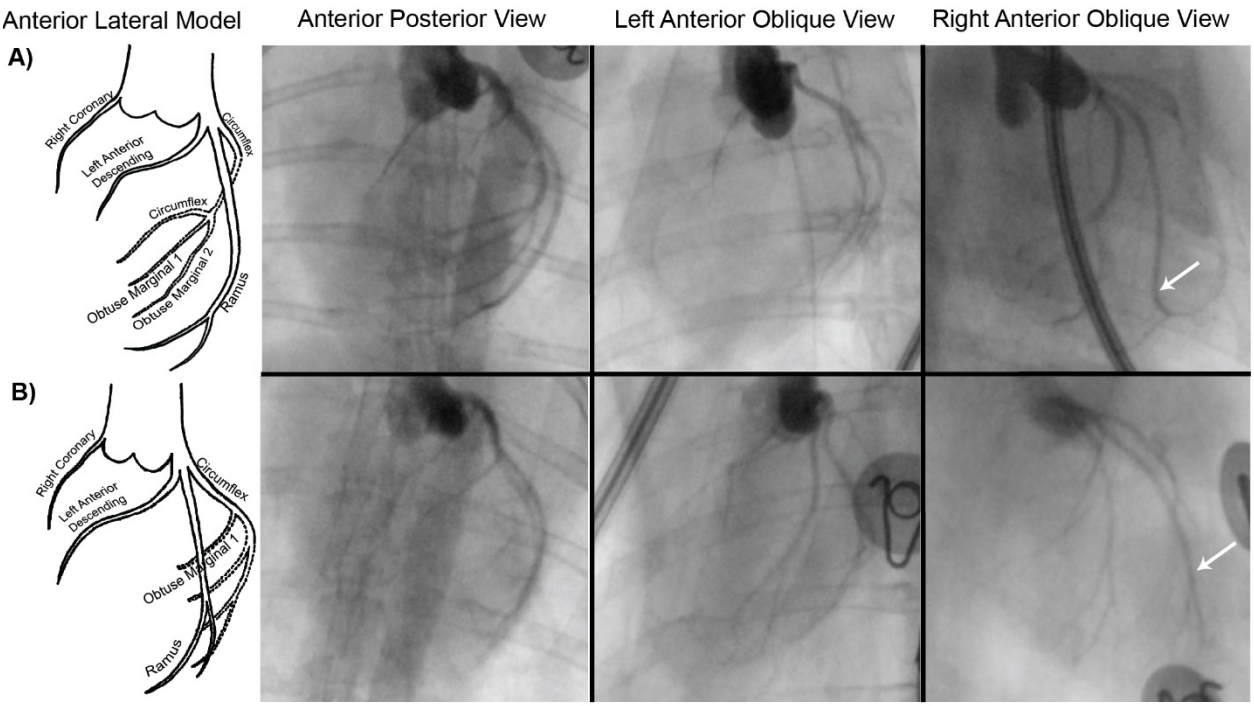

A) Young rabbit heart with distal branching of the ramus and well-developed circumflex system. The OM1 is relatively minor. The LAD is minor. **B)** Aged rabbit heart with ramus showing distal branching. The circumflex artery is well developed with a significant OM1. The LAD is minor and the first septal is pronounced. White arrow denotes coil target location. *PJM performed the angiography, KRM assisted in the design of this experiment.*

Figure 2.3: Quadrifurcation of the Left Main Coronary Artery: Aged Rabbit

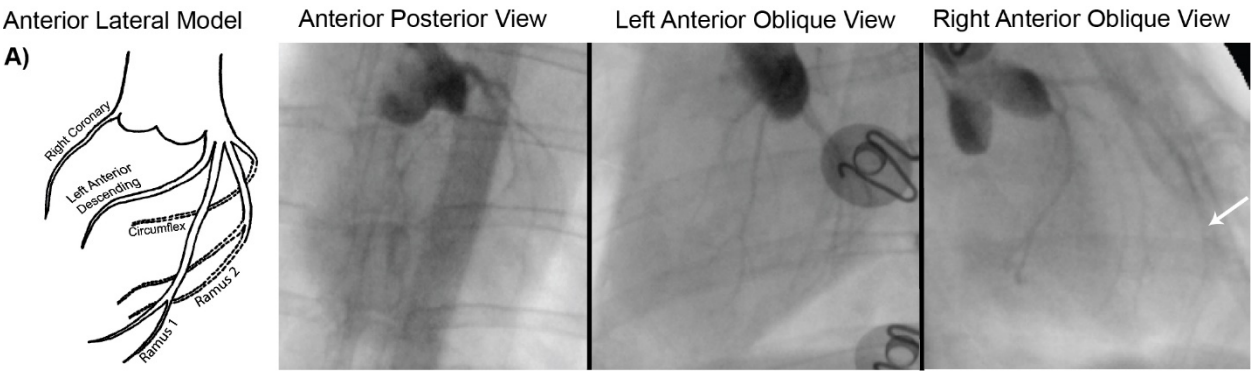

A) Aged quadrifurcated rabbit exhibits a substantial ramus 1 with distal branching and a smaller ramus 2 with proximal branching. The LAD is minor, and the circumflex exhibits distal branching. The LAD is not visible from the RAO view. White arrow denotes coil target location. *PJM performed the angiography, KRM assisted in the design of this experiment.*

Figure 2.4: Instance of Right Coronary Dominance in Aged Rabbit

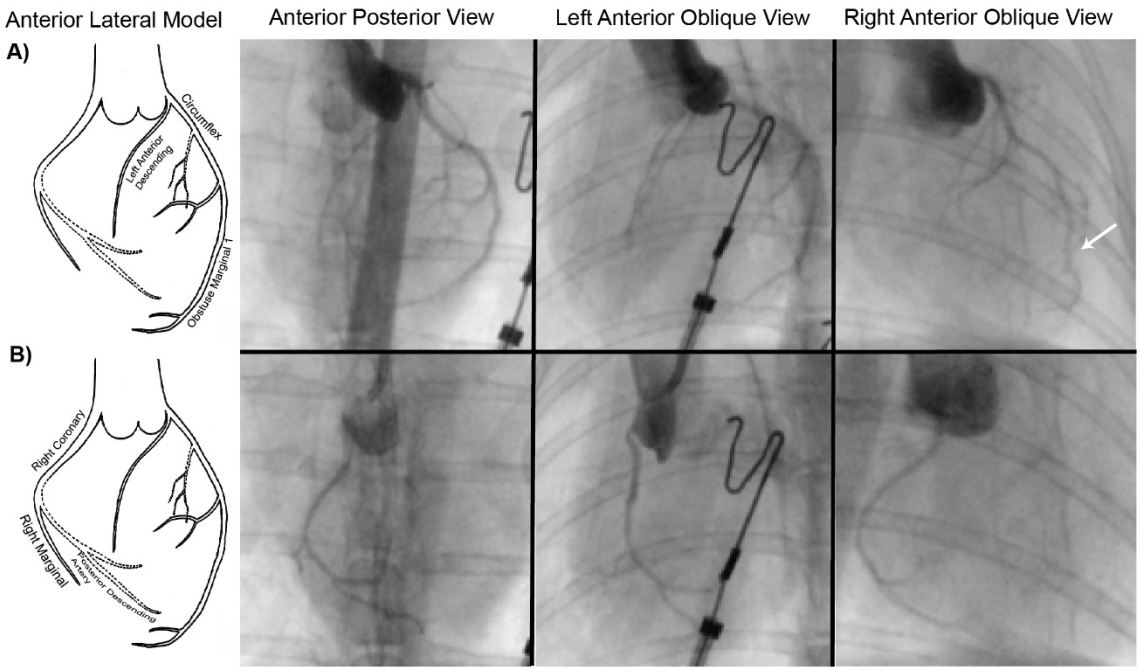

A) The left coronary system of an aged right dominant rabbit. The circumflex is minor and the OM1 is by far the major artery on the left side. The LAD is paralleled by a proximal branch **B)** The right coronary system provides the posterior perfusion with a clearly defined posterior descending artery and a substantial right marginal. *PJM performed the angiography, KRM assisted in the design of this experiment.*

Figure 2.5: Location Specific Coil Embolization Yields Anatomy-Independent Scars

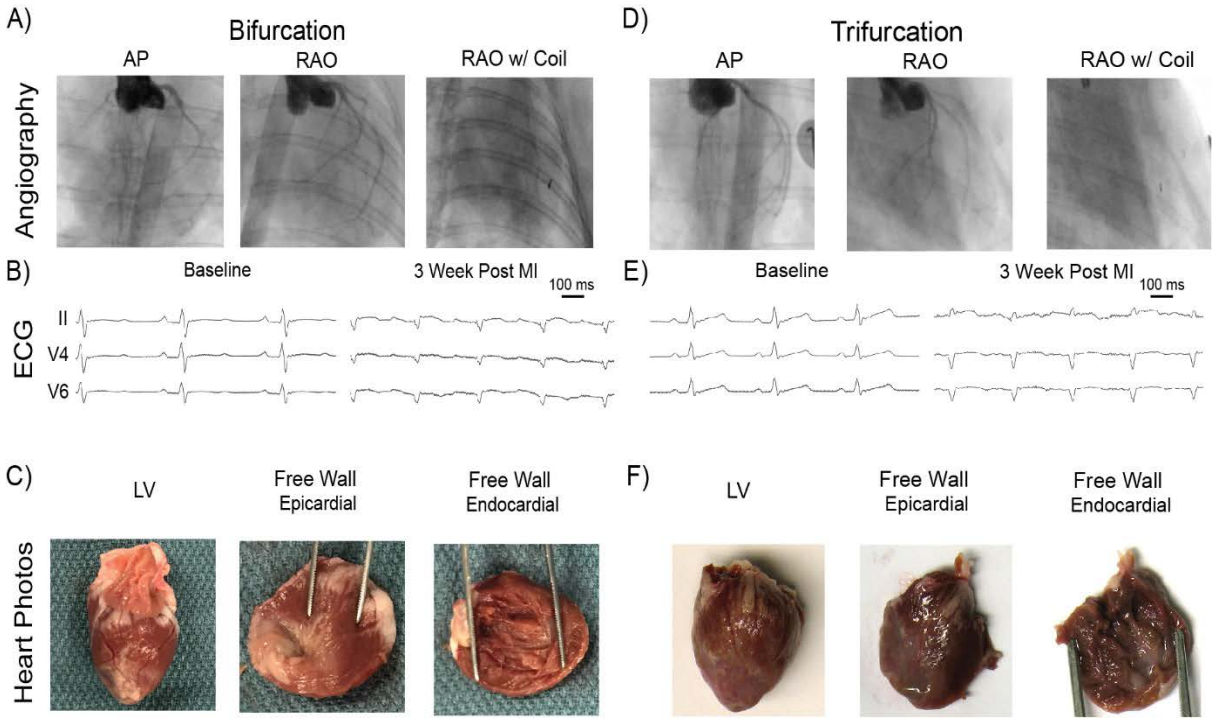

A) Aged bifurcated rabbit with a very high take off of OM1 and distal branching of OM1. We occluded the first obtuse marginal above the branch point. **B)** The baseline ECG was normal. At three weeks, the ECG shows, pathological Q waves and ST inversion. **C)** The epicardial surface of the excised heart shows an infarct of 30% of the left ventricle and these findings are confirmed by the endocardial view. **D)** Aged trifurcated rabbit heart with a significant circumflex system and distal branching of the ramus artery. The OM1 is quite large, perfusing the posterior aspect of the heart. This rabbit also had relative diminutive first septal artery and a large LAD. We occluded the ramus above the distal branch point. **E)** The baseline ECG was normal. At three weeks, the ECG shows QRS widening, pathological Q waves and ST inversion. **F)** The epicardial surface of the excised heart shows an infarct of 30% of the left ventricle and these findings are confirmed by the endocardial view. *KRM assisted in acquiring the angiograms and ECGs, harvesting the*

tissue, and collecting gross histology photos. PJM performed the surgeries and procedures.

Figure 2.6: Target Location of the Coil

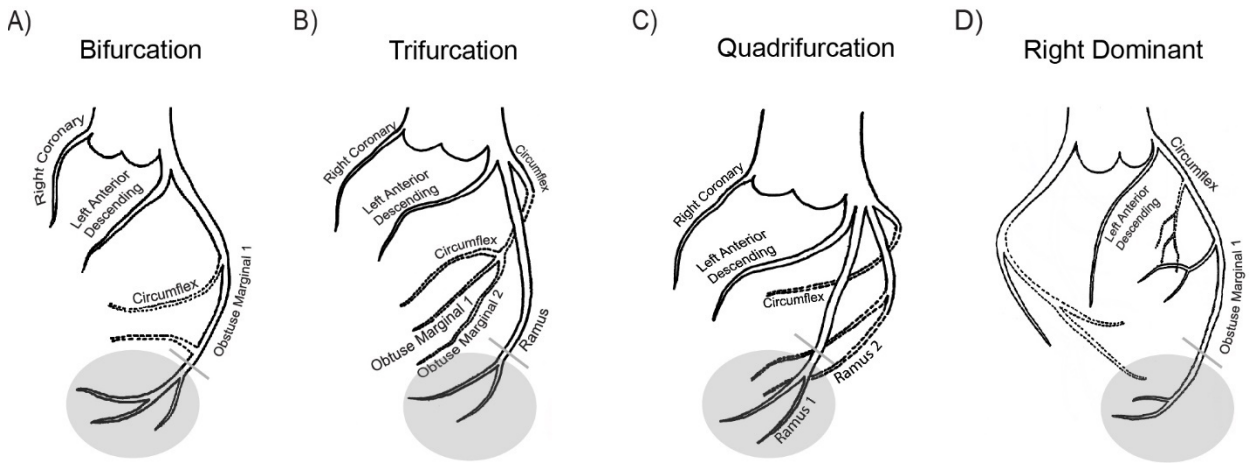

This figure demonstrates the target location for each type of anatomy we encounter in the rabbit. **(A)** Bifurcation. The coil should be placed down the OM1 distal to the proximal branch point. **(B)** Trifurcation. The coil should be placed down the ramus, proximal to the distal branch point. **(C)** Quadrifurcation. The coil should be placed down the Ramus 1, proximal to the branch point. **(D)** Right dominant. The coil should be placed down the OM1, similar to the bifurcation case. The grey bar in each diagram notates the coil location and the grey shading denotes of region of myocardium to be infarcted.

Figure 2.7: Comparison of Scar Size Across Age Groups

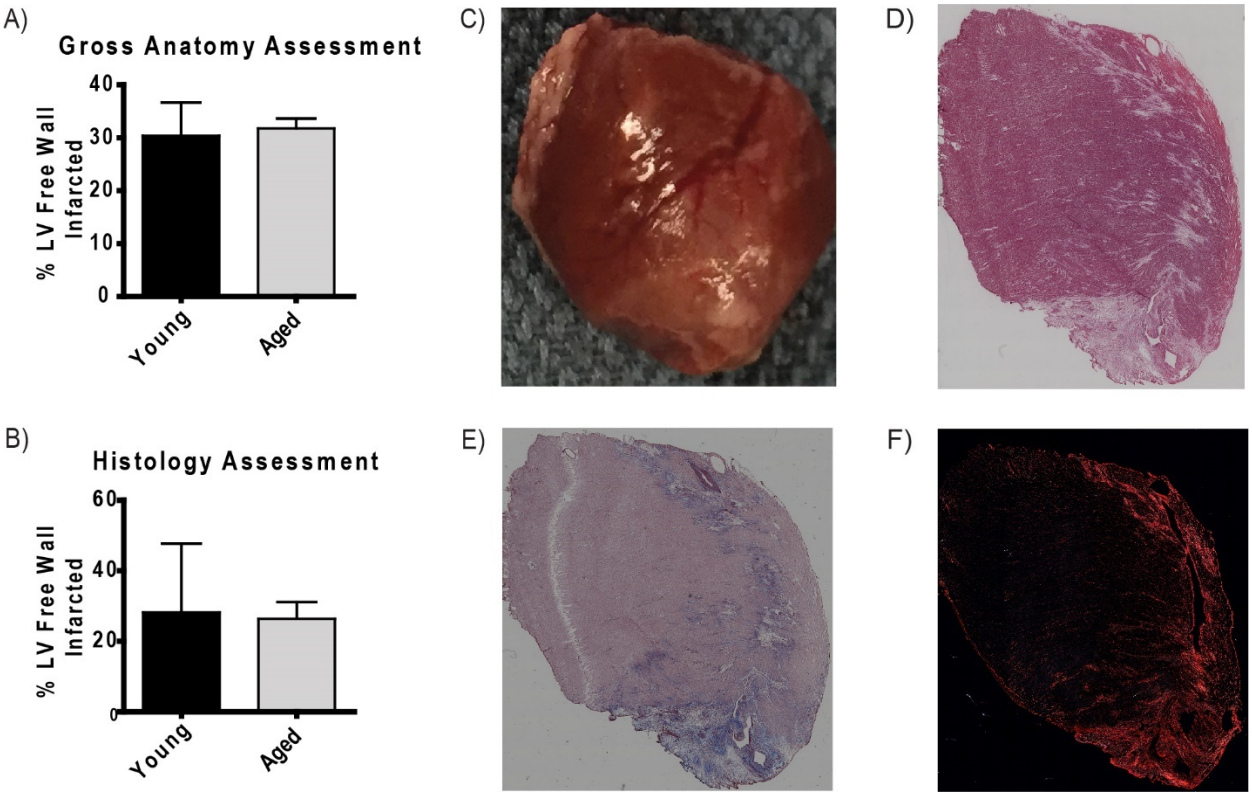

Minimally invasive procedure produces infarcts of the same size. A) Infarct size assessed by epicardial and endocardial area measurements of the scar and total LV free wall in eight young and nine aged infarcted hearts (n.s., p=0.63). B) Infarct size assessed by Masson's trichrome fibrosis staining in histology sections in five young and eight aged infarcted hearts (n.s., p=0.84). C) Gross anatomy of LV free wall confirms presence of apical infarct. D) Hematoxylin and Eosin staining (H&E) were performed to visualize myocytes in red/pink and fibrosis in white. E) Fibrosis in both infarct border zone and scar zone were assessed using Mason's trichrome staining where red/purple color indicates myocytes, and blue indicates fibrosis F) Sirius red collagen stain. All

histology was performed on 10 µM serial frozen sections. Error bars shown represent Mean ± SD.

Table 2.1: Left Coronary Anatomy

	Branching of Coil Artery	Young	Aged*	Total	Total
Bifurcation	Distal	23	23	46	64
	Proximal	7	11	18	
Trifurcation	Distal	6	16	22	34
	Proximal	1	11	12	
Quadrifurcation	Distal	0	3	3	3
Total		37	64	101	101

*two-tailed, 2x3 fisher's exact contingency table

Overview of left coronary anatomy patterns in young and aged rabbit hearts. Since arterial branching affects coil placement, we focus on the branching of the artery perfusing the anterior, apical left ventricle or what we refer to as the "coil artery". One hundred and one rabbits were studied and characterized by coronary angiography. Aged rabbit hearts display a higher degree of left main coronary branching, as assessed by 2x3 fisher's exact test ($p<0.05$).

Table 2.2: Coil Placement Rubric

Anatomy	Major Branching	Coil Location
Bifurcation	*Distal*	*Proximal to Branching*
	Proximal	*Anterior Branch*
Trifurcation	*Distal*	*Proximal to Branching*
	Proximal	*Anterior Branch*
Quadrifurcation		*Proximal Ramus 1*

A coil placement rubric to standardize infarct size and location across all coronary branching patterns. With distal branching of the OM1 or Ramus, a coil is placed proximal to the branch point. In the instance of proximal branching of the OM1 or Ramus, a coil is directed into the anterior branch. To account for quadrifurcation, a coil is placed in the proximal Ramus 1, ideally at the middle ventricle.

2.8 References

1. Deo R, Albert CM: **Epidemiology and genetics of sudden cardiac death**. *Circulation* 2012, **125**(4):620-637.
2. Zheng ZJ, Croft JB, Giles WH, Mensah GA: **Sudden cardiac death in the United States, 1989 to 1998**. *Circulation* 2001, **104**(18):2158-2163.
3. Adabag AS, Luepker RV, Roger VL, Gersh BJ: **Sudden cardiac death: epidemiology and risk factors**. *Nature reviews Cardiology* 2010, **7**(4):216-225.
4. Zipes DP, Wellens HJ: **Sudden cardiac death**. *Circulation* 1998, **98**(21):2334-2351.
5. Varro A, Lathrop DA, Hester SB, Nanasi PP, Papp JG: **Ionic currents and action potentials in rabbit, rat, and guinea pig ventricular myocytes**. *Basic Res Cardiol* 1993, **88**(2):93-102.
6. Salata JJ, Jurkiewicz NK, Jow B, Folander K, Guinosso PJ, Jr., Raynor B, Swanson R, Fermini B: **IK of rabbit ventricle is composed of two currents: evidence for IKs**. *The American journal of physiology* 1996, **271**(6 Pt 2):H2477-2489.
7. Mitsos S, Katsanos K, Dougeni E, Koletsis EN, Dougenis D: **A critical appraisal of open- and closed-chest models of experimental myocardial ischemia**. *Lab Anim (NY)* 2009, **38**(5):167-177.
8. Walker NL, Burton FL, Kettlewell S, Smith GL, Cobbe SM: **Mapping of epicardial activation in a rabbit model of chronic myocardial infarction**. *J Cardiovasc Electrophysiol* 2007, **18**(8):862-868.

9. Fujita M, Morimoto Y, Ishihara M, Shimizu M, Takase B, Maehara T, Kikuchi M: **A new rabbit model of myocardial infarction without endotracheal intubation**. *J Surg Res* 2004, **116**(1):124-128.

10. Mahaffey KW, Raya TE, Pennock GD, Morkin E, Goldman S: **Left ventricular performance and remodeling in rabbits after myocardial infarction. Effects of a thyroid hormone analogue**. *Circulation* 1995, **91**(3):794-801.

11. Taylor DA, Atkins BZ, Hungspreugs P, Jones TR, Reedy MC, Hutcheson KA, Glower DD, Kraus WE: **Regenerating functional myocardium: improved performance after skeletal myoblast transplantation**. *Nat Med* 1998, **4**(8):929-933.

12. Podesser B, Wollenek G, Seitelberger R, Siegel H, Wolner E, Firbas W, Tschabitscher M: **Epicardial branches of the coronary arteries and their distribution in the rabbit heart: the rabbit heart as a model of regional ischemia**. *Anat Rec* 1997, **247**(4):521-527.

13. Hu N, Straub CM, Garzarelli AA, Sabey KH, Yockman JW, Bull DA: **Ligation of the left circumflex coronary artery with subsequent MRI and histopathology in rabbits**. *J Am Assoc Lab Anim Sci* 2010, **49**(6):838-844.

14. Edwards R, Yousef Z, Rakhit R, Wright M, Rosenthal E, Redwood S, Marber M: **A model of closed chest regional myocardial infarction in the rabbit: a clinically relevant in vivo assay system of post-infarction remodelling**. *Basic Res Cardiol* 2002, **97**(5):374-383.

15. Ziv O, Schofield L, Lau E, Chaves L, Patel D, Jeng P, Peng X, Choi BR, Koren G: **A novel, minimally invasive, segmental myocardial infarction with a clear**

healed infarct borderzone in rabbits. *Am J Physiol Heart Circ Physiol* 2012, **302**(11):H2321-2330.

16. Marber MS, Latchman DS, Walker JM, Yellon DM: **Cardiac stress protein elevation 24 hours after brief ischemia or heat stress is associated with resistance to myocardial infarction**. *Circulation* 1993, **88**(3):1264-1272.

17. Saba S, Mathier MA, Mehdi H, Gursoy E, Liu T, Choi BR, Salama G, London B: **Prevention of adverse electrical and mechanical remodeling with biventricular pacing in a rabbit model of myocardial infarction**. *Heart Rhythm* 2008, **5**(1):124-130.

18. McLachlan CS, McGuire MA: **Characterization and incidence of inducible monomorphic ventricular tachycardia in a postinfarction rabbit model**. *J Electrocardiol* 2007, **40**(1):89-93.

19. Isorni MA, Casanova A, Piquet J, Bellamy V, Pignon C, Puymirat E, Menasche P: **Comparative Analysis of Methods to Induce Myocardial Infarction in a Closed-Chest Rabbit Model**. *Biomed Res Int* 2015, **2015**:893051.

20. Day SB, Johnson JA: **The distribution of the coronary arteries of the rabbit**. *Anat Rec* 1958, **132**(4):633-643.

21. von Holst D, Hutzelmeyer H, Kaetzke P, Khaschei M, Rödel HG, Schrutka H: **Social rank, fecundity and lifetime reproductive success in wild European rabbits (Oryctolagus cuniculus)**. *Behavioral Ecology and Sociobiology* 2002, **51**(3):245-254.

22. Kennedy DJ, Vetteth S, Periyasamy SM, Kanj M, Fedorova L, Khouri S, Kahaleh MB, Xie Z, Malhotra D, Kolodkin NI *et al*: **Central role for the cardiotonic steroid**

marinobufagenin in the pathogenesis of experimental uremic cardiomyopathy. *Hypertension* 2006, **47**(3):488-495.

23. Burton RA, Schneider JE, Bishop MJ, Hales PW, Bollensdorff C, Robson MD, Wong KC, Morris J, Quinn TA, Kohl P: **Microscopic magnetic resonance imaging reveals high prevalence of third coronary artery in human and rabbit heart**. *Europace* 2012, **14 Suppl 5**:v73-v81.

24. Agelaki MG, Pantos C, Korantzopoulos P, Tsalikakis DG, Baltogiannis GG, Fotopoulos A, Kolettis TM: **Comparative antiarrhythmic efficacy of amiodarone and dronedarone during acute myocardial infarction in rats**. *Eur J Pharmacol* 2007, **564**(1-3):150-157.

25. Li T, Wei X, Watkins AC, Sanchez PG, Wu ZJ, Griffith BP: **Prophylactic amiodarone and lidocaine improve survival in an ovine model of large size myocardial infarction**. *J Surg Res* 2013, **185**(1):152-158.

26. Zagorianou A, Marougkas M, Drakos SG, Diakos N, Konstantopoulos P, Perrea DN, Anastasiou-Nana M, Malliaras K: **The effect of long-term amiodarone administration on myocardial fibrosis and evolution of left ventricular remodeling in a porcine model of ischemic cardiomyopathy**. *Springerplus* 2016, **5**(1):1568.

27. Lindsey ML, Gannon J, Aikawa M, Schoen FJ, Rabkin E, Lopresti-Morrow L, Crawford J, Black S, Libby P, Mitchell PG *et al*: **Selective matrix metalloproteinase inhibition reduces left ventricular remodeling but does not inhibit angiogenesis after myocardial infarction**. *Circulation* 2002, **105**(6):753-758.

28. Shibutani, DHTOTETACKHYKHS, Okumura TIaK: **Amiodarone Attenuates the Upregulated Matrix Metalloproteinase-2 Activity in a Rat Myocardial Infarction Model**. *Hirosaki Medical Journal* 2009, **60**(1/2/3/4):45-53.

29. Karth GD, Buberl A, Nikfardjam M, Meyer B, Wollenek G, Grimm M, Lassnigg A, Brannath W, Hiesmayr M, Heinz G: **Role of amiodarone on the systemic inflammatory response induced by cardiac surgery: proinflammatory actions**. *Can J Anaesth* 2007, **54**(4):262-268.

30. Lee BH, Kim WH, Choi MJ, Rho JR, Kim WG: **Chronic heart failure model in rabbits based on the concept of the bifurcation/trifurcation coronary artery branching pattern**. *Artif Organs* 2002, **26**(4):360-365.

Chapter 3: Diminished Autophagy Contributes to Aberrant Ca2+ Homeostasis and Arrhythmogenesis in Aging Rabbit Hearts

This content of this chapter was submitted to *Aging Cell* and is currently under review.

The author contributed to this manuscript by preparing cells for transmission electron microscopy (TEM), collaborating with the Lifespan Biostatistics core to analyze TEM images, performing all ROS, TMRM, and calcium imaging confocal experiments, in addition to autophagy flux assays, and western blotting experiments.

Kevin R. Murphy[1,2], Leroy L. Cooper[1,3], Yi Chun Lu[1], Jin O'Uchi[1], John M. Sedivy[2], Dmitry Terentyev[1], Gideon Koren[1]

[1]Cardiovascular Research Center, Division of Cardiology, Cardiovascular Institute, Warren Alpert Medical School of Brown University, Providence RI, USA
[2]Department of Molecular Biology, Cellular Biology, and Biochemistry, Brown University, Providence RI, USA
[3]Department of Biology, Vassar College, Poughkeepsie, NY, USA

Corresponding Author:
Gideon Koren, MD (gideon_koren@brown.edu)
1 Hoppin Street
Coro West, 5th Floor, CVRC
Providence RI, 02903

Keywords: ryanodine receptor, aging, sarcoplasmic reticulum, mitochondria, reactive oxygen species, and redox modification

3.1 Summary

Human aging is associated with a 10-20-fold increase in the incidence of sudden cardiac death from malignant tachyarrhythmia. We previously reported that thiol oxidation of sarcoplasmic reticulum Ca^{2+} release channel ryanodine receptors (RyR2s) by mitochondria-derived reactive oxygen species (mito-ROS) contributes to defective Ca^{2+} homeostasis in cardiomyocytes from aging rabbit hearts. However, mechanisms responsible for the increase in mito-ROS in the aging heart remain poorly understood. Here we test the hypothesis that age-associated decrease in autophagy is a major contributor to enhanced mito-ROS production and thereby pro-arrhythmic disturbances in Ca^{2+} homeostasis. Ventricular tissues from aged rabbits displayed significant downregulation of proteins involved in mitochondrial autophagy compared with young controls. Blocking autophagy with chloroquine (1 μM, 3 hrs) increased mito-ROS production by 20% and elicited depolarization of mitochondrial membrane potential ($\Delta\psi m$) to 50% of control levels in HL-1 cardiomyocytes. Blocking autophagy significantly increased the oxidation levels of RyR2, which resulted in enhanced propensity to pro-arrhythmic spontaneous Ca^{2+} release under β-adrenergic stimulation. The aberrant Ca^{2+} release was abolished by treatment with the mito-ROS scavenger MitoTEMPO (25 μM). Importantly, the autophagy enhancer Torin1 (250 nM, 4 hrs incubation) and ATG7 overexpression reduced the rate of mito-ROS production and restored both $\Delta\psi m$ and defective Ca^{2+} handling in primary rabbit myocytes from aging hearts. We conclude that decreased autophagy is a major cause of increased mito-ROS production in the aging heart. Our data suggest that promoting autophagy may reduce pathologic mito-ROS

during normal aging and reduce pro-arrhythmic spontaneous Ca^{2+} release via oxidized RyR2s.

3.2 Introduction

Sudden cardiac death due to malignant ventricular tachyarrhythmias remains a major cause of mortality in the United States, with ~300,000 cases reported each year [1]. Risk of sudden cardiac death increases 5-40–fold in people aged over 65 years compared to younger individuals [2, 3]. We have used a rabbit model to study the mechanisms of arrhythmogenesis in the aging heart. The rabbit heart closely resembles the human heart in its electrical and contractile properties [4]. Our studies of the aged rabbit heart demonstrated conduction abnormalities, myocardial stiffening, and increased interstitial fibrosis [4]. Moreover, aged rabbit cardiomyocytes have depolarized membrane potentials, increased mitochondria-derived reactive oxygen species (mito-ROS), Ca^{2+} leak from the oxidation of the calcium handling RyR2 receptor by mito-ROS, and increased formation of spontaneous calcium waves (SCWs) [5]. Mitochondria participate in a variety of intracellular tasks such as energy production, nutrient sensing, calcium (Ca^{2+}) buffering, and more [6]. Excessive production of ROS by defective mitochondria can lead to aberrant intracellular Ca^{2+} homeostasis by oxidizing the sarcoplasmic reticulum (SR) Ca^{2+} release channel ryanodine receptor (RyR2) and predisposes the aging heart to lethal ventricular tachyarrhythmias [5, 7, 8]. However, mechanisms underlying impaired mito-ROS generation and concomitant pro-arrhythmic changes in Ca^{2+} cycling, characteristic of aging, are not well understood.

Intracellular Ca^{2+} release from the SR mediated by RyR2 is a critical determinant of cardiac contractility. Abnormally high RyR2 activity has been implicated in arrhythmogenesis and is present in a variety of diseases such as heart failure and myocardial infarction [9-12]. We recently reported that in aging rabbit hearts abnormally high RyR2 activity leads to spontaneous Ca^{2+} release, i.e., Ca^{2+} waves (SCWs) that can translate into arrhythmogenic disturbances in plasmalemmal membrane potential such as early and delayed afterdepolarizations (EADs and DADs respectively) [5]. We demonstrated that hyperactivity of RyR2 in old hearts is caused by oxidation of reactive cysteines on the channels by excessive ROS emitted by mitochondria and that treatment of aged myocytes with mitochondria-specific scavenger MitoTEMPO effectively restores intracellular Ca^{2+} cycling. However, the mechanisms responsible for increased ROS production by mitochondria in aging myocytes are yet to be determined.

The mitochondrial population is a vast network controlled by cycles of fission and fusion and is regulated by mitophagy, or autophagy at the organelle level specific to mitochondria. Mitochondrial fission is a culling mechanism for damaged mitochondria, while fusion recombines fragmented, healthy mitochondria into larger, bio-energetically favorable structures. Damaged smaller mitochondria resulting from fission are cleared from the mitochondrial network by mitophagy, which is a self-degradative catabolic process [13, 14]. Mitophagy involves upregulation of general autophagy machinery components followed by the recognition of damaged mitochondria as a target for clearance. Autophagy sequesters unnecessary or dysfunctional cellular components, including proteins, organelles, or even bacteria in a double-membrane structure called an autophagosome that is then degraded by lysosomal acidic hydrolases [14, 15]. Without

efficient autophagy (and its mitochondria-specific form, mitophagy), damaged mitochondria would remain in the cell and generate harmful ROS [16-18]. Because both autophagy and the mitochondrial specific mitophagy are impaired in the aged heart [19-21], we hypothesized that decreased autophagy may predispose the aging heart to arrhythmogenesis.

Here we show that blocking autophagy with chloroquine, which blocks lysosomal acidification and prevents autophagosome fusion and therefore subsequent degradation [22], promoted generation of SCWs at the cellular scale because of RyR2 oxidation. By contrast, enhancing autophagy in cultured primary aged myocytes using torin1, a potent inhibitor of the negative autophagy regulator mTOR [23], reduced the instance of spontaneous Ca^{2+} release. In addition to pharmacologic experiments, we overexpressed ATG7 to enhance autophagy, as ATG7 is an essential component of the autophagosome, and is sufficient to increase autophagy flux [24, 25]. The results showed a significant reduction of age-related instance of spontaneous Ca^{2+} release. We conclude that defective autophagy contributes to the age-associated increase of mito-ROS production and pro-arrhythmic Ca^{2+} mishandling.

3.3 Results

Autophagy is Downregulated in the Aging Rabbit Heart

First, we examined the ultrastructure of CMs isolated from young and aged left ventricular free wall [26] using transmission electron microscopy. Analysis of primary CMs from young and aged hearts revealed that the arrangement of mitochondria in aged CMs is both disorganized and fragmented (Fig. 1A), with cumulative size distribution (Fig. 1B) in which aged mitochondria are skewed smaller. Furthermore, mitochondria from aged

CMs have more variance in mitochondrial cross-sectional area than young CMs (0.6 μm vs 0.9 μm) ($p<0.05$) (Fig. 1C). These results indicate that mitochondria from aged CMs vary in size to a greater degree than mitochondria from young CMs, which are more homogenous; this is reflected in the slopes of the distribution lines of young and aged mitochondria in Fig. 1B. We then performed western blot analysis against proteins important in mitochondrial regulation of fission (DRP1) and fusion (MFN2) to better understand why mitochondria in aged CMs are more heterogeneous. Immunoblots with homogenates prepared from left ventricular free walls revealed 2.25-fold greater DRP1 expression in aged hearts relative to young samples ($p<0.05$, Fig 1D), but no change in expression of MFN2. We then performed western blot analysis of homogenates prepared from young and aged hearts against markers of autophagy and mitophagy to understand why defective mitochondria remain in aged CM. Classical autophagy machinery components [27, 28] such as the autophagosome scaffolding protein p62, is increased 1.5-fold in aged samples ($p<0.05$). Light-chain 3 cleavage ratio (II/I) is 1.7-fold higher in aged compared to young samples ($p<0.01$) and is consistent with decreased autophagy. PINK1, the ubiquitin-mediated mitophagy kinase, is decreased by 20% in aged relative to young samples ($p<0.05$). Lastly, the transcriptional autophagy effector p53, is 2.5-fold more abundant in aged compared to young samples ($p<0.05$) (Fig. 1E). Overall, we observed that mitochondria in aged CMs are more heterogeneous, undergo increased mitochondrial fission, and display protein profiles consistent with decreased autophagy.

Autophagy Inhibition Decreases Δψm, Increases Mito-ROS, and Promotes Spontaneous Ca^{2+} Release in HL-1 CMs

We treated cells from the previously established HL-1 atrial cardiomyocyte cell line [29] with 1 μM chloroquine or vehicle control for 3 hours. At baseline HL-1 cardiomyocytes (CMs) produced low levels of mito-ROS. Compared with control cells, chloroquine-treated cells exhibited decreased autophagy flux (shown as high-ratio positive puncta in Fig. 2A) using adenovirus containing TF-LC3-GFP. The ratio of red channel (autolysosomes) to green channel (autophagosomes) decreased 44% after addition of chloroquine, indicating that autophagy is decreased after treatment. Western blot analysis reveal that these cells expressed 1.75-fold more p62 compared to control cells ($p<0.05$) (Fig. 2B). Direct measurement of mitochondrial ROS using the specific fluorescent superoxide indicator MitoSOX showed a 43% increase in mito-ROS (100 ± 20% vs. 143 ± 50%) ($p<0.05$) after chloroquine treatment (fluorescence signal is plotted as a heatmap in Fig 3A). In addition, general ROS was measured using the fluorescent indicator CM-H2DCFDA (Fig. 2C). Chloroquine treatment increased ROS generation compared to control (0.23 ± 0.06 $F*s^{-1}$ vs 0.13 ± 0.09 $F*s^{-1}$) ($p<0.05$), and ROS generation was rescued by the application of the mitochondrial ROS scavenger MitoTEMPO (0.16 ± 0.07 $F*s^{-1}$) ($p<0.05$) [30] (Fig. 2D). Live cell measurements of Δψm using the fluorescence indicator TMRM showed chloroquine-mediated decrease of Δψm compared to vehicle control (2.1 ± 0.4 vs. 1.58 ± 0.6 $\Delta F*F_0^{-1}$) ($p<0.05$) (Fig. 2E). These data indicate that autophagy blockade in HL-1 CMs decreased the Δψm and increased mito-ROS.

To test the functional effects of decreased autophagy on pro-arrhythmic Ca^{2+} handling, we performed live-cell Ca^{2+} imaging of HL-1 CMs with 1 Hz field-stimulation (Fig. 3A). Quantification of Ca^{2+} handling parameters revealed that the number of cells exhibiting pro-arrhythmic global SCWs was markedly increased after autophagy block. Fifty-eight percent of control cells exhibited SCWs compared to 95% of chloroquine-treated cells ($p<0.05$) (Fig. 3B). Further, the latency at which SCWs formed was drastically decreased in chloroquine treatment compared to control (1.9 ± 1.1 sec vs. 8.8 ± 5.8 sec) ($p<0.05$). Because multiple physiological changes may be elicited by autophagy block with chloroquine, we applied the superoxide scavenger MitoTEMPO (25 μM, 10 min) [31] to HL-1 CMs treated with chloroquine. There was no change in the proportion of cells exhibiting SCWs after acute application of MitoTEMPO; however, scavenging mito-ROS significantly improved the latency to SCW compared to chloroquine (5.6 ± 3.2 sec vs. 1.9 ± 1.1 sec) ($p<0.05$).

Given the increase in SCW formation in HL-1 CMs after autophagy block, we assessed the levels of oxidation of the RyR2. Protein lysates conjugated with C2-Maleimide (Fig. 3C), a free thiol fluorescence indicator [32], were resolved in non-reducing conditions using PAGE. After C2-Maleimide fluorescence signal was imaged, immunoblots were performed on the same gel to obtain RyR2 signal. RyR2 signal was used to normalize the C2-maleimide signal against total RyR2. Densitometry showed a two-fold reduction in maleimide signal indicating that blocking autophagy increases thiol oxidation on the RyR2 ($p<0.05$).

Increasing Autophagy in Aged Rabbit CMs Restores Δψm, Decreases ROS, and Reduces SCWs

We next treated aged CMs with Torin1 (250 nM, 4hrs), an mTOR inhibitor 1,000x more selective than rapamycin [23], to enhance autophagy. TF-LC3-GFP analysis reveals a 3.8-fold increase in autophagy flux after Torin1 treatment compared to control (Fig. 4A). Aged rabbit CMs treated with Torin1 (Fig. 4) revealed 34% reduction in baseline ROS compared to vehicle control as assessed by using the general ROS indicator CM-H2DCFDA (100 ± 37.6% vs. 65.9 ± 24.8%) ($p<0.01$) and a lower production rate (2.71 ± 0.19 vs. 1.85 ± 0.14 $F*s^{-1}$) ($p<0.01$) (Fig. 4B). Enhancing autophagy restored Δψm in Torin1-treated CMs compared to vehicle control (1.85 ± 0.57 vs. 1.45 ± 0.46 $\Delta F*F_0$) ($p<0.05$) (Fig. 4C). To functionally validate the improvement of ROS and Δψm, live cell Ca^{2+} imaging was performed. Representative line scan images are shown in Fig. 4D after 1 Hz field stimulation. Strikingly, after enhancing autophagy, there was a 48% reduction in the number of cells that display pro-arrhythmic SCWs compared to vehicle control ($p<0.05$, Fishers Exact test).

Finally, to interrogate the specificity of the pharmacologic experiments, we overexpressed ATG7, in aged rabbit CMs. The results showed that autophagy flux was enhanced 3.6-fold in ATG7 overexpressing aged CMs compared to controls (Fig. 5A). These cells have less baseline ROS (100% vs. 73%) and a lower production rate (4.31 ± 0.30 vs 3.56 ± 0.27 $\Delta F*s^{-1}$) ($p<0.05$) (Fig. 5B). ATG7 overexpression showed a trend to restoring Δψm as compared to control (1.53 ± 0.11 vs. 1.33 ± 0.12 $\Delta F*F_0$) ($p=0.10$) (Fig. 5C). Next, we functionally validated the intervention using live cell Ca^{2+} imaging.

Representative line scan images are shown after 1Hz field stimulation (Fig. 5D). Similar to Torin1 autophagy enhancement, there was a two-fold reduction in the number of cells that display pro-arrhythmic SCWs compared to control with ATG7 overexpression ($p<0.05$, Fishers Exact test). *In toto,* these data implicate autophagy as an age-related molecular mechanism that underlies the pro-arrhythmic changes in mammalian CMs that lead to changes in calcium cycling (Fig. 6).

3.4 Discussion

Here we show that decreased autophagy during normal aging is a mechanism underlying pro-arrhythmic changes of Ca^{2+} homeostasis in the aging heart (Fig. 6). We demonstrated that:: 1) aging hearts contain a heterogeneous mitochondrial population (assessed by transmission electron microscopy) along with markers suggesting decreased levels of autophagy and mitophagy; 2) decreased autophagy in HL-1 cells contributes to Δψm depolarization and excessive generation of mito-ROS capable of oxidizing the SR Ca^{2+} release channel RyR2, leading to increased propensity for pro-arrhythmic SCWs; 3) enhancing autophagy in aged CMs restored Δψm, decreased mito-ROS, and blocked the formation of SCWs. Our data implicate autophagy as a mechanism that may underlie age-related increase in mito-ROS production and thereby Ca^{2+}-mediated cardiac arrhythmia.

Autophagy in Aging

Autophagy is generally accepted to decrease with age in many organs, especially the aging heart, as we report here [19, 24, 28, 33]. Since it is a critical regulator of cellular homeostasis, targeting autophagy may be a useful strategy in treating age-related

disease. As a cellular regulator, autophagy is responsible for the removal of damaged organelles; with defective autophagy, the cell fails to clear damaged mitochondria that are smaller and produce high levels of ROS. Our data suggest that during aging, mitochondrial size variance increases along with levels of the fission factor DRP1, but there is no change in production of the fusion factor MFN2. Concurrently, autophagy components involved in the maturation of the autophagosome are downregulated with age (Fig. 1), which is consistent with previously published work [21, 24]. Despite signals from mitochondria such as decreased Δψm or mito-ROS (Fig. 2), CMs are unable to mount the proper autophagy response to clear mitochondria.

Aging Influences Cardiac Mitochondrial Physiology

Several other autophagy components are reported to decrease with age and can affect mitochondrial physiology and turnover. For instance, the kinase Pink1, which is associated with the E3 ligase Parkin, is decreased during normal cardiac aging and functionally blocks the removal of damaged mitochondria with altered Δψm [28]. Depolarization of the Δψm has been shown to stimulate mito-ROS in smooth muscle cells via SODII and lead to local spontaneous Ca^{2+}-release events known as sparks [34]. Here we use acute pharmacological manipulations of autophagy to down- or up-regulate autophagy; chloroquine blocks lysosomal acidification and therefore blocks autophagy. We chose to use HL-1 cardiomyocytes that contain healthy mitochondria, intact calcium-handling systems, and are tractable for the studies presented. Previous reports indicate short exposure to micromolar range chloroquine after two hours leads to decreased autophagy flux [35], therefore we treated our myocytes with 1 μM chloroquine for three

hours. Autophagy block with chloroquine did decrease autophagy flux as measured by the indicator TF-LC3-GFP and led to accumulation p62 polypeptides (Fig 2). Functionally, our manipulation increased mito-ROS and depolarized the Δψm (Fig 2).

Age-Related Dysfunctional Ca^{2+} Release Underlies Increased Arrhythmic Potential

Cardiac contraction relies on Ca^{2+} release from intracellular Ca^{2+} stores mediated by the SR Ca^{2+} release channel RyR2. In cardiac disease or aging, RyR2 becomes more active, which helps to maintain cardiac output to meet baseline metabolic demands [5]. However, during stress, hyperactivity of RyR2s has been associated with SCWs, which could translate into disturbances in membrane potential, i.e. delayed or early afterdepolarizations leading to malignant arrhythmias and sudden cardiac death [10]. Posttranslational modifications of the channel, including phosphorylation by PKA and/or CaMKII and oxidation of reactive cysteines, have been implicated in the RyR2 hyperactivity characteristic of cardiac disease and aging [10, 36]. ROS scavengers were proven to stabilize aberrant Ca^{2+} release and lessen triggers for arrhythmia in conditions accompanied by oxidative stress, including heart failure [37] and myocardial infarction [10]. Likewise, we previously reported that in aging rabbit ventricular CMs the scavenging of mito-ROS restores the oxidative state of RyR2s, stabilizing Ca^{2+} release and resulting in decreased SCWs under β-adrenergic stimulation to mimic stress [5]. Calcium imaging revealed alteration in several key parameters such as increased propensity for spontaneous calcium release (measured by decreased latency to spontaneous wave after pacing train), and a greater proportion of cells after autophagy block that displayed spontaneous activity (Fig 3). Interestingly, we found that this dysfunction is rescued by scavenging mito-ROS via application of MitoTEMPO. These data are in line with our

previous report [5] that mito-ROS oxidizes the RyR2 during aging, leading to enhanced SR calcium leak and generation of SCWs. Targeted enhancement of autophagy effectively stabilized RyR2-mediated Ca^{2+} release via downregulation of mito-ROS production (Fig 4 & 5).

Targeting mito-ROS in Aging to Reduce Cardiomyocyte Arrhythmogenesis

Mitochondria participate in numerous processes including bioenergetics, intracellular signaling, and immune response [34, 38-41]. Previous reports implicate mTOR as an important signaling intermediate between the mitochondria and nucleus that helps maintain mitochondrial function [42, 43]. Our data show that inhibition of mTOR by Torin1 improves aged CM physiology as assessed by a variety of mitochondrial functions, including decreased ROS production and hyperpolarization of depolarized $\Delta\psi m$ in the aging CM (Fig. 4), in accordance with other reports [42, 44, 45]. Calcium imaging of Torin1-treated aged CMs reveals a two-fold decrease in the number of cells exhibiting pro-arrhythmic SCW activity (Fig. 4). To directly address the possibility that the functional changes we observe are an off-target effect of Torin1 treatment, we overexpressed the autophagy effector ATG7. Similar to Torin1 treatment, we see that ATG7 overexpressing aged myocytes reveal a two-fold decrease in the number of cells exhibiting pro-arrhythmic SCW activity (Fig. 5). Given these data, we propose the strategy of scavenging mito-ROS with mitochondria-specific superoxide-specific ROS scavengers, or by enhancing autophagy to reduce the number of age-related pro-arrhythmic spontaneous calcium release events at the cellular scale.

3.5 Conclusion

We demonstrate that enhancing autophagy using acute application of Torin1 or ATG7 overexpression in primary CMs from aged rabbits effectively mimics the effects of ROS scavengers at the cellular level, reducing mito-ROS and effectively stabilizing RyR2-mediated Ca^{2+} release (Fig. 4 & 5). Conversely, blocking autophagy in HL-1 CMs promotes the oxidation of RyR2 and ROS-dependent pro-arrhythmic disturbances in Ca^{2+} handling, as manifested in an increased propensity for generation of pro-arrhythmic SCWs (Fig. 3). In combination with our previously published results, our data suggest autophagy (Fig. 6) as a target for modulation of mito-ROS in the aging mammalian heart to prevent Ca^{2+}-dependent arrhythmia.

3.6 Experimental Procedures:

Cell Culture

Primary rabbit cardiomyocytes were isolated from young (4.5-9 months) or aged (>4 years) New Zealand White rabbits (RSI Farms, Mocksville, NC, USA) as previously described, by Langendorff perfusion with a solution containing collagenase II (#CLS-2, Worthington Biochemical, Lakewood, NJ, USA) [5]. Myocytes were plated for 1 hour in M199 (#M4530, Sigma, St. Louis, MO, USA) supplemented with 10% FBS, penicillin (100 u/mL), and streptomycin (0.1 u/mL) (#P4333, Sigma, St. Louis, MO, USA). HL-1 cardiomyocytes were cultured as previously described [29]. Briefly, cells were propagated on cell culture–grade plastics coated with fibronectin/gelatin (#F1141, # G9391, respectively, Sigma, St. Louis, MO, USA) and split 1:2 every other day and kept in Claycomb Medium (#51800C, Sigma, St. Louis, MO, USA) with 10% FBS, penicillin-

streptomycin (above), and norepinephrine (100 μM) (#A0937, Sigma, St. Louis, MO, USA).

Transmission Electron Microscopy of Primary Isolated Ventricular Rabbit Myocytes

Primary rabbit left ventricular cardiomyocytes were plated on Permanox Lab-Tek chamber slides and fixed with 1.25% glutaraldehyde in 0.15M sodium cacodylate buffer. Following fixation, cells were buffer-rinsed and post-fixed with 1% osmium tetroxide. After rinsing, cells were stained en bloc with 2% aqueous uranyl acetate and dehydrated through a graded ethanol series. Media chambers and gaskets were removed. Slides were covered with Epox 812 resin and placed over resin-filled slide-duplicating molds and polymerized overnight. The resin was separated from the slide, and cultures were examined by light microscopy to identify regions of interest. Selected areas were cut out and mounted on blocks for sectioning. Ultra-thin sections (50-60 nm) were prepared using a Reichert Ultracut S microtome, retrieved onto 300 mesh copper grids, and contrasted with uranyl acetate and lead citrate. Sections were examined using a Morgagni 268 transmission electron microscope. Images were collected with an AMT Advantage 542 CCD camera system. Mitochondrial structure was analyzed using the publicly available ImageJ and region of interest (ROI) manager plugin to manually select and gate individual mitochondria. Parameters such as area and aspect ratio of ROI were measured using ImageJ's internal algorithms.

Western Blotting of Autophagy and Mitochondrial Proteins:

Protein expression was determined using the following antibodies in immunoblotting: p62 1:1000 (insert company), PINK1 1:1000 (Cell Signaling #9646), p53 (Abcam #ab17869), LC3 (Abgent # AM1800A), DRP1 1:500 (Abcam #AB56788), and MFN2 1:500 (Sigma #WH0009927M3). Left ventricular free-wall tissue was homogenized in protein lysis buffer (50mM Tris HCL pH7.5, 150mM NaCl, 1mM EDTA, 10% Glycerol, 1mM PMSF, 1 tablet Complete MINI protease inhibitor). Samples were centrifuged at 2.5k RPM for 15 minutes, aliquoted, and stored at -80°C. 15-25ug protein was loaded into 4-15% TGX gels (#4561086, BioRad, Hercules, CA, USA) via SDS-PAGE, transferred onto PVDF membranes, and probed with mouse or rabbit antibodies specific for these proteins and subsequently probed with donkey anti-mouse or anti-rabbit secondary antibodies (Thermo Fisher). Blots were developed with SuperSignal West Pico (#34080, Thermo Fisher, Waltham, MA, USA), imaged with ChemiDoc 2000 (BioRad, Hercules, CA, USA), and quantified and analyzed using ImageLab (BioRad, Hercules, CA, USA) and ImageJ (US National Institutes of Health, Bethesda, MD, USA) software.

SDS-Page and Western Blotting for RyR2 Oxidation Using C2-Maleimide:

RIPA Extraction buffer (50mM Tris HCLpH7.5, 100mM NaCl, 10mM EDTA, 1% Triton X-100, 1% NP-40, 0.2$ SDS, 1 tablet Complete MINI protease inhibitor, pH 7.5) was added to cell culture plates, scraped, collected, and kept on ice for 45 minutes with vigorous vortexing every 15 minutes. Lysates were spun at 4°C for 30 minutes at 5,800g. 25 μL of concentrated supernatant was treated with 40 μL of 0.225 mM Alexa 647 C2-Maleimide and incubated for 2 hrs at room temperature in the dark, rotating. 450 μL ice-

cold acetone was added and incubated for 1 hr at -20°C. The protein pellet was resuspended in 1x Laemlli buffer (#161-0737, BioRad, Hercules, CA, USA) and loaded into a 4-15% TGX gel (#4561086, BioRad, Hercules, CA, USA). Before transfer, the gels were imaged with ChemiDoc 2000 (BioRad, Hercules, CA, USA) using the Alexa 647 preset. Protein was then transferred onto PVDF membranes and probed with anti-RyR 1:1,000 (#MA3-916, Thermo Fisher, Waltham, MA, USA) and subsequently probed with a donkey anti-mouse secondary antibody (#PA1-28748, Thermo Fisher, Waltham, MA, USA). Blots were developed as described above.

Fluorescence Microscopy Measurements of Autophagy Flux Using a TF-LC3-GFP Biosensor:

Autophagy flux was measured using the tandem fluorescence LC3-GFP adenovirus. Cardiomyocytes were measured in Tyrode solution (140 mM NaCl, 5.4 mM KCl, 1.8 mM Ca^{2+} 1 mM $MgCl_2$, 10 mM HEPES, 5.6 mM glucose, pH = 7.3 using NaOH). Cells were infected for 48hrs with 1 MOI of adenovirus containing TF-LC3-GFP. Z-stack images were taken in 1 μm steps through the cell. Two images per stack were collected where the biosensor was excited first at 460-500 nm and emission was collected at 500-560nm to image the GFP fluorophore and second at 540-580nm and emission was collected at 600-660nm. Using NIS Elements V3 software (Nikon Instruments) focused images were created from the stack. Ratio images were generated by dividing the red channel by green channel. Pixels over ratio=1 represent autolysomsomal region. Total area of ratio>1 were calculated with respect to total surface area to measure autophagy flux.

Confocal Microscopy Measurements of Intracellular ROS and Δψm:

ROS production by cardiomyocytes was measured in Tyrode solution (140 mM NaCl, 5.4 mM KCl, 1.8 mM Ca^{2+} 1 mM $MgCl_2$, 10 mM HEPES, 5.6 mM glucose, pH = 7.3 using NaOH) using the ROS-sensitive dye 5-(and-6)-chloromethyl-2',7'-dichlorodihydrofluoroscein diacetate (CM-H2DCFDA, 7.5 μM, incubated for 20 min) as previously described [5]. The DCFDA dye was excited with the 488 nm line of an argon laser in x–y mode, and emission was collected at 500–530 nm. The rate of ROS production was measured in cardiomyocytes *in vitro* and *ex vivo* as well as those pretreated with mito-TEMPO (25 μM for 10 min). Mitochondrial ROS production by cardiomyocytes was measured in Tyrode solution using the mitochondria superoxide-sensitive fluorescent indicator MitoSOX Red (1 μM, incubated in cell culture medium for 30 min). The dye was excited with the 514 nm line of an HeNe laser in x–y mode, and emission was collected at 640-660 nm. Mitochondrial membrane potential was monitored with a voltage-sensitive fluorescent indicator, tetramethylrhodamine methyl ester (TMRM) as previously described [39]. In brief, cardiomyocytes were loaded with 1 nM TMRM (10min), and TMRM fluorescence was measured in x–y mode. TMRM was excited at 543 nm with a helium–neon laser, and the emission signals were collected at 570–650 nm. TMRM fluorescence was normalized to the minimum fluorescence signal obtained with the mitochondrial uncoupler carbonyl cyanide p-(trifluoromethoxy) phenylhydrazone (FCCP, 50 μM).

Confocal Microscopy Measurements of Intracellular Ca^{2+}

Intracellular Ca^{2+} cycling activity in isolated rabbit ventricular myocytes was monitored using a Leica SP2 confocal laser scanning system equipped with a 60x 1.4 NA oil-immersion objective in linescan and x–y mode using Ca^{2+}-sensitive indicators Fluo-3 (Molecular Probes, Carlsbad, CA, USA), respectively. Cells were loaded with Fluo-3 for 10 min, and after 20 min de-esterification, the dye was excited with the 488 nm line of an argon laser. Emission was collected at 500–600 nm. Cardiomyocytes were studied in Tyrode solution (140 mM NaCl, 5.4 mM KCl, 1.8 mM Ca^{2+} 1 mM $MgCl_2$, 10 mM HEPES, 5.6 mM glucose, pH = 7.3 using NaOH). Myocytes were paced via field stimulation at 1 Hz using extracellular platinum electrodes. To assess the SR Ca2+ load and decay kinetics, 10mM caffeine was applied at the end of the experiments.

To test the propensity for triggered activity, myocytes were paced at 1 Hz for 30 seconds, and the latency between the last stimulus in the pacing train and the first SCW was calculated. To assess the effect of mitochondria-derived ROS on cardiomyocytes from aged rabbits, myocytes were pretreated with the mitochondria-specific ROS scavenger (2-(2,2,6,6-tetramethylpiperidin-1-oxyl-4-ylamino)-2-oxoethyl) triphenylphosphonium chloride (mito-TEMPO, 25 μM, Enzo Life Sciences, Farmingdale, NY, USA) for 10 min. The intracellular Ca^{2+} cycling measurements were performed under β-adrenergic stimulation with 100 nM ISO for HL-1 cardiomyocytes and 30 nM ISO for aged rabbit cardiomyocytes.

Statistical Analysis

Data are presented as mean ± standard deviation (SD) of *n* measured cells or hearts. Statistical comparisons between groups were performed in OriginPro 2017 with Student's *t* test (paired and unpaired) unless otherwise stated. Differences that are not statistically different are noted as NS. Differences were considered statistically significant at $p<0.05$.

Acknowledgements

This work was supported by NIH grants R01-HL110791 (to G. Koren), R21-AG049608 (to J. Sedivy and G. Koren), and R01-HL121796 (to D. Terentyev). We would like to thank Dr. William Claycomb for generously providing the HL-1 CM cell line. We would also like to thank the Sadoshima lab for providing adenovirus containing TF-LC3-GFP, LacZ, and ATG7. Dr. Alison Chambers provided helpful consultation for statistical analysis of some datasets presented. Lastly, we would like to thank Dr. Karim Roder for his helpful comments during the preparation of this manuscript.

Competing Interests

None declared.

Author Contributions

K.R.M, D.T., J.S., and G.K. contributed to the conception and design of the study. K.R.M, J.O., and D.T. worked on interpretation of data and writing the manuscript. K.R.M, L.L.C, Y.L., and D.T. performed experiments and analyzed the results. All authors read

and approved the final submission. All experiments were carried out in the Cardiovascular Research Center of the Cardiovascular Institute at Lifespan.

3.7 Figures

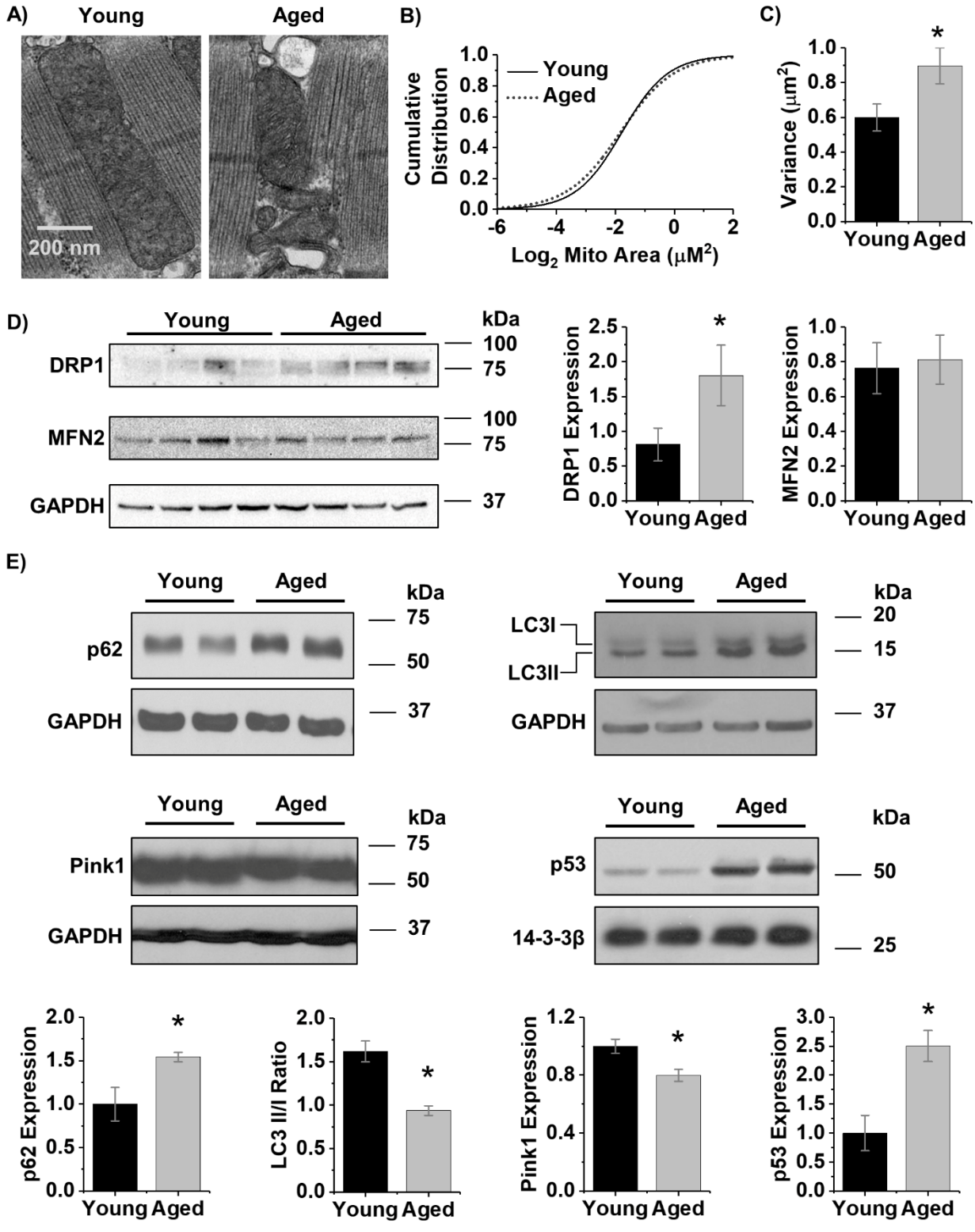
A)
Young
Aged
200 nm
B)
Cumulative Distribution
Young
Aged
Log2 Mito Area (μM2)
C)
Variance (μm2)
Young Aged
D)
Young
Aged
kDa
DRP1
MFN2
GAPDH
100
75
37
DRP1 Expression
MFN2 Expression
E)
p62
LC3I
LC3II
Pink1
p53
14-3-3β
20
15
50
25
p62 Expression
LC3 II/I Ratio
Pink1 Expression
p53 Expression

Figure 3.1: CM Aging Leads to Heterogeneous Mitochondria and Decreased Markers of Autophagy.

A) Representative transmission electron micrographs of acutely disassociated CMs from young and aged rabbit hearts, scale bar = 200 nm (n=4 hearts, >30 cells/age). B) Cumulative distribution of mitochondrial log2 cross-sectional areas assessed by image analysis of electron micrographs in young and aged CMs. Analysis of data was performed using GLIMMIX procedure in SAS Version 9.4 (SAS Inc.). Multiple comparisons testing was performed using Holm–Bonferroni corrections, *<p,0.05. C) Variance in mitochondrial log2 cross-sectional areas (n=4 hearts with 8 CMs per heart). D) Representative immunoblots for mitochondrial fission and fusion proteins, DRP1 and MFN2 with densitometry using young and aged whole left ventricular homogenates (n=4 hearts). E) Representative immunoblots for autophagy (p62, LC3) and mitophagy proteins (Pink1 and p53) using young and aged whole left ventricular homogenates (n-4). *p<0.05, all values are mean ± SEM.

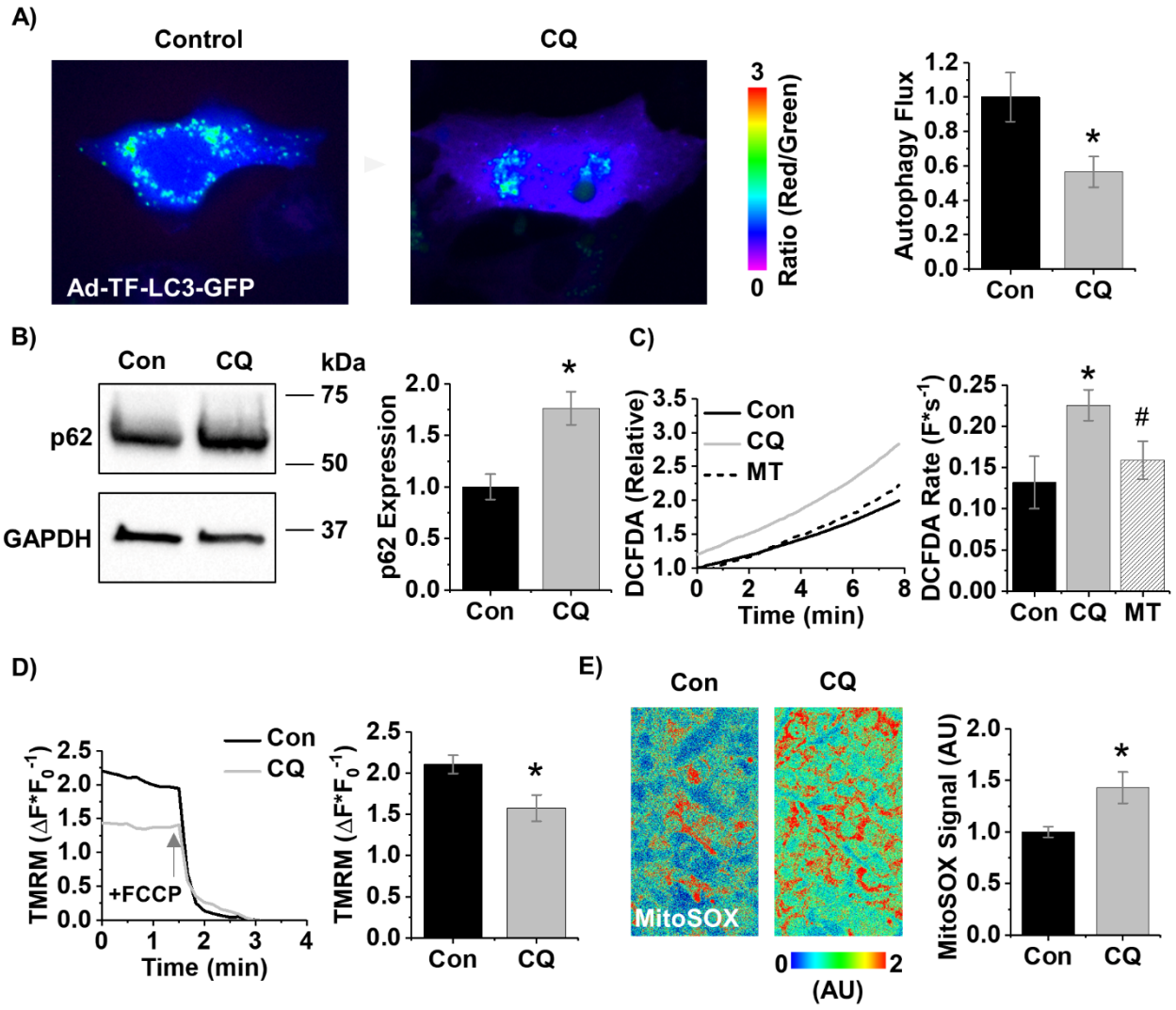

Figure 3.2: Chloroquine decreases autophagy in HL-1 CMs.

A) Confocal XY images of HL-1 CMs infected with Ad-TF-LC3-GFP visualizing autolysosomes as puncta. Examples of autophagosomes shown by white arrow (n=8 CMs). B) Representative immunoblots for the autophagy protein p62 (n=3). C) Changes in DCFDA fluorescence in chloroquine and vehicle treated CMs, and from CMs treated with 25 μM MitoTEMPO for 10 min following chloroquine treatment. Mean data represent ROS production rate. D) Traces and mean data of normalized TMRE fluorescence of chloroquine and vehicle treated CMs. Data are normalized to the minimum TMRE

fluorescence in the presence of the uncoupling agent FCCP. n=3 biological preparations. E) Representative confocal images of HL1 cells stained with MitoSOX acquired in XYT mode. Relative MitoSOX fluorescence is plotted. $^{*}p<0.05$, all values are mean ± SEM.

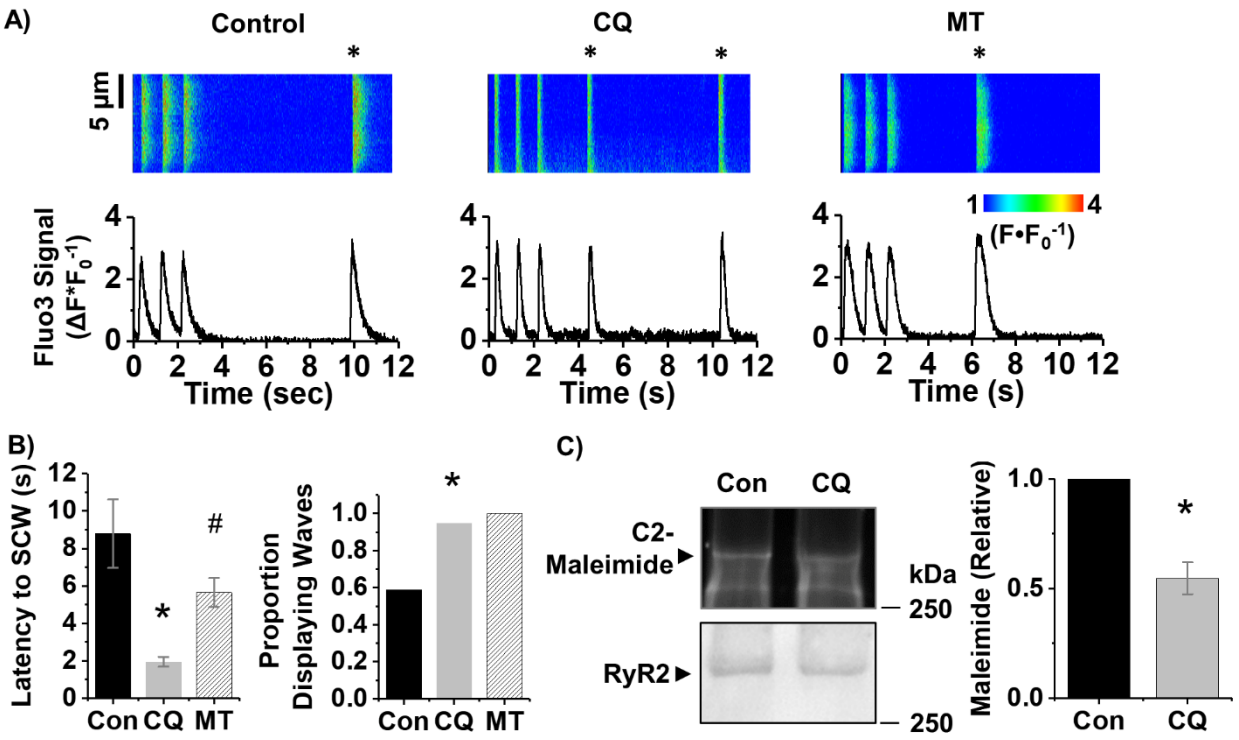

Figure 3.3: Inhibition of Autophagy Reduces Refractoriness of RyR2-mediated Ca^{2+} Release under β-Adrenergic Stimulation.

A) Confocal line scan images and Fluo3 profiles at the end of 1 min 1 Hz pacing train with HL-1 CMs treated with chloroquine (1 µm, 3 hr) or vehicle; all with 100 nM isoproterenol. SCWs are indicated by an asterisk. n=3 biological replicates with at least 10 cells. B) Mean data for SCW latency and proportion of cells exhibiting SCWs. C) Representative C2-Maleimide fluorescence of RyRs from HL-1 CMs treated with chloroquine or vehicle. Relative maleimide fluorescence scored between conditions. n=3 biological preparations from sequential passages. *p<0.05, all values are mean ± SEM.

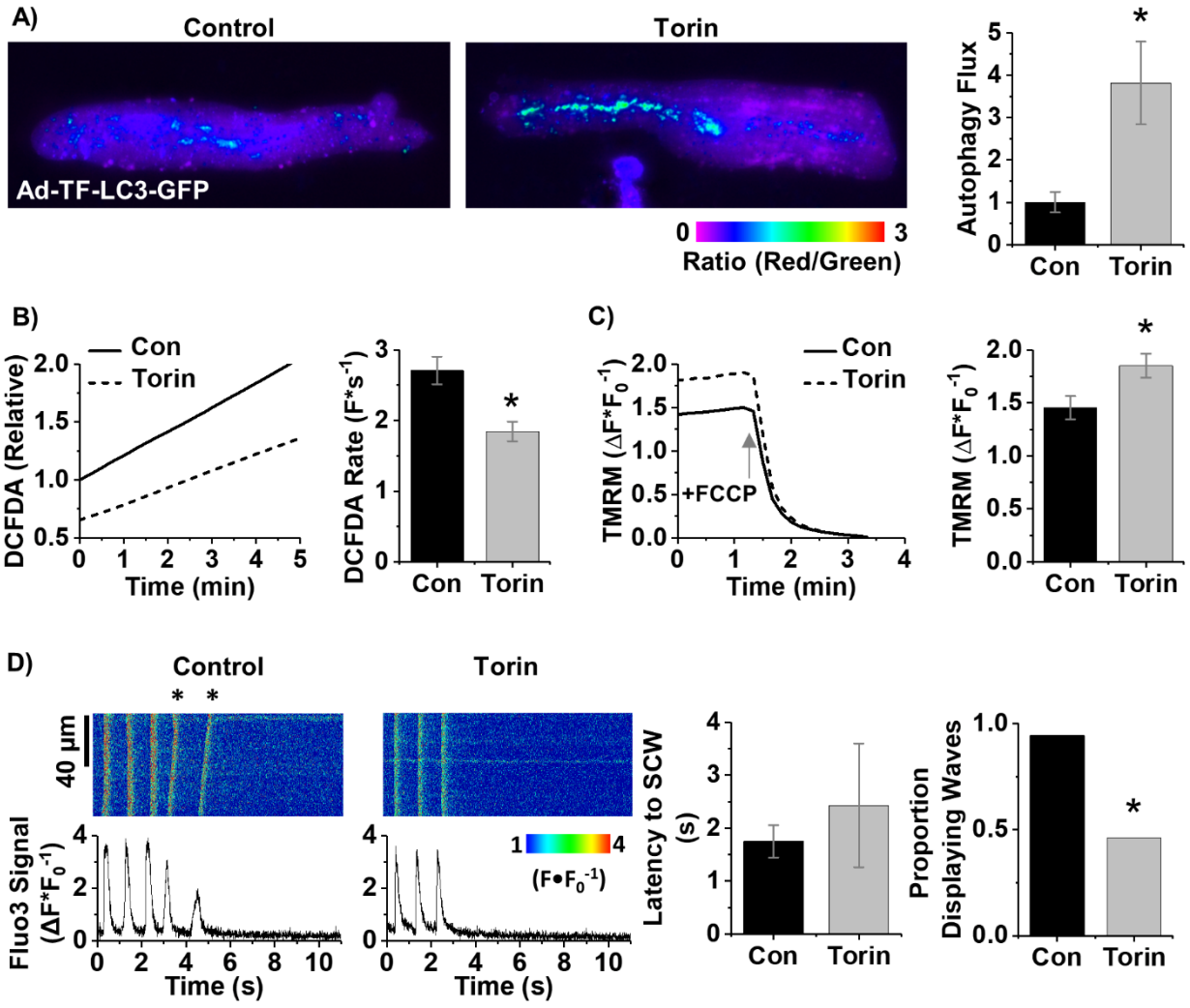

Figure 3.4: Enhancing Autophagy in Aged Rabbit CMs Reduces ROS, Restores Δψm, and Reverses Effects of Aging of RyR-Mediated Ca^{2+} Release.

A) Changes in DCFDA fluorescence in Torin1 (250 nm, 4 hr) and vehicle treated aged rabbit CMs. Mean data represent ROS production rate. B) Traces and mean data of normalized TMRM fluorescence of Torin1 and vehicle treated CMs. Data are normalized to the minimum TMRM fluorescence in the presence of the uncoupling agent FCCP (50 µM). C) Confocal line scan images and Fluo3 profiles at the end of 30 sec 1 Hz pacing train with aged rabbit CMs treated with Torin1 or vehicle; all with 25 nM isoproterenol.

SCWs are indicated by an asterisk. n=3 biological replicates. *p<0.05, all values are mean ± SEM.

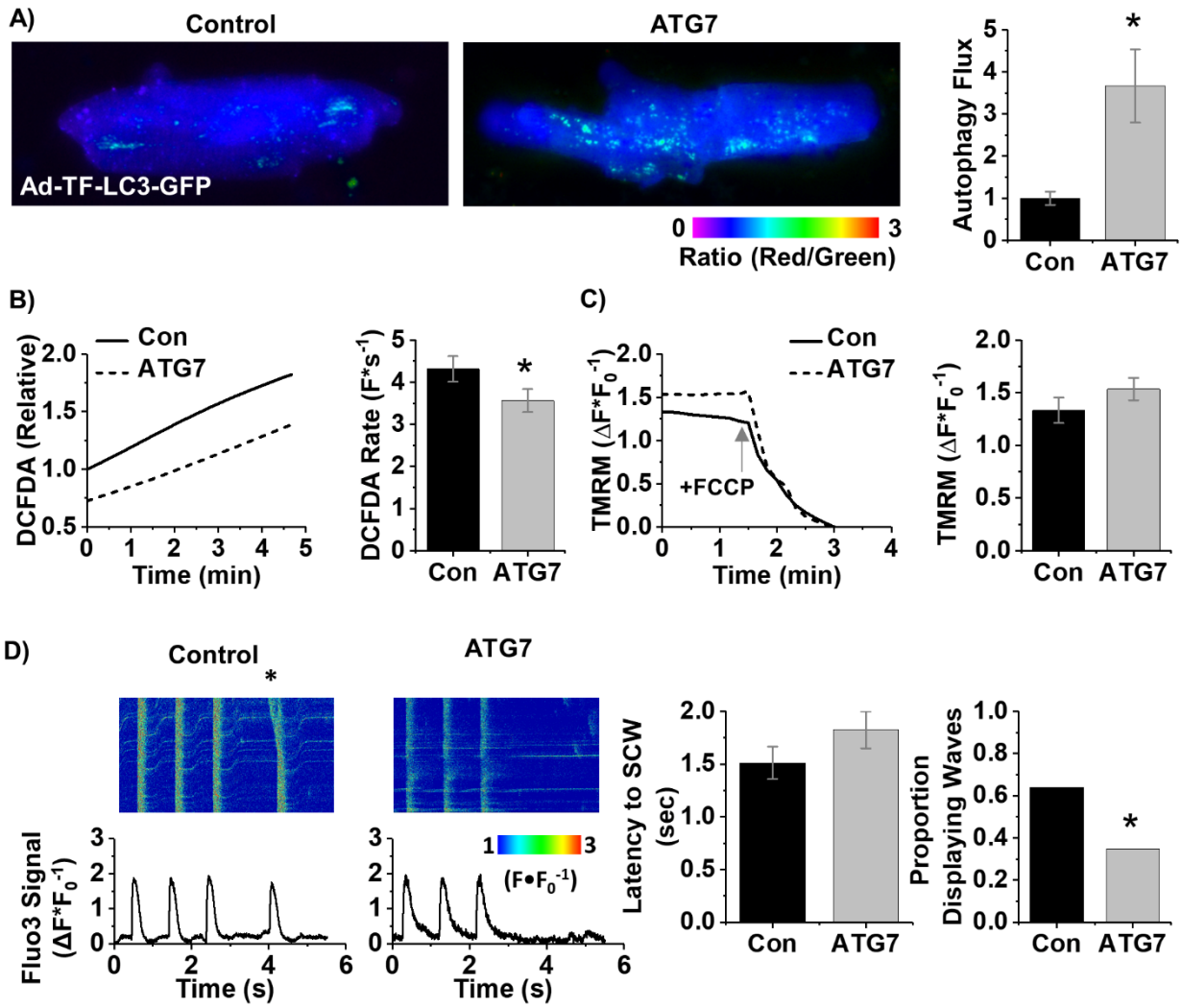

Figure 3.5: Genetically Enhancing Autophagy in Aged Rabbit CMs Reduces ROS, Restores Δψm, and Reverses Effects of Aging of RyR-Mediated Ca^{2+} Release.

A) Changes in DCFDA fluorescence in ATG7 and vector control treated aged rabbit CMs. Mean data represent ROS production rate. B) Traces and mean data of normalized TMRM fluorescence of ATG7 and vector control treated CMs. Data are normalized to the minimum TMRM fluorescence in the presence of the uncoupling agent FCCP (50 μM). C) Confocal line scan images and Fluo3 profiles at the end of 30 sec 1 Hz pacing train with aged rabbit CMs treated with ATG7 or vector control; all with 25 nM isoproterenol. SCWs

are indicated by an asterisk. n=3 biological replicates. *$p<0.05$, all values are mean ± SEM.

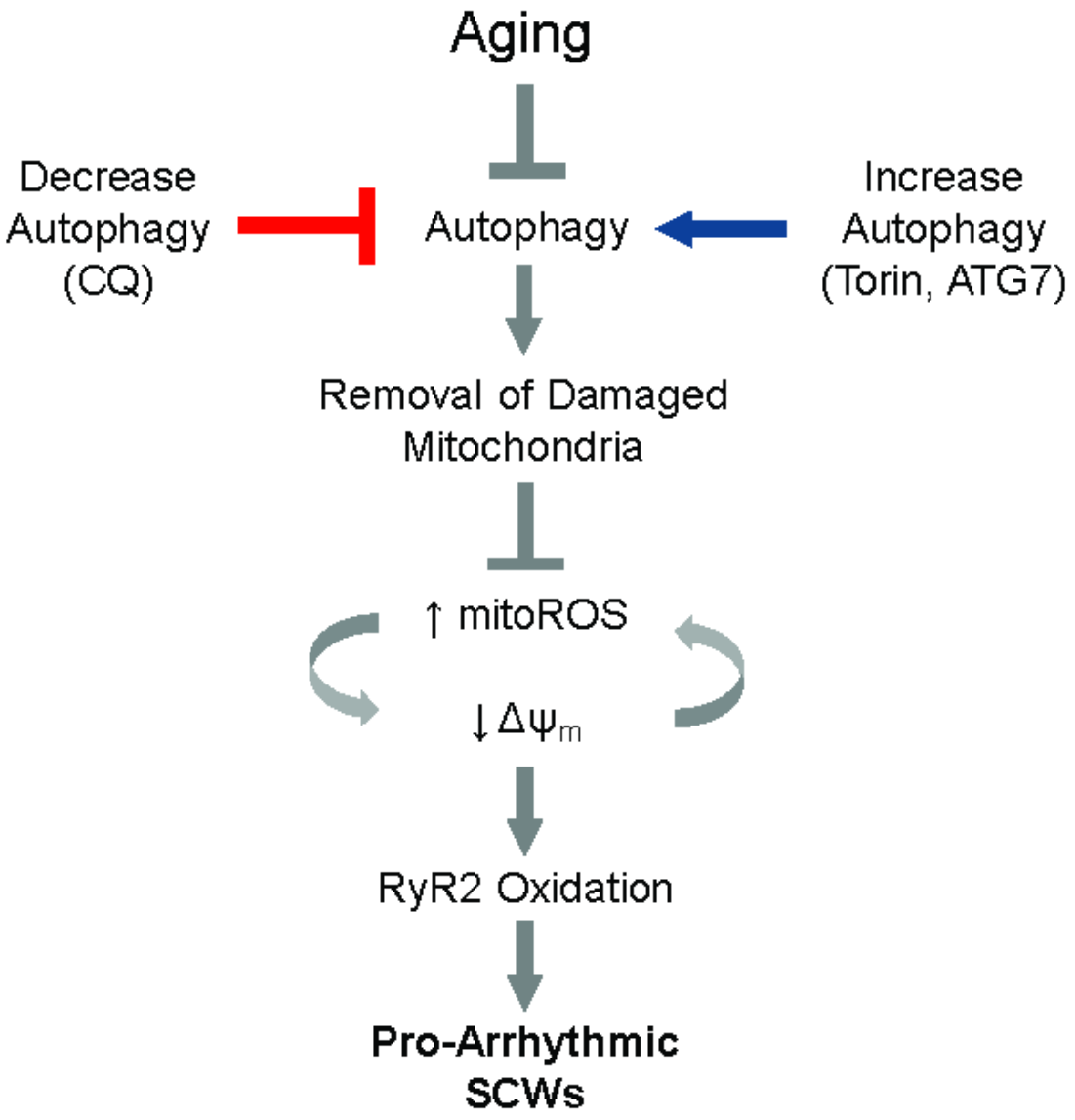

Figure 3.6: Proposed Model of Autophagy Control of Ca2+-Mediated Cardiac Arrhythmia.

Autophagy is a major cause of increased mito-ROS production in the aging heart. Blocking or enhancing autophagy is sufficient to modify pathologic mito-ROS production and Δψm during normal aging thereby controlling the instance of pro-arrhythmic spontaneous Ca2+ release via oxidized RyR2s.

3.7 Literature Cited

1. Deo R, Albert CM: **Epidemiology and genetics of sudden cardiac death**. *Circulation* 2012, **125**(4):620-637.
2. Zheng ZJ, Croft JB, Giles WH, Mensah GA: **Sudden cardiac death in the United States, 1989 to 1998**. *Circulation* 2001, **104**(18):2158-2163.
3. Podrid PJ, Myerburg RJ: **Epidemiology and stratification of risk for sudden cardiac death**. *Clin Cardiol* 2005, **28**(11 Suppl 1):I3-11.
4. Cooper LL, Odening KE, Hwang MS, Chaves L, Schofield L, Taylor CA, Gemignani AS, Mitchell GF, Forder JR, Choi BR *et al*: **Electromechanical and structural alterations in the aging rabbit heart and aorta**. *Am J Physiol Heart Circ Physiol* 2012, **302**(8):H1625-1635.
5. Cooper LL, Li W, Lu Y, Centracchio J, Terentyeva R, Koren G, Terentyev D: **Redox modification of ryanodine receptors by mitochondria-derived reactive oxygen species contributes to aberrant Ca2+ handling in ageing rabbit hearts**. *J Physiol* 2013, **591**(23):5895-5911.
6. Dai WW, Jin GQ: **[The crosstalking between aging and autophagy]**. *Sheng Li Ke Xue Jin Zhan* 2012, **43**(4):247-250.
7. Scridon A, Gallet C, Arisha MM, Orea V, Chapuis B, Li N, Tabib A, Christe G, Barres C, Julien C *et al*: **Unprovoked atrial tachyarrhythmias in aging spontaneously hypertensive rats: the role of the autonomic nervous system**. *Am J Physiol Heart Circ Physiol* 2012, **303**(3):H386-392.

8. Janczewski AM, Lakatta EG: **Modulation of sarcoplasmic reticulum Ca(2+) cycling in systolic and diastolic heart failure associated with aging**. *Heart Fail Rev* 2010, **15**(5):431-445.

9. Plummer BN, Cutler MJ, Wan X, Laurita KR: **Spontaneous calcium oscillations during diastole in the whole heart: the influence of ryanodine reception function and gap junction coupling**. *Am J Physiol Heart Circ Physiol* 2011, **300**(5):H1822-1828.

10. Belevych AE, Terentyev D, Terentyeva R, Ho HT, Gyorke I, Bonilla IM, Carnes CA, Billman GE, Gyorke S: **Shortened Ca2+ signaling refractoriness underlies cellular arrhythmogenesis in a postinfarction model of sudden cardiac death**. *Circ Res* 2012, **110**(4):569-577.

11. Wehrens XH, Lehnart SE, Marks AR: **Intracellular calcium release and cardiac disease**. *Annu Rev Physiol* 2005, **67**:69-98.

12. Zima AV, Bovo E, Mazurek SR, Rochira JA, Li W, Terentyev D: **Ca handling during excitation-contraction coupling in heart failure**. *Pflugers Archiv : European journal of physiology* 2014, **466**(6):1129-1137.

13. Kubli DA, Gustafsson AB: **Mitochondria and mitophagy: the yin and yang of cell death control**. *Circ Res* 2012, **111**(9):1208-1221.

14. Ashrafi G, Schwarz TL: **The pathways of mitophagy for quality control and clearance of mitochondria**. *Cell Death Differ* 2013, **20**(1):31-42.

15. Ravikumar B, Futter M, Jahreiss L, Korolchuk VI, Lichtenberg M, Luo S, Massey DC, Menzies FM, Narayanan U, Renna M *et al*: **Mammalian macroautophagy at a glance**. *J Cell Sci* 2009, **122**(Pt 11):1707-1711.

16. Sharp WW, Fang YH, Han M, Zhang HJ, Hong Z, Banathy A, Morrow E, Ryan JJ, Archer SL: **Dynamin-related protein 1 (Drp1)-mediated diastolic dysfunction in myocardial ischemia-reperfusion injury: therapeutic benefits of Drp1 inhibition to reduce mitochondrial fission**. *FASEB J* 2014, **28**(1):316-326.

17. Miquel J, Economos AC, Fleming J, Johnson JE, Jr.: **Mitochondrial role in cell aging**. *Exp Gerontol* 1980, **15**(6):575-591.

18. Terman A, Kurz T, Navratil M, Arriaga EA, Brunk UT: **Mitochondrial turnover and aging of long-lived postmitotic cells: the mitochondrial-lysosomal axis theory of aging**. *Antioxid Redox Signal* 2010, **12**(4):503-535.

19. Lopez-Otin C, Blasco MA, Partridge L, Serrano M, Kroemer G: **The hallmarks of aging**. *Cell* 2013, **153**(6):1194-1217.

20. Dai DF, Rabinovitch PS, Ungvari Z: **Mitochondria and cardiovascular aging**. *Circ Res* 2012, **110**(8):1109-1124.

21. Taneike M, Yamaguchi O, Nakai A, Hikoso S, Takeda T, Mizote I, Oka T, Tamai T, Oyabu J, Murakawa T *et al*: **Inhibition of autophagy in the heart induces age-related cardiomyopathy**. *Autophagy* 2010, **6**(5):600-606.

22. Shintani T, Klionsky DJ: **Autophagy in health and disease: a double-edged sword**. *Science* 2004, **306**(5698):990-995.

23. Thoreen CC, Kang SA, Chang JW, Liu Q, Zhang J, Gao Y, Reichling LJ, Sim T, Sabatini DM, Gray NS: **An ATP-competitive mammalian target of rapamycin inhibitor reveals rapamycin-resistant functions of mTORC1**. *J Biol Chem* 2009, **284**(12):8023-8032.

24. Martinez-Lopez N, Athonvarangkul D, Singh R: **Autophagy and aging**. *Adv Exp Med Biol* 2015, **847**:73-87.

25. Bhuiyan MS, Pattison JS, Osinska H, James J, Gulick J, McLendon PM, Hill JA, Sadoshima J, Robbins J: **Enhanced autophagy ameliorates cardiac proteinopathy**. *J Clin Invest* 2013, **123**(12):5284-5297.

26. Morrissey PJ, Murphy KR, Daley JM, Schofield L, Turan NN, Arunachalam K, Abbott JD, Koren G: **A novel method of standardized myocardial infarction in aged rabbits**. *Am J Physiol Heart Circ Physiol* 2017, **312**(5):H959-H967.

27. Ohsumi Y: **Molecular dissection of autophagy: two ubiquitin-like systems**. *Nat Rev Mol Cell Biol* 2001, **2**(3):211-216.

28. Hoshino A, Mita Y, Okawa Y, Ariyoshi M, Iwai-Kanai E, Ueyama T, Ikeda K, Ogata T, Matoba S: **Cytosolic p53 inhibits Parkin-mediated mitophagy and promotes mitochondrial dysfunction in the mouse heart**. *Nat Commun* 2013, **4**:2308.

29. Claycomb WC, Lanson NA, Jr., Stallworth BS, Egeland DB, Delcarpio JB, Bahinski A, Izzo NJ, Jr.: **HL-1 cells: a cardiac muscle cell line that contracts and retains phenotypic characteristics of the adult cardiomyocyte**. *Proc Natl Acad Sci U S A* 1998, **95**(6):2979-2984.

30. Liu M, Liu H, Dudley SC, Jr.: **Reactive oxygen species originating from mitochondria regulate the cardiac sodium channel**. *Circ Res* 2010, **107**(8):967-974.

31. Ni R, Cao T, Xiong S, Ma J, Fan GC, Lacefield JC, Lu Y, Le Tissier S, Peng T: **Therapeutic inhibition of mitochondrial reactive oxygen species with mito-**

TEMPO reduces diabetic cardiomyopathy. *Free radical biology & medicine* 2016, **90**:12-23.

32. Hanna AD, Lam A, Tham S, Dulhunty AF, Beard NA: **Adverse effects of doxorubicin and its metabolic product on cardiac RyR2 and SERCA2A**. *Mol Pharmacol* 2014, **86**(4):438-449.

33. Siddall HK, Yellon DM, Ong SB, Mukherjee UA, Burke N, Hall AR, Angelova PR, Ludtmann MH, Deas E, Davidson SM *et al*: **Loss of PINK1 increases the heart's vulnerability to ischemia-reperfusion injury**. *PLoS One* 2013, **8**(4):e62400.

34. Xi Q, Cheranov SY, Jaggar JH: **Mitochondria-derived reactive oxygen species dilate cerebral arteries by activating Ca2+ sparks**. *Circ Res* 2005, **97**(4):354-362.

35. Iwai-Kanai E, Yuan H, Huang C, Sayen MR, Perry-Garza CN, Kim L, Gottlieb RA: **A method to measure cardiac autophagic flux in vivo**. *Autophagy* 2008, **4**(3):322-329.

36. Chandel NS, Schumacker PT, Arch RH: **Reactive oxygen species are downstream products of TRAF-mediated signal transduction**. *J Biol Chem* 2001, **276**(46):42728-42736.

37. Terentyev D, Gyorke I, Belevych AE, Terentyeva R, Sridhar A, Nishijima Y, de Blanco EC, Khanna S, Sen CK, Cardounel AJ *et al*: **Redox modification of ryanodine receptors contributes to sarcoplasmic reticulum Ca2+ leak in chronic heart failure**. *Circ Res* 2008, **103**(12):1466-1472.

38. Chen Y, McMillan-Ward E, Kong J, Israels SJ, Gibson SB: **Mitochondrial electron-transport-chain inhibitors of complexes I and II induce autophagic**

cell death mediated by reactive oxygen species. *J Cell Sci* 2007, **120**(Pt 23):4155-4166.

39. Cordeiro B, Terentyev D, Clements RT: **BKCa channel activation increases cardiac contractile recovery following hypothermic ischemia/reperfusion**. *Am J Physiol Heart Circ Physiol* 2015, **309**(4):H625-633.

40. Nakai A, Yamaguchi O, Takeda T, Higuchi Y, Hikoso S, Taniike M, Omiya S, Mizote I, Matsumura Y, Asahi M *et al*: **The role of autophagy in cardiomyocytes in the basal state and in response to hemodynamic stress**. *Nat Med* 2007, **13**(5):619-624.

41. Sovari AA, Rutledge CA, Jeong EM, Dolmatova E, Arasu D, Liu H, Vahdani N, Gu L, Zandieh S, Xiao L *et al*: **Mitochondria oxidative stress, connexin43 remodeling, and sudden arrhythmic death**. *Circ Arrhythm Electrophysiol* 2013, **6**(3):623-631.

42. Matsui Y, Takagi H, Qu X, Abdellatif M, Sakoda H, Asano T, Levine B, Sadoshima J: **Distinct roles of autophagy in the heart during ischemia and reperfusion: roles of AMP-activated protein kinase and Beclin 1 in mediating autophagy**. *Circ Res* 2007, **100**(6):914-922.

43. Taneike M, Nishida K, Omiya S, Zarrinpashneh E, Misaka T, Kitazume-Taneike R, Austin R, Takaoka M, Yamaguchi O, Gambello MJ *et al*: **mTOR Hyperactivation by Ablation of Tuberous Sclerosis Complex 2 in the Mouse Heart Induces Cardiac Dysfunction with the Increased Number of Small Mitochondria Mediated through the Down-Regulation of Autophagy**. *PLoS One* 2016, **11**(3):e0152628.

44. Bitto A, Lerner C, Torres C, Roell M, Malaguti M, Perez V, Lorenzini A, Hrelia S, Ikeno Y, Matzko ME *et al*: **Long-term IGF-I exposure decreases autophagy and cell viability**. *PLoS One* 2010, **5**(9):e12592.

45. Lerner C, Bitto A, Pulliam D, Nacarelli T, Konigsberg M, Van Remmen H, Torres C, Sell C: **Reduced mammalian target of rapamycin activity facilitates mitochondrial retrograde signaling and increases life span in normal human fibroblasts**. *Aging Cell* 2013, **12**(6):966-977.

Chapter 4: The Role of Senescencent Myofibroblasts in Arrhythmogenesis in the Aged, Infarcted Heart

This chapter presents unpublished data.

The author contributed to this manuscript by performing histology (immunohistochemistry), *β*-galactosidase assays, and qPCRs. The author also served as the co-mentor to Yueming Cao, a Brown University undergraduate student volunteer, who performed analysis of rabbit cardiac histology under the direction of the author and his advisor. Tae Yun Kim and Bum Rak Choi performed and analyzed all optical mapping and electrophysiological data presented here as part of our collaboration.

Kevin R. Murphy[1,2], Patrick Morrissey[1], Yueming Cao[1], Yi Chun Lu[1], Jean M. Daley[1], Lorraine Schofield[1], Nilufer N. Turan[1], Karuppiah Arunachalam[1,3], Tae Yun Kim[1], Bum Rak Choi[1], and Gideon Koren[1]

[1]Cardiovascular Research Center, Division of Cardiology, Rhode Island Hospital, Warren Alpert Medical School of Brown University, Providence RI

[2]Department of Molecular Biology, Cellular Biology and Biochemistry, Brown University, Providence RI

[3]Department of Internal Medicine, Rhode Island Hospital, Warren Alpert Medical School of Brown University, Providence RI

Keywords: cellular senescence, *β*-galactosidase, fibrosis,

4.1 Abstract

Aging is associated with a more than 5 to 40-fold increase in the incidence of sudden cardiac death (SCD) over the age of 65. Our laboratory has developed a minimally invasive myocardial infarction (MI) model in young (5 – 9 months) and old (4 – 6 years) female New Zealand White rabbits that closely recapitulates human pathophysiology. Using this method, we generate reproducible infarcts of 25-35% of the free wall of the left ventricles (LV) of young and aged rabbits [1, 2]. The aged MI is extremely malignant, featuring increased incidence of VT/VF peri-procedurally. Further, ventricular fibrillation (VF) begets VF in the aged infarcted heart. Peri-procedural VF requires more defibrillation attempts due to recurrent VF. Aged animals that survived MI procedure display APD remodeling, slowing of conduction in the infarct border zone, and increased dominant VF frequencies 3-weeks post-MI. A small proportion of the surviving MI population (16%) experienced sudden cardiac death, which indicated our model shares the malignancy of MI seen in the human population [3].

This chapter also examines and compares the healing of the infarcted hearts in aged vs. young hearts. We hypothesized that age-related senescence response of aged cardiac myofibroblasts differs from that of young myofibroblasts and that these differences contribute to the pathogenesis of increased arrhythmogenesis of the aged hearts. We used senescence-associated beta galactosidase (SA-βGal) staining to quantify senescence in the scar zone, infarct border zone (IBZ), and remote zone (RZ). Our preliminary data revealed marked differences in the senescence response of cardiac myofibroblasts in young and aged hearts. After 3-weeks post-MI, we observed significantly more senescent myofibroblasts in the aged scar than young (21% ± 5% vs.

10% ± 3%) ($p<0.05$). Our data also showed that genes in the pathways that regulate senescence, such as p16, p21, p53, and TGF-β are transcriptionally upregulated in the 3-week post-MI group in both young and aged hearts. Senescence-associated secretory phenotypes (SASP) in scar zone are differentially expressed in scar vs remote zones as well as aged vs young hearts. Analysis of senescence patterns over a time course of 3-weeks post-MI revealed a delayed and persistent senescence response in the aging infarcted scar zone. In conclusion, our data demonstrate that myocardial infarction in the aged heart is associated with malignant arrhythmias and SCD. Moreover, the healing response of the aging heart post MI differs from that of the young heart. The persistent senescence in the infarct zone is likely to remodel neighboring myocardium. Targeting senescent cardiac myofibroblasts in the post-MI aged hearts may reduce chronic inflammation and arrhythmogenesis.

4.2 Introduction

Sudden cardiac death due to malignant ventricular tachyarrhythmia is a leading cause of death in industrialized countries each year [4]. Aging is a key risk factor for SCD, where one's risk increases 5-40-fold over age 65 [5, 6]. We have shown that aged rabbit hearts display mechanical and electrical differences compared to young hearts. Aged hearts display aortic stiffening in addition to increase in systolic stiffness and contractility and diastolic stiffness. Electrophysiological and optical mapping studies show aged-related anisotropic conduction velocity in addition to slower, age-related ventricular and His-Purkinje conduction [7]. Underlying all these changes is a marked increase in fibrosis assessed by histochemistry and MRI [8].

Initial efforts in collaboration with the Choi Lab at Brown University showed that despite changes in electrophysiology such as conduction disturbances, arrhythmia inducibility in aged rabbit hearts was not high and equivalent to young rabbit hearts under tachypacing, redox stress (H_2O_2), and isoproterenol with minimal success triggering arrhythmia. Because in 65% of human cases of SCD ischemic stress such as MI precede the fatal event [5, 6], we hypothesized that ischemic stress during aging may potentiate arrhythmias. Therefore, we developed a minimally invasive MI procedure to recapitulate physiology and SCD seen in the human heart post-MI [1, 2, 8]. After infarction aged hearts are extremely arrhythmogenic. Infarcted rabbits in the aging population displayed incidence of spontaneous VT/VF recorded by *in vivo* telemetry [1].

Cellular senescence plays an important role in wound healing and tissue repair [9-11]. Senescence is differentially regulated with age [12] and has negative impacts on tissue health [13-16]. Despite naturally occurring in aged tissues, senescent cells have remained elusive in aged cardiac tissues. Initial studies in our lab failed to detect senescent cells in young or aged rabbit hearts. One group showed that senescent myofibroblasts are present in infarct border zone in young mice 7 days after undergoing coronary artery ligation [16]. A recent study showed that the senescence of myofibroblasts is critical for limiting the fibrosis response in young hearts [17]. Importantly, senescent cells affect the surrounding tissues through paracrine effects. This process is the senescence-associated secretory phenotype [18]. For example, the secretion of cytokines, chemokines, growth factors, and matrix remodeling proteins all disrupt normal tissue homeostasis and promote a pro-inflammatory response [19, 20].

The goal of this study was to test the hypothesis that MI in the aged rabbits is associated with SCD. In addition, we hypothesized that changes in cellular senescence response to myocardial infarction during aging promote a pro-inflammatory phenotype that affects arrhythmogenesis. Importantly, we sought to investigate whether the senescence associated secretory phenotype is present and/or exacerbated during aging. Our results showed that aging MI leads the increased incidence of VT/VF peri-procedurally and that age hearts require more defibrillation attempts compared to young hearts. Aged hearts post-MI displayed APD remodeling, slow conduction and altered properties of VF. The results show that senescence of myofibroblasts occurs in both young and aged animals, but that the senescence response is delayed and persistent over 3-weeks post-MI. Strikingly, at 3-weeks post-MI factors such as p16, p21, and TGF-β are upregulated (to a greater extent) in the scar zones of aged rabbit infarcts compared to young, displayed more SA-βGal-positive myofibroblasts, and an upregulated, pro-inflammatory senescence-associated secretory phenotype. We conclude that the aged infarct heals differently and contains more senescent myofibroblasts in the scar zone that may lead to a persistent inflammatory response that can trigger lethal arrhythmia sustained by the aging heart.

4.3 Methods

Animal Ethical Statement

This investigation conformed to the current Guide for Care and Use of Laboratory Animals published by the National Institutes of Health (NIH Publication No. 85–23,

revised 1996), as well as the standards recently delineated by the American Physiological Society (Guiding Principles for Research Involving Animals and Human Beings), and was approved by the Institutional Animal Care and Use Committee at Rhode Island Hospital. Adult female rabbits (3.5–5.5 kg) ages 6–12 mo were used for young group, and ages 4.0-5.5 yo were used for aged group [21]. The prophylactic drug regimen includes 3 days of oral amiodarone, 400 mg given twice daily 6 to 8 hours apart prior and 400 mg the day following the experimental MI. Rabbits were anesthetized with intramuscular ketamine/xylazine (25 mg/kg/3.75 mg/kg) and buprenorphine (0.03 mg/kg), intubated, and ventilated with isoflurane (1–2%, FiO_2 0.5). Blood pressure and peripheral oxygen saturation were measured continuously. A continuous 12-lead ECG was recorded during the induction of myocardial infarction. Procedurally, a bolus of intravenous amiodarone (5 mg/kg) is given during a 20 minute period before and again 40 minutes after coronary coil placement, with a continuous infusion (12.5 mcg/kg/min) between the boluses. Additionally, premature ventricular contractions (PVC's) are suppresed with intravenous lidocaine using a bolus of 1 mg/kg and an 40 mcg/kg/min infusion.

Tissues

Rabbit hearts were excised from young (6-12 months) and old (4-6 years) female, New Zealand White rabbits (RSI Farms, Mocksville, NC, USA) as previously described [2]. The rabbits were anaesthetized with ketamine (60 $mg \cdot kg^{-1}$), xylazine (15 $mg \cdot kg^{-1}$ IM) and buprenorphine (0.03 $mg \cdot kg^{-1}$ SQ), and sodium pentobarbital (150 $mg \cdot kg^{-1}$, IV). Hearts were quickly excised after thoracotomy and washed in PBS. Heart tissue for histological

analysis was coated and embedded in optimal cutting temperature (OCT) compound solution (Fisher Scientific, Waltham, MA, USA) and rapidly frozen on liquid nitrogen. Heart tissue for biochemical analysis was snap frozen in liquid nitrogen and stored immediately at -80°C.

Optical Mapping of Epicardial Surface and Data Analysis

Hearts were excised and retrogradely perfused through the aorta with 20ml/min rate in a Langendorff perfusion system (Radnoti Glass Technology, Monrovia) with (in $mmol*L^{-1}$) 130 NaCl, 24 $NaHCO_3$, 1.0 $MgCl_2$, 4.0 KCl, 1.2 NaH_2PO_4, 5 Dextrose, 25 Mannitol, 1.25 $CaCl_2$, at pH 7.4, and gassed with 95% O2 and 5% CO2. Fluorescence images from the anterior surface and LV free wall of the heart were captured using a CMOS camera (100x100 pixels, Ultima-L, SciMedia, Japan), and the field of view was set to 2.0x2.0 cm^2 (spatial resolution of 200x200 μm^2). The sampling rate was set to 1,000 frames/s, and data were analyzed with a custom-built software program developed in Interactive Data Language (Harris Geospatial Solutions). Hearts were stained with a voltage-sensitive dye, di-4-ANEPPS (Thermo Fisher Scientific), using 25 µL of stock solution (1 $mg*ml^{-1}$ of dimethyl sulfoxide, DMSO) delivered through a bubble trap, above the aortic cannula.

The action potential durations were calculated the difference between activation and repolarization time points. The activation and repolarization time points at each site were determined from fluorescence (F) signals by calculating $(dF/dt)_{max}$ and $(d2F/dt2)_{max}$. Data were filtered using a spatial Bilateral filter (5x5 pixel), and first/second derivatives were calculated using a temporal polynomial filter (3^{rd} order, 13 points). Action potential

conduction velocity was calculated using, the spatial gradient of activation time (11x11 pixels) and spatial resolution of acquired image (200 μm/pixel).

β-galactosidase Assay

β-galactosidase staining was performed with modifications as previously performed by Dimri *et al.* and Debacq-Chainiaux *et al*. [22, 23]. Tissue sections immediately after cutting were immersed in 0.5% glutaraldehyde (in 1X PBS) for 15 minutes then placed in fresh 1x PBS. Sections were then incubated at 37°C with no CO_2 with fresh *β*-galactosidase staining solution (40 mM citric acid/Na phosphate buffer, 5 mM $K_4[Fe(CN)_6]\cdot 3H_2O$, 5 mM $K_3[Fe(CN)_6]$, 150 mM sodium chloride, 2 mM magnesium chloride and 1 $mg\cdot ml^{-1}$ X-gal) for 18hours. Sections were counterstained with haematoxylin and eosin as previously described [24].

RNA Isolation and cDNA Synthesis

Tissue from LV scar zone, infarct border zone, and remote zone (40-50 mg) was processed using the RNeasy Fibrous Tissues kit (Qiagen, Valencia, CA, USA) using the predefined protocol. The nucleic acid concentration of the RNA was determined using the NANODROP 2000c Spectrophotometer (Thermo Fisher, Waltham, MA, USA). Reverse transcription was performed to produce cDNA using the iScript reverse transcription kit (BioRad, Hercules, CA, USA). Reverse transcriptions were performed using the C1000 Thermocycler (Biorad, Hercules, CA, USA).

Forward/reverse Primer Design and Conventional PCR

Primer sets were designed for each gene of interest as well as endogenous control. National Center for Biotechnology Information gene database (https://www.ncbi.nlm.nih.gov/gene) was used to obtain accession numbers for each gene, and Primer Blast tool (https://www.ncbi.nlm.nih.gov/tools/primer-blast/) was used to yield several primer sets for each gene. Primer sets were selected for each gene of interest for subsequent testing.

Quantitative PCR (qPCR) for Primer Efficiency and Validation

The efficiencies of the selected primer set for each gene were determined (Table 4.2) to accurately calculate normalized change gene expression (ΔC_T). SybrGreen-based qPCR using 40 ng, 4 ng, 0.4 ng, 0.04 ng, and 0.004 ng of cDNA from rabbit LV free wall tissue was performed in triplicate for each primer set using a ViiA7 qPCR machine (Thermo Fisher, Waltham, MA, USA). SRP14 control [25] and no template were used as positive and negative controls, respectively. Standard curves, melt curves, and primer efficiency were reported by the ViiA7 QuantStudio software.

Statistical Analysis

Data are presented as mean ± SD of *n* measured cells or rabbits. Statistical comparisons between groups were performed with Student's *t* test unless otherwise stated. Differences were considered statistically significant at $p< 0.05$.

Analysis of gene transcript expression data was performed using GLIMMIX procedure in SAS Version 9.4 (SAS Inc.). Multiple comparisons of dCT target expression testing were performed using Holm–Bonferroni corrections. Heatmaps of fold-change expression values were constructed using Origin Pro 2017. For all analyses, differences were considered statistically significant at $p<0.05$.

4.4 Results

Aged Rabbit Hearts are Prone to Arrhythmia and Sudden Cardiac Death

Myocardial infarctions were performed in young and aged rabbits. 76% of all animals survived MI procedure (38 of 47 young vs. 46 of 64) (Table 4.1). MI in our aging population was extremely arrhythmogenic, where aged rabbits that died peri-procedurally died almost exclusively from arrhythmia (5 of 9 young vs. 17 of 18 aged) ($p<0.05$, fishers exact test) (Table 4.1). These rabbits experienced VT/VF peri-procedurally whereas young rabbits do not die exclusively from VT/VF but also from hemodynamic stress or other non-VT complications. A small percentage (16%) of the surviving animals experienced unwitnessed sudden death. Of those rabbits surviving the MI procedure that died suddenly, most animals experienced SCD within 72 hours of MI (5 of 6 young vs. 11 of 12 aged) (Table 4.1).

A subset of the rabbit population was closely monitored peri-procedurally for occurrence of arrhythmia (VT/VF) and number of defibrillation attempts required for successful cardioversion. The results showed that aged rabbits experience VF more frequently than young (6 of 31 young vs. 21 of 56 aged) ($p<0.05$) (Fig 4.1A). Further, aged rabbits require 5.4 defibrillation attempts to successfully cardiovert compared to 3.1

attempts for young rabbits ($p<0.05$) (Fig. 4.1B). VF-begets-VF in the aging heart. Most defibrillation attempts were not successful, under 30% (Fig 4.1C). Figure 4.1D illustrates the onset of VF in young and aged rabbits and the average result after defibrillation attempt. Lastly, although there is no significant difference in the survivorship between age groups, aged animals display a trend of lower survivorship after MI procedure (Fig 4.1E).

Optical Mapping of Infarcted Young and Aged Rabbit Hearts

High resolution optical mapping of the epicardial surface of infarcts (achieved with our minimally invasive MI procedure [1, 2]) showed prolonged action potential duration (APD) in infarct border zone vs. remote zone in aged hearts (180.1 ms vs. 170.3 ms) (Fig 4.2). Aged hearts also presented slowed conduction velocity in the infarct border zone vs. remote zone (0.34 ± 0.09 m/s vs. 0.95 ± 0.13 m/s) ($p<0.05$). Interestingly, a previously studied cohort of young animals showed a shortened infarct border zone APD compared to remote zone (200.1 ms vs. 217.7 ms) (Fig 4.2C) ($p<0.05$). This electrical remodeling of prolonged APD and slowed conduction in the infarct border zone of aged hearts was associated with cardiac alternans mainly in the border zone and frequent reentrant arrhythmia formation. Further analysis of the action potentials in young and aged mice revealed an increased VF frequency in aged hearts. Despite the prolongation of APD in the border zone of aged infarcts, the VF frequency was greater than in young hearts (Fig 4.3) ($p<0.05$).

The Aging Scar is Enriched with Senescent Myofibroblasts

Blocking of the first marginal brunch of the circumflex artery leads to a scar of about 30% of the free wall of the left ventricle (Fig 2.7 from **Chapter 2**). To analyze the histopathology of the healing infarcted heart, the rabbit heart was therefore divided into three zones: the scar zone that includes the area of the transmural infarct, the infarct border zone, and the remote zone that was not directly affected by the procedure (Figure 4.4B). After three weeks of healing, the remote zone and infarct border zone exhibits electrical remodeling of the APD (Fig 4.4C) and the presence of arrhythmogenic APD alternans (Fig 4.4D). In order to better understand the remodeling effects our functional experiments uncovered, we next investigated the presence of cellular senescence in young and aged hearts three weeks post-MI. Tissue sections were incubated in SA-βGal using previously established methods [22]. Fig 4.5A shows a representative aged MI cross-sectional view that contains protected transverse muscle strands, infarct/scar, a clearly delineated infarct border zone, and remote zone tissue. SA-βGal experiments and 40x imaging revealed the presence of SA-βGal-positive cells in the infarct and border zones of both young and aged animals (Fig 4.5B). Interestingly, there are no senescent cells in the remote zones of either aged or young tissues which corroborate previous findings from our lab. Quantification of the numbers of senescent cells showed an accumulation in aged scar zones compared to young (21% ± 5% vs. 10% ± 3% SA-βGal-positive) ($p<0.05$) (Fig 4.5C) with no difference in the myocardium leading up to the scar border.

Senescent cells are present after injury in the heart and the response is differentially expressed with age. Immunohistochemistry was performed on serial

sections to SA-βGal stained sections to identify the cell type undergoing this shift. Indeed, in both aged and young animals α-SMA positive cells co-localize in serial sections with SA-βGal positive cells (Fig 4.5D). This indicated that in accord with previous wound healing studies, senescent myofibroblast accumulated in response to injury and disease [26, 27].

Senescence Response to Injury in the Aging Heart Is Dynamic and Persistent

To test the hypothesis that cellular senescence is dysregulated during aging, we performed a time course of SA-βGal staining in sections after one, two, and three weeks post-MI (Fig 4.6). SA-βGal was measured as the number of senescent fibroblasts as a percentage of total cells. Young vs. aged senescence in the infarct border zone were as follows: one-week post-MI (14% ± 4% vs. 6% ± 6%), two weeks post-MI (6% ± 4% vs. 7% ± 4%), and three weeks post-MI (2% ± 1% vs. 1% ± 0%). In the scar zone one-week post-MI (21% ± 9% vs. 14% ± 9%), two weeks post-MI (13% ± 3% vs. 24% ± 3%) ($p<0.05$), and three weeks post MI (10% ± 3% vs. 21% ± 5%) ($p<0.05$). No cellular senescence was detected in remote zone, in accord with previous experiments from our lab where normal healthy hearts do not exhibit any cellular senescence (data not shown). These data support a model of delayed and persistent senescence response through the scar of the aged, infarcted heart.

Pathways Controlling Cellular Senescence and SASP are Altered Transcriptionally After Injury and During Age

To identify the molecular controllers of cellular senescence in infarction tissues, gene expression analysis by qPCR was performed. All custom designed, rabbit-specific, primer sequences and genomic targets can be found in *Table 4.2***.** Analysis of p16, p21, and p53 show upregulation in response to injury (scar zone has the highest fold change expression compared to remote) ($p<0.05$) and to age (aged hearts contain higher fold change expression compared to young) ($p<0.05$). For the first time we present data in an age appropriate model of MI comparing senescence response in young and aged hearts. Transcript analysis showed the upregulation of genes controlling the senescence response such as p16 and p21 after injury, and highlights the dramatic enrichment of senescence in the aged scar zone compared to young injury (Fig 4.7 and Table 4.3). Further analysis of SASP revealed dramatic increased expression of SASP factors, especially in the aged scar. Transcripts previously characterized as part of the SASP such as immune factors IL-6, CCL2 (MCP-1), and CXCL2 or matrix remodeling factors such as MMP9, TIMP1, and TIMP2 were analyzed. Expression of these targets was mildly upregulated in the injury zones of young animals, however the aged scar exhibited the highest fold change enrichment ($p<0.05$) (Fig 4.7 and Table 4.3). These data indicate the genetic program during aging is upregulated after injury compared to young.

4.5 Discussion

The Aged Heart is Arrhythmogenic

Changes in electrotonic tone are extremely arrhythmogenic [28]. Structural remodeling post-MI may underlie the formation and propagation of extra systolic activity that can develop to sustained and lethal arrhythmia [29]. These localized disturbances due to tissue heterogeneity are thought to slow conduction velocity and promote the formation of ectopic activity [30]. Indeed, fibrotic, aged rabbit hearts contained a prolonged APD in the IBZ compared to young hearts and displayed a decrease in conduction velocity. VT/VF is easily induced in aged hearts post-MI under ramp pacing protocol. VT/VF post-MI occurs spontaneously after myocardial infarction, similarly to humans. Indeed, with transmural scar formation optical mapping showed APD differences between the remote and border zones, which underlies pro-arrhythmic alternans in the infarct border zone.

In addition to functional changes post-MI, during the MI procedure it was noted that aged animals were susceptible to an increased incidence of lethal VT/VF compared to young animals. The events required more defibrillation attempts and were generally less successful. In addition to the electrical remodeling visualized after MI via optical mapping we reported a significant increase in the arrhythmogenesis of the aged myocardium peri-procedurally.

Cellular Senescence is Present Post-MI in Cardiac Myocardium

At baseline, senescent fibroblasts are not present in cardiac tissue. Post-MI senescent cells have been reported in low quantities in mouse MI models following left coronary artery ligation using young mice. This report showed that p53/p21 pathway was responsible for the senescent response in myofibroblasts post MI [16]. Because oxidative stress is a potent inducer of cellular senescence, we tested if cellular senescence was differentially induced with aging in response to MI injury.

Using tissue sections from rapidly frozen hearts we characterized the cellular senescence response post-MI using SA-βGal staining to directly visualize senescent cells. Sections of whole LV free wall revealed a significant accumulation of senescent cells through the scar zone 3 weeks post-MI. Quantification of proportion of cells that exhibit senescent phenotype revealed a two-fold enrichment in aged scars compared to young. Indeed, previous reports have implicated cellular senescence in the heart as a modifier of fibrosis [16]. However, the question remains whether modifying senescence in the heart post-MI will modify the scar and/or alter electrical behavior in the infarct border zone. One potential effect of modifying senescence is that the extracellular matrix is differentially maintained by the SASP post-MI [17]. Another possibility is the SASP could recruit an arrhythmogenic inflammatory response. Indeed, cell types in immune response such as macrophages can modulate electrical conduction [31] and participate in arrhythmogenesis via interleukin production [32]. Chronic inflammation after aged MI may be a cause of APD prolongation in the infarct border zone [33, 34].

We showed a dynamic response over a three-week time course post-MI where senescent myofibroblasts are quickly cleared from young hearts, but expression is

delayed and persistent in aged hearts. Chronic or persistent senescent cells can secrete increased amounts of proinflammatory proteins and contribute to chronic inflammation [35]. Alternatively, a persistent senescence response could be due to the failure to clear senescent cells. Innate immune response is critical for the clearance of senescent cells via antigen-specific mechanisms, and defective adaptive immunity impedes the clearance of senescent cells [36]. These hypotheses are yet to be tested in aged cardiac tissue. This chronic inflammatory response is likely pro-arrhythmogenic in the aging heart.

Senescence Post-MI is Delayed and Persistent During Aging

Three weeks post-MI analysis of rabbit aged hearts showed a marked increase in SA-βGal staining as well as a pro-senescence and inflammatory molecular signature compared to young infarcts. Senescence is a wound healing response *in vivo*, therefore we sought to investigate the cellular senescence response post-MI at one, two, and three weeks. We found a delayed and persistent senescence response in aged hearts post-MI.

Senescence in the infarct border zone cleared quickly after one week. It appeared that young hearts mount a large response initially whereas aged animals do not mount a response. The scar zone senescence response in young MI peaked at or before one week and the cells were cleared over three weeks. In contrast, aged hearts achieved maximum senescence response at two weeks post-MI that persisted through three weeks. Hence, the aged heart appears to exhibit a delayed and persistent senescence response during aging.

The chronic expression of senescent cells has been linked to a pro-inflammatory state due to secreted SASP factors [19]. Our data showed increased expression of pro-

inflammatory factors such as CCL2 and CXCL2. These proteins are responsible for attraction of monocytes and macrophages, respectively. Persistent expression of the factors could lead to a chronic inflammatory phenotype. Chronic inflammation during aging, or inflammaging, has been linked to atrial and ventricular arrhythmias in aged patients [37]. Others have reported that inflammation can be an arrhythmic trigger [38, 39].

Persistent expression of MMPs and TIMPs could modify the extracellular matrix leading to the formation of lethal arrhythmia [40, 41]. Changes in collagen in the matrix can affect tissue anisotropy through fibroblasts [42]. Extracellular matrix composition alterations are linked with changes in gap junction proteins like Cx43 and ion channel expression [43]. Changes in MMPs and TIMPs and the ratios at which they express to modify the matrix have been shown to underlie malignant ventricular arrhythmia [44].

Conclusion

We posit the persistence of senescent myofibroblasts through the scar will negatively modify the surrounding tissue microenvironment underlying the pro-arrhythmic changes observed during aging post-MI. Aged hearts are prone to VT/VF peri-procedurally indicating that aging is an important factor that predisposes the heart to the propagation of lethal arrhythmia. Although the senescence response may initially be critical for limiting fibrosis and scar formation, the long-term expression will promote negative effects and the upregulation of a secreted program of chemokines, interleukins, and matrix remodeling factors that lead to a prolonged inflammatory, malignant state post-MI. The upregulation and persistence of chronic inflammatory response may promote

triggered activity surrounding the scar zone. Therefore, cellular senescence is a novel target post-MI to reduce the amount of age-related arrhythmia and sudden cardiac death.

Acknowledgements

The authors would like to thank Dr. Christoph Schorl at the Brown University genomics core facility for his expertise and consultation. Both he and Dr. Marco DeCecco were extremely helpful in designing and validating rabbit specific primer sets for senescence and SASP targets.

4.6 Figures and Tables

Figure 4.1: Aging MI Display Increased Propensity for Arrhythmia Peri-Procedurally

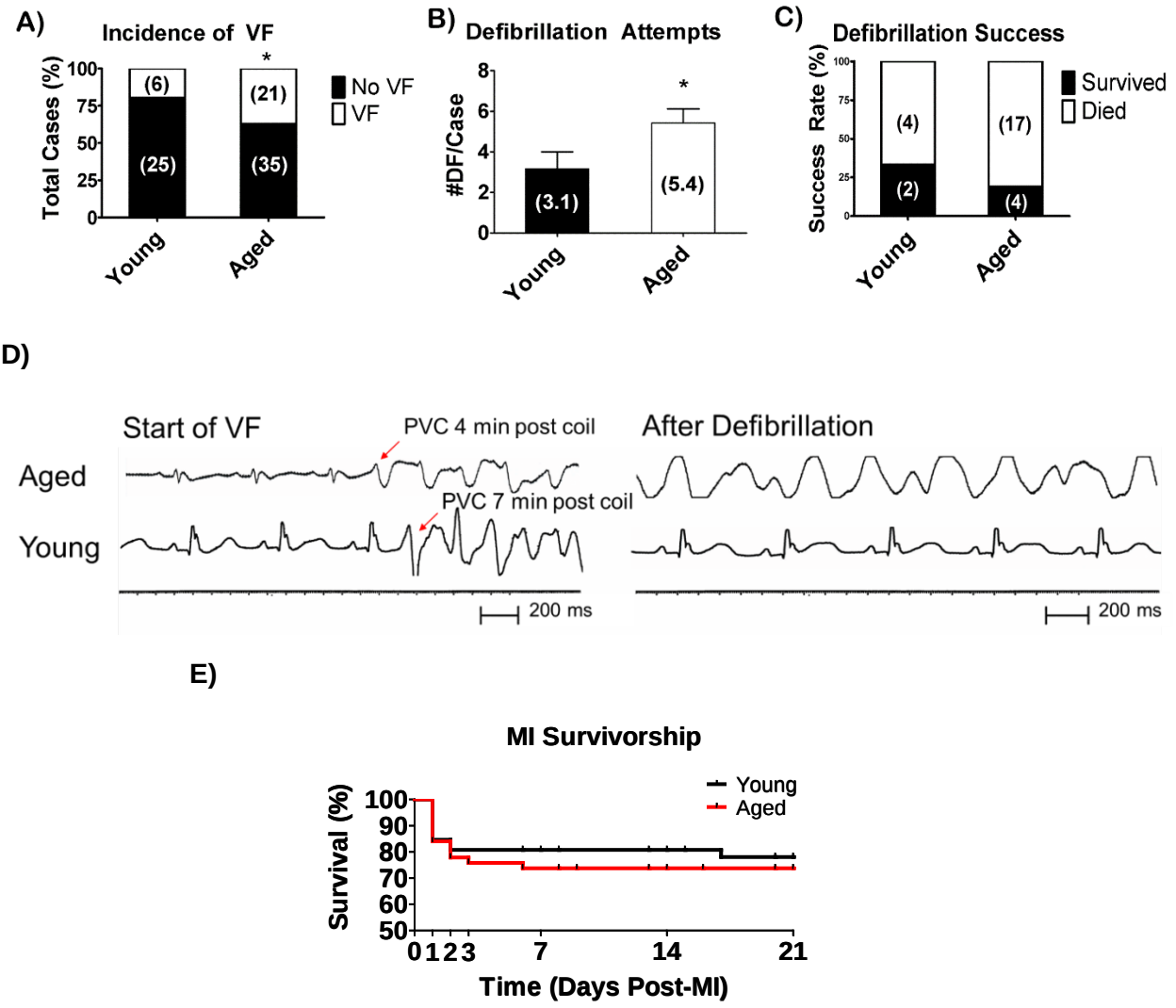

(A) Aged animals display increased peri-procedural death due to VT/VF (p = .03 Fisher's exact 2X2). (B) Incidence of VF and defibrillation in aged and young animals. (C) Aged animals require more DF attempts (p<0.05, student's t-test). (D) Instance of recurrent VF after defibrillation in an aged rabbit after 4 DF attempts. Instance of successful defibrillation in one young animal. (E) Kaplan-Meier curve showing

survivorship of animals that finished the MI procedure. All values are mean ± SEM, *p<0.05.

The arrhythmia analysis was performed by Patrick Morrisey. The survival statistics were performed by the author.

Figure 4.2: Aged MI Exhibit Conduction Abnormalities in the IBZ

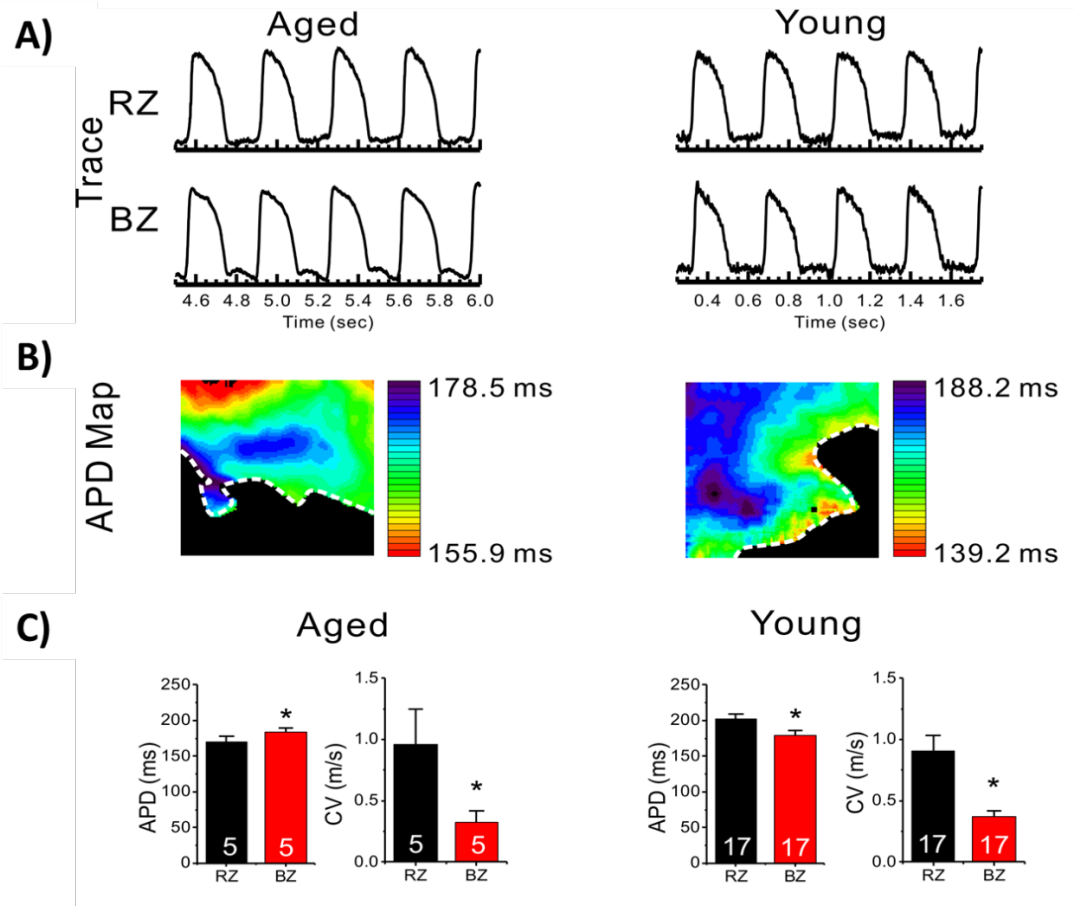

(A) Action Potential tracings from the Remote zone and infarct zone. (B) Action Potential duration maps show differences around the scar (black area) (C) In aged rabbits (n=5), APD in the border zone was significantly prolonged. In contrast, APD in young rabbits (n=17) was significantly shortened. Both young and old hearts show slow conduction in the infarct border zone.

These experiments were performed by Dr. Tae Yun Kim and Dr. Bum Rak Choi and developed in collaboration with the Choi lab at CVRC.

Figure 4.3 Dominant VF Frequencies in MI Hearts

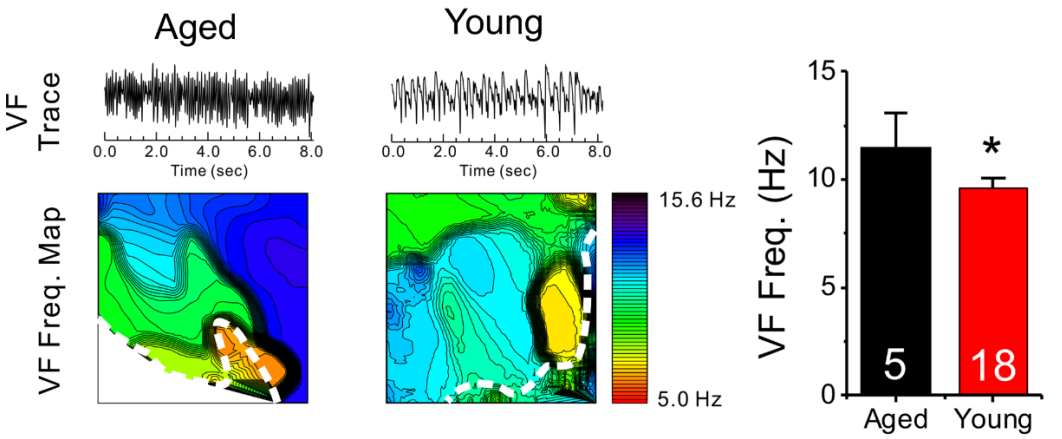

Optical action potentials of VF in Aged and Young hearts. VF frequency maps show more area with higher VF frequency in aged hearts. Despite prolongation of APD in MI border zone in aged rabbits, VF frequencies were higher compared to young MI. All values are mean ± SEM, *p<0.05.

These experiments were performed by Dr. Tae Yun Kim and Dr. Bum Rak Choi and developed in collaboration with the Choi lab at CVRC.

Figure 4.4: Infarcted Rabbit Hearts Display Electrical Remodeling

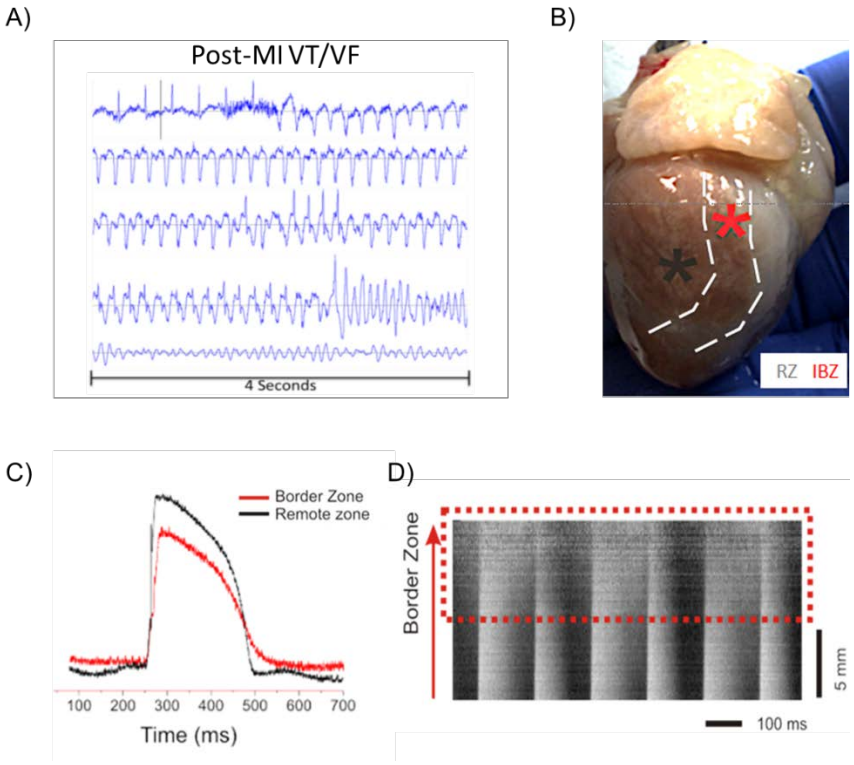

(A) *In vivo* telemetry showing initiation of VT degrading to VF in rabbits 18 hours post-MI. (B) Gross anatomical view of a rabbit heart post-MI. White lines demarcate (from left to right) the remote zone, infarct border zone, and scar zone. (C) APDs from remote zone and infarct border zone. Microelectrodes were placed at the sites notated by stars in panel B. (D) The infarct border zone shows larger APD alternans than the remote zone, associated with conduction block and VF induction.

These experiments were performed by Dr. Tae Yun Kim and Dr. Bum Rak Choi and developed in collaboration with the Choi lab at CVRC.

Figure 4.5: The Aging Scar Contains More Senescent Myofibroblasts

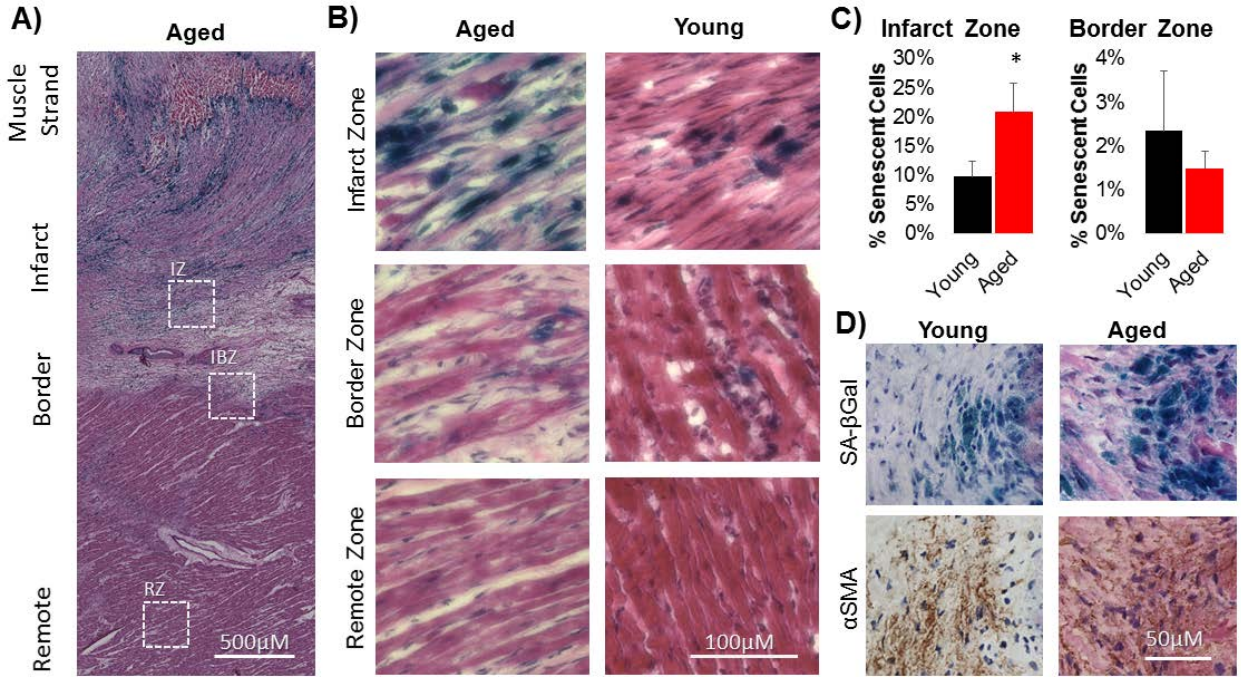

(A) Aged heart stained with X-Galactosidase to look for Senescence Associated β-Galactosidase (SA-βGal), an indicator of senescence in cells. H&E was used as the counter stain. Regions were identified as remote, border, infarct, and muscle strand. (B) Zoomed-in view of infarct zone, border zone, and remote zone in aged vs. young hearts. (C) Aged hearts have more senescent cells in the infarct zone. (D) Visuals of SA-βGal patterns and αSMA staining in the same region in young vs. aged hearts. n= 5 young and 8 aged animals. All values are mean ± SEM, *p<0.05, student's t-test.

Figure 4.6: Senescence Response is Delayed and Persistent in Aging MI

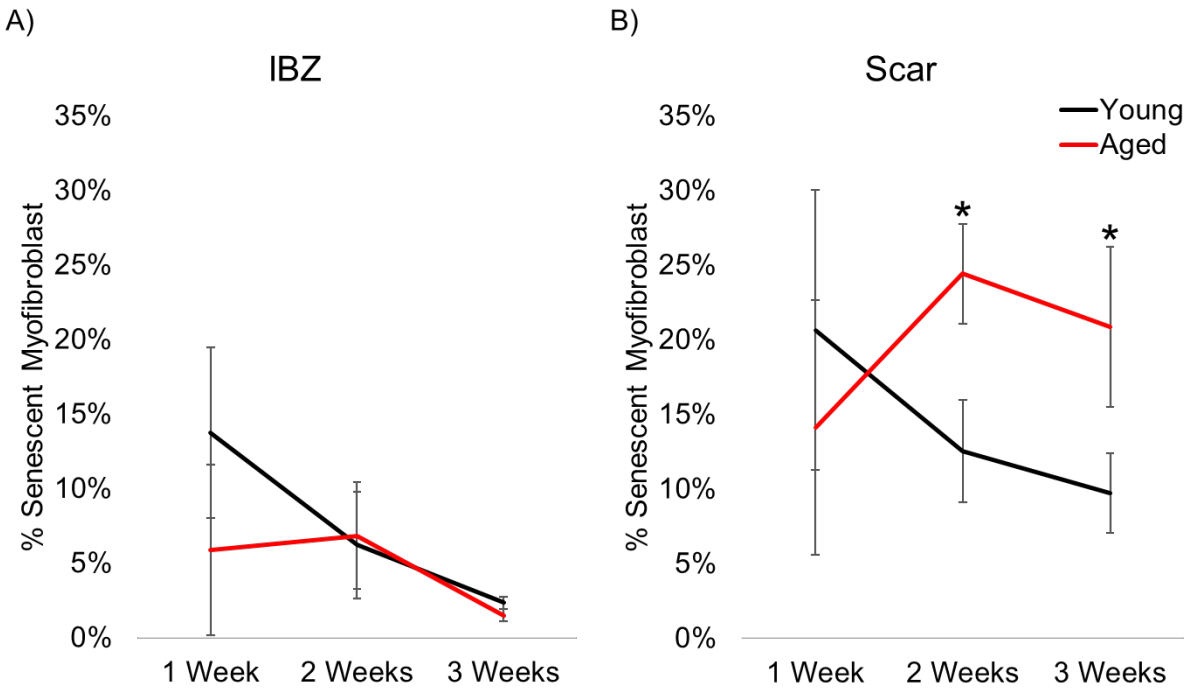

Time course of SA-βGal staining post-MI after one, two, or three weeks. (A) Senescence is quantified in the infarct border zone. (B) Senescence is quantified in the scar zone. n=3 young and 4 aged animals at one and two weeks. n=5 young and 8 aged at three weeks. All values are mean ± SEM, *p<0.05, student's t-test.

Figure 4.7: The Genetic Program of Senescence is Upregulated During Cardiac Injury and Aging

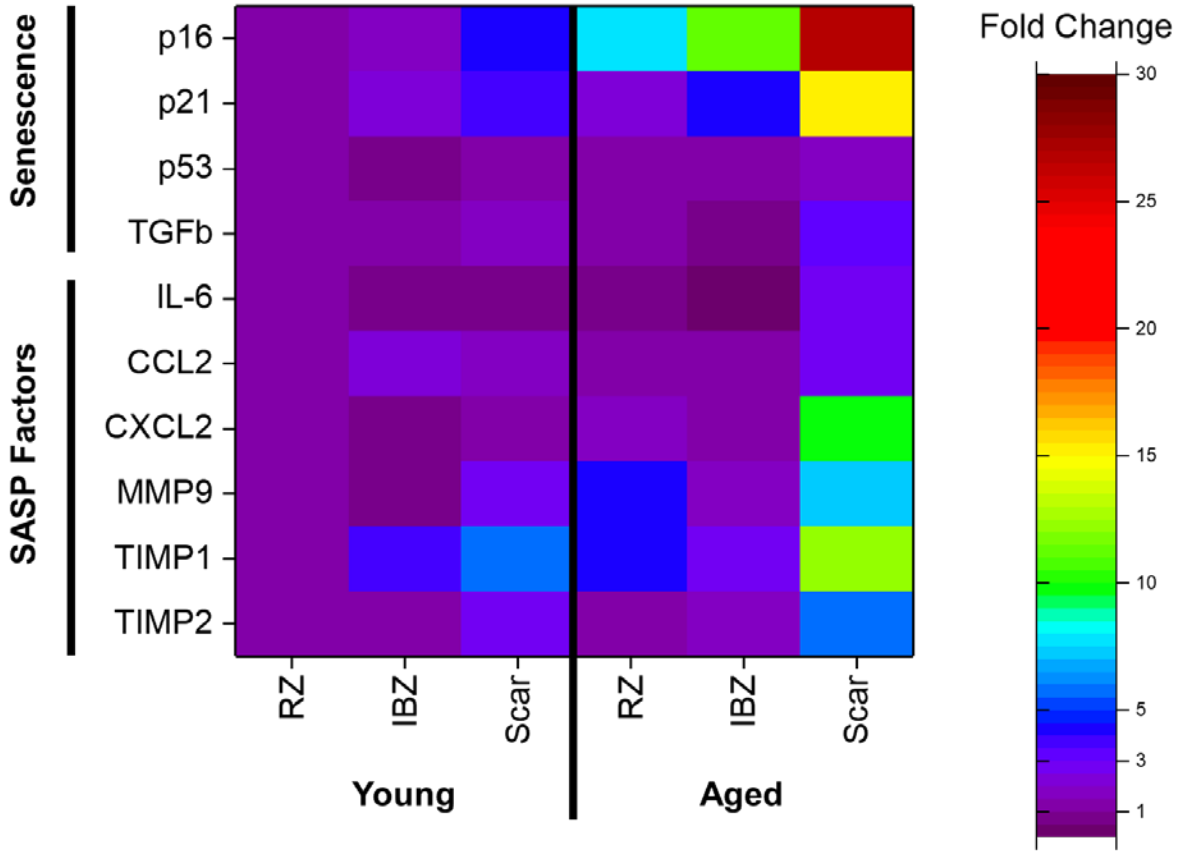

Young and aged samples from remote zone, infarct border zone, and scar zone were isolated 3 weeks post-MI and were analyzed for the indicated mRNA by qPCR. Signals were normalized to the young remote zone. Signals higher than baseline reported in young remote zone are shown as increasing temperature on the heatmap. n=6 animals per age group.

Table 4.1: MI in Aged Rabbits is Arrhythmogenic

	Count	Procedural Deaths*		Procedural Survival	Sudden Cardiac Death		Completion
		VT/VF	*Non-VT/VF*		*Acute (<72hr)*	*Chronic (>72hr)*	
Young	47	5	4	38	5	1	32 (68%)
Aged	64	17	1	46	11	1	34 (53%)
TOTAL	111	27 (24%) *		84 (76%)	18 (16%)		66 (60%)

Overview of rabbit survival statistics of the novel minimally invasive myocardial infarction procedure. Procedure death and survival are reported as a percentage of the total count. Rabbits that experienced sudden cardiac death or protocol completion were reported as a fraction of animals that survived the infarction procedure. *$p<0.05$, fishers exact test.

Table 4.2: Rabbit Specific Primers used for qPCR

	Primer/probe Sequences (5'-3')	Efficiency
SRP14	Accession: XM_002717984.2 Forward: 5' – TTCCAGAAATGCCGGTTGTC – 3' Reverse: 5' – CAAAGCCCTCCACAGAACCTT – 3'	102%
p16	Accession: XM_008255019.2 Forward: 5' – GCCGAAGGCGGTAACCA -3' Reverse: 5' – GCTTCGATGCTGGACTTCTCA – 3'	96%
p21	Accession: XM_002714669.2 Forward: 5' – GAGACTGCGACGCACTCATG – 3'' Reverse: 5' – CGCTCCCAGGCGAAGTT – 3''	98%
p53	Accession: XM_017348089.1 Forward: 5' – CCTGGAGCTCTGGTCTGAGATC – 3' Reverse: 5' – CCACCACGTCAAATACCCCTAA – 3'	100%
TGFβ	Accession: XM_008249704.2 Forward: 5' – CACCCGCGTGCTAATGGT – 3' Reverse: 5' – CCGGAGCTCTGACGTGTTAAA – 3'	97%
IL-6	Accession: NM_001082064.2 Forward: 5' – GAAAACACCAGGGTCAGCAT – 3' Reverse: 5' – TGAGGGTGGCTTCTTCATTC – 3'	107%
CCL2	Accession: NM 001082294.1 Forward: 5' – TGAATTCCCCAGTCACCTGC – 3' Reverse: 5' – TTGGGACACTTGGTGCTGTT – 3'	97%
CXCL2	Accession: XM_002717021.3 Forward: 5' – AGACCGTGCAGGGCATTC – 3' Reverse: 5' – GACTTGAGCGTGGCTATGACTTC – 3'	101%
MMP9	Accession: NM_001082203.1 Forward: 5' – TCCAACTTTGACAGCGACA – 3' Reverse: 5' - GGAGTGATCCAAGCCCAGTG – 3'	109%
TIMP1	Accession: XM_008272340.2 Forward: 5' – GCAACTCCGACCTTGTCATC – 3' Reverse: 5' – AGCGTAGGTCTTGGTGAAGC – 3'	100%
TIMP2	Accession: XM_008252510.2 Forward: 5' – GCGAGAAGGAGGTGGACT – 3' Reverse: 5' – TTGTCGGGGCCTTTGAACAT – 3'	103%

Table 4.3: Fold-Change Gene Expression of Senescence and SASP Targets

	Young			Aged		
	RZ	IBZ	Scar	RZ	IBZ	Scar
p16	1.00	1.93*	4.32*	7.73*	11.39*,†	26.54*,†,§
p21	1.00	2.04	3.53*	2.30	4.23*,†	15.03*,†,§
p53	1.00	0.90	1.27	1.12	1.18	1.75*,†,§
TGFβ	1.00	1.02	1.86*	1.16	0.95	3.04*,†,§
IL-6	1.00	0.70	0.85	0.54	0.23	2.75†,§
CCL2	1.00	2.00	1.77	1.38	1.07	2.81*,†,§
CXCL2	1.00	0.92	1.24	1.62	1.38†	9.71*,†,§
MMP9	1.00	0.51	2.53	4.44	1.52	7.16§
TIMP1	1.00	3.94	5.94*	4.29	2.71	12.04§
TIMP2	1.00	1.39*	2.79*	1.29	1.79†	5.86†,§

*p<0.05 compared to young RZ. †<0.05 compared to aged RZ. §<0.05 compared to aged IBZ.

4.7 References

1. Ziv O, Schofield L, Lau E, Chaves L, Patel D, Jeng P, Peng X, Choi BR, Koren G: **A novel, minimally invasive, segmental myocardial infarction with a clear healed infarct borderzone in rabbits**. *Am J Physiol Heart Circ Physiol* 2012, **302**(11):H2321-2330.
2. Morrissey PJ, Murphy KR, Daley JM, Schofield L, Turan NN, Arunachalam K, Abbott JD, Koren G: **A novel method of standardized myocardial infarction in aged rabbits**. *Am J Physiol Heart Circ Physiol* 2017, **312**(5):H959-H967.
3. Adabag AS, Therneau TM, Gersh BJ, Weston SA, Roger VL: **Sudden death after myocardial infarction**. *JAMA* 2008, **300**(17):2022-2029.
4. Deo R, Albert CM: **Epidemiology and genetics of sudden cardiac death**. *Circulation* 2012, **125**(4):620-637.
5. Zheng ZJ, Croft JB, Giles WH, Mensah GA: **Sudden cardiac death in the United States, 1989 to 1998**. *Circulation* 2001, **104**(18):2158-2163.
6. Podrid PJ, Myerburg RJ: **Epidemiology and stratification of risk for sudden cardiac death**. *Clin Cardiol* 2005, **28**(11 Suppl 1):I3-11.
7. Koura T, Hara M, Takeuchi S, Ota K, Okada Y, Miyoshi S, Watanabe A, Shiraiwa K, Mitamura H, Kodama I *et al*: **Anisotropic conduction properties in canine atria analyzed by high-resolution optical mapping: preferential direction of conduction block changes from longitudinal to transverse with increasing age**. *Circulation* 2002, **105**(17):2092-2098.
8. Cooper LL, Odening KE, Hwang MS, Chaves L, Schofield L, Taylor CA, Gemignani AS, Mitchell GF, Forder JR, Choi BR *et al*: **Electromechanical and structural**

alterations in the aging rabbit heart and aorta. *Am J Physiol Heart Circ Physiol* 2012, **302**(8):H1625-1635.

9. Tchkonia T, Zhu Y, van Deursen J, Campisi J, Kirkland JL: **Cellular senescence and the senescent secretory phenotype: therapeutic opportunities**. *J Clin Invest* 2013, **123**(3):966-972.
10. Demaria M, Ohtani N, Youssef SA, Rodier F, Toussaint W, Mitchell JR, Laberge RM, Vijg J, Van Steeg H, Dolle ME *et al*: **An essential role for senescent cells in optimal wound healing through secretion of PDGF-AA**. *Dev Cell* 2014, **31**(6):722-733.
11. Vande Berg JS, Robson MC: **Arresting cell cycles and the effect on wound healing**. *Surg Clin North Am* 2003, **83**(3):509-520.
12. Baker DJ, Childs BG, Durik M, Wijers ME, Sieben CJ, Zhong J, Saltness RA, Jeganathan KB, Verzosa GC, Pezeshki A *et al*: **Naturally occurring p16(Ink4a)-positive cells shorten healthy lifespan**. *Nature* 2016, **530**(7589):184-189.
13. Baker DJ, Wijshake T, Tchkonia T, LeBrasseur NK, Childs BG, van de Sluis B, Kirkland JL, van Deursen JM: **Clearance of p16Ink4a-positive senescent cells delays ageing-associated disorders**. *Nature* 2011, **479**(7372):232-236.
14. Campisi J: **Aging, cellular senescence, and cancer**. *Annu Rev Physiol* 2013, **75**:685-705.
15. Menendez JA, Alarcon T: **Senescence-Inflammatory Regulation of Reparative Cellular Reprogramming in Aging and Cancer**. *Front Cell Dev Biol* 2017, **5**:49.

16. Zhu F, Li Y, Zhang J, Piao C, Liu T, Li HH, Du J: **Senescent cardiac fibroblast is critical for cardiac fibrosis after myocardial infarction**. *PLoS One* 2013, **8**(9):e74535.

17. Meyer K, Hodwin B, Ramanujam D, Engelhardt S, Sarikas A: **Essential Role for Premature Senescence of Myofibroblasts in Myocardial Fibrosis**. *J Am Coll Cardiol* 2016, **67**(17):2018-2028.

18. Coppe JP, Patil CK, Rodier F, Sun Y, Munoz DP, Goldstein J, Nelson PS, Desprez PY, Campisi J: **Senescence-associated secretory phenotypes reveal cell-nonautonomous functions of oncogenic RAS and the p53 tumor suppressor**. *PLoS Biol* 2008, **6**(12):2853-2868.

19. Franceschi C, Campisi J: **Chronic inflammation (inflammaging) and its potential contribution to age-associated diseases**. *J Gerontol A Biol Sci Med Sci* 2014, **69 Suppl 1**:S4-9.

20. Rodier F, Coppe JP, Patil CK, Hoeijmakers WA, Munoz DP, Raza SR, Freund A, Campeau E, Davalos AR, Campisi J: **Persistent DNA damage signalling triggers senescence-associated inflammatory cytokine secretion**. *Nat Cell Biol* 2009, **11**(8):973-979.

21. von Holst D, Hutzelmeyer H, Kaetzke P, Khaschei M, Rödel HG, Schrutka H: **Social rank, fecundity and lifetime reproductive success in wild European rabbits (Oryctolagus cuniculus)**. *Behavioral Ecology and Sociobiology* 2002, **51**(3):245-254.

22. Debacq-Chainiaux F, Erusalimsky JD, Campisi J, Toussaint O: **Protocols to detect senescence-associated beta-galactosidase (SA-betagal) activity, a**

biomarker of senescent cells in culture and in vivo. *Nat Protoc* 2009, **4**(12):1798-1806.

23. Dimri GP, Lee X, Basile G, Acosta M, Scott G, Roskelley C, Medrano EE, Linskens M, Rubelj I, Pereira-Smith O *et al*: **A biomarker that identifies senescent human cells in culture and in aging skin in vivo**. *Proc Natl Acad Sci U S A* 1995, **92**(20):9363-9367.

24. Fischer AH, Jacobson KA, Rose J, Zeller R: **Hematoxylin and eosin staining of tissue and cell sections**. *CSH Protoc* 2008, **2008**:pdb prot4986.

25. Pilbrow AP, Ellmers LJ, Black MA, Moravec CS, Sweet WE, Troughton RW, Richards AM, Frampton CM, Cameron VA: **Genomic selection of reference genes for real-time PCR in human myocardium**. *BMC Med Genomics* 2008, **1**:64.

26. Krizhanovsky V, Yon M, Dickins RA, Hearn S, Simon J, Miething C, Yee H, Zender L, Lowe SW: **Senescence of activated stellate cells limits liver fibrosis**. *Cell* 2008, **134**(4):657-667.

27. Jun JI, Lau LF: **The matricellular protein CCN1 induces fibroblast senescence and restricts fibrosis in cutaneous wound healing**. *Nat Cell Biol* 2010, **12**(7):676-685.

28. Connolly A, Trew ML, Smaill BH, Plank G, Bishop MJ: **Local Gradients in Electrotonic Loading Modulate the Local Effective Refractory Period: Implications for Arrhythmogenesis in the Infarct Border Zone**. *IEEE Trans Biomed Eng* 2015, **62**(9):2251-2259.

29. de Bakker JM, van Capelle FJ, Janse MJ, Tasseron S, Vermeulen JT, de Jonge N, Lahpor JR: **Slow conduction in the infarcted human heart. 'Zigzag' course of activation**. *Circulation* 1993, **88**(3):915-926.

30. Rutherford SL, Trew ML, Sands GB, LeGrice IJ, Smaill BH: **High-resolution 3-dimensional reconstruction of the infarct border zone: impact of structural remodeling on electrical activation**. *Circ Res* 2012, **111**(3):301-311.

31. Hulsmans M, Clauss S, Xiao L, Aguirre AD, King KR, Hanley A, Hucker WJ, Wulfers EM, Seemann G, Courties G *et al*: **Macrophages Facilitate Electrical Conduction in the Heart**. *Cell* 2017, **169**(3):510-522 e520.

32. Monnerat G, Alarcon ML, Vasconcellos LR, Hochman-Mendez C, Brasil G, Bassani RA, Casis O, Malan D, Travassos LH, Sepulveda M *et al*: **Macrophage-dependent IL-1beta production induces cardiac arrhythmias in diabetic mice**. *Nat Commun* 2016, **7**:13344.

33. Lazzerini PE, Capecchi PL, Bertolozzi I, Morozzi G, Lorenzini S, Simpatico A, Selvi E, Bacarelli MR, Acampa M, Lazaro D *et al*: **Marked QTc Prolongation and Torsades de pointes in Patients with Chronic Inflammatory Arthritis**. *Front Cardiovasc Med* 2016, **3**:31.

34. Kofron CM, Kim TY, King ME, Xie A, Feng F, Park E, Qu Z, Choi BR, Mende U: **Gq-activated fibroblasts induce cardiomyocyte action potential prolongation and automaticity in a three-dimensional microtissue environment**. *Am J Physiol Heart Circ Physiol* 2017, **313**(4):H810-H827.

35. Freund A, Orjalo AV, Desprez PY, Campisi J: **Inflammatory networks during cellular senescence: causes and consequences**. *Trends Mol Med* 2010, **16**(5):238-246.

36. Kang TW, Yevsa T, Woller N, Hoenicke L, Wuestefeld T, Dauch D, Hohmeyer A, Gereke M, Rudalska R, Potapova A *et al*: **Senescence surveillance of pre-malignant hepatocytes limits liver cancer development**. *Nature* 2011, **479**(7374):547-551.

37. Lewek J, Kaczmarek K, Cygankiewicz I, Wranicz JK, Ptaszynski P: **Inflammation and arrhythmias: potential mechanisms and clinical implications**. *Expert Rev Cardiovasc Ther* 2014, **12**(9):1077-1085.

38. Klein RM, Vester EG, Brehm MU, Dees H, Picard F, Niederacher D, Beckmann MW, Strauer BE: **[Inflammation of the myocardium as an arrhythmia trigger]**. *Z Kardiol* 2000, **89 Suppl 3**:24-35.

39. Zhang Y, Wang YT, Shan ZL, Guo HY, Guan Y, Yuan HT: **Role of inflammation in the initiation and maintenance of atrial fibrillation and the protective effect of atorvastatin in a goat model of aseptic pericarditis**. *Mol Med Rep* 2015, **11**(4):2615-2623.

40. Mirza M, Strunets A, Shen WK, Jahangir A: **Mechanisms of arrhythmias and conduction disorders in older adults**. *Clin Geriatr Med* 2012, **28**(4):555-573.

41. Nguyen TP, Qu Z, Weiss JN: **Cardiac fibrosis and arrhythmogenesis: the road to repair is paved with perils**. *J Mol Cell Cardiol* 2014, **70**:83-91.

42. Lindsey ML, Goshorn DK, Squires CE, Escobar GP, Hendrick JW, Mingoia JT, Sweterlitsch SE, Spinale FG: **Age-dependent changes in myocardial matrix**

metalloproteinase/tissue inhibitor of metalloproteinase profiles and fibroblast function. *Cardiovasc Res* 2005, **66**(2):410-419.

43. Stein M, Noorman M, van Veen TA, Herold E, Engelen MA, Boulaksil M, Antoons G, Jansen JA, van Oosterhout MF, Hauer RN *et al*: **Dominant arrhythmia vulnerability of the right ventricle in senescent mice**. *Heart Rhythm* 2008, **5**(3):438-448.

44. Flevari P, Theodorakis G, Leftheriotis D, Kroupis C, Kolokathis F, Dima K, Anastasiou-Nana M, Kremastinos D: **Serum markers of deranged myocardial collagen turnover: their relation to malignant ventricular arrhythmias in cardioverter-defibrillator recipients with heart failure**. *Am Heart J* 2012, **164**(4):530-537.

Chapter 5: Conclusion and Future Directions

Humans risk for sudden cardiac death increases dramatically with age. The focus of this dissertation was to uncover molecular changes in the aging heart that underlie the increased predilection for arrhythmia and sudden cardiac death. We used hearts from aged rabbits, a physiologically relevant system to study the human hearts, to address the following specific aims:

Specific Aim 1: To create a coronary anatomy atlas of the structures present in young and aged rabbits. (A) Collect and analyze coronary angiography to determine the configurations of the anatomy. (B) Create a rubric for coil implantation to generate standardized location and size for infarction regardless of anatomy or any other factor. (C) Validate the surgical rubric using historical and functional experimental methods.

Specific Aim 2: To characterize structural changes in the mitochondria of aging cardiac myocytes and their regulatory factors, and to quantify changes in autophagy during aging in the cardiac myocyte. To inhibit or enhance autophagy in healthy and aged cardiac myocytes and measure the effect on ROS, mitochondria, and spontaneous pro-arrhythmic calcium release.

Specific Aim 3: To quantify the kinetics of cellular senescence of cardiac myofibroblasts and fibrosis in young and aged rabbit hearts post MI histologically and biochemically. To characterize the senescence-associated secretory phenotype (SASP) in samples isolated from infarcted young and aged rabbit hearts.

Our results show that the aging heart is prone to develop more malignant arrhythmia following site-specific occlusion of the first marginal brunch of the circumflex coronary artery. Moreover, the mitochondria in aged cardiac myocytes produce increased mito-ROS which is pro-arrhythmogenic. We identified autophagy as a regulator and therapeutic target for reducing mito-ROS production and abnormal calcium release by increasing autophagy. Finally, we show that following acute injury (myocardial infarction) the aging heart accumulates senescent myofibroblasts in the infarct zone which likely contribute to the abnormal characteristics of APD in the IBZ of aged rabbits.

5.1 Creation of A Novel Method of Standardized Myocardial Infarction in Young and Aged Rabbits

The risk for sudden cardiac death increases greatly with age. It is becoming increasingly clear that age-appropriate models of human disease are critical to understand age-related mechanisms of disease. In **Chapter 2**, we created an atlas of the rabbit coronary anatomy to allow for site specific occlusion using our previously established surgical model of myocardial infarction [1]. Traditional methods using blind coronary artery ligation results in a wide degree of variability in infarct size and location from animal to animal. This is due to large diversity of coronary anatomy and therefore the area at risk when the artery is ligated in a blinded fashion. To thoroughly create a rubric for artery occlusion in the rabbit and overcome some of these problems, we analyzed coronary angiography over 100 rabbits that have undergone our MI procedure. We found that regardless of age or sex the coronary anatomy exists in predominantly four major categories: bifurcation, trifurcation, and quadfurcation of the left main descending

artery, as well as right dominance. Based on our analysis we created a rubric that contains a recommendation for which artery to target in each anatomical configuration and the suggested placement of prothrombotic coil. We demonstrated using echocardiography, gross anatomy analysis, and histological staining that our approach led to consistent and reproducible infarcts.

5.2 Diminished Autophagy During Aging Leads to Aberrant Calcium Handling and Pro-Arrhythmic Cellular Behavior

The underlying mechanisms in pro-arrhythmic calcium handling in aging myocytes have largely remained elusive. Previously, we showed that increased mito-ROS during aging leads to the formation of pro-arrhythmic spontaneous calcium waves implicated in the formation of lethal arrhythmia [2]. Therefore, in **Chapter 3**, we directly tested the role of autophagy in promoting mito-ROS generation. We found that cardiac myocytes from aged rabbit hearts contained a dysfunctional population of mitochondria due to dysregulated fission and fusion. We also reported that autophagy is downregulated in the aged heart by assessing protein expression of several factors for general autophagy as well as mitophagy. To directly connect decreased autophagy with mitochondrial dysfunction we blocked autophagy in HL-1 cardiac myocytes *in vitro* using chloroquine. We found that blocking autophagy increased mito-ROS which led to oxidation of RyR2 leading to generation of SCWs. We then treated primary aged rabbit cardiac myocytes with the drug Torin1 and overexpressed ATG7 to enhance autophagy. The results showed that enhancing autophagy reduced the ROS burden and led to a two-fold reduction in the instance of spontaneous calcium release. Thus, in **Chapter 3** we showed

that autophagy is a novel target capable of reducing mito-ROS generation that is pro-arrhythmic in the aging myocyte, and enhancing autophagy can prevent the formation of spontaneous calcium release that may trigger lethal arrhythmia.

5.3 Cellular Senescence is Delayed and Persistent in the Aged Infarcted Heart

In over 65% of cases of SCD, previous ischemic injury is reported [3, 4]. The risk of SCD increases 5-40-fold after age 65, making age an important risk factor for SCD. The underlying mechanisms of SCD, especially after ischemic injury, remain poorly understood. Therefore, we used our rabbit model described in **Chapter 2** to study wound healing in an age-appropriate model of myocardial infarction. Previous literature suggests cellular senescence is an important process involved in wound healing and tissue repair in both the dermis [5] and liver [6]. Cellular senescence is a specialized state cells enter where they stop dividing, yet remain metabolically active [7, 8]. A key feature of senescent cells the senescence-associated secretory phenotype (SASP) which has deleterious effects on the surrounding tissue by secreting chemokines, cytokines, and matrix remodelling proteins [9, 10]. However, the role senescence plays in arrhythmia and age-related SCD remained elusive. Therefore, in **Chapter 4** we reported an increased instance of peri-procedural arrhythmia in aged animals. We conducted optical mapping experiments that revealed changes in APD in the infarct border zone and remote zone, especially during aging. Further, the aged heart displayed conduction disturbances in the infarct border zone. Hearts were then processed for the detection of cellular senescence using histological and biochemical methods. SA-βGal staining revealed an enrichment of senescent myofibroblasts in the

scar zone of aged hearts as compared to infarcted young hearts. Furthermore, the scar zones were enriched with p16, p21, and TGF-β transcripts. Several pro-inflammatory cytokines like IL-6, CCl2, and CXCL2 were enriched in the aged scar, along with matrix remodelling factors like MMP9, TIMP1, and TIMP2. We also studied a three-week time course post-MI that revealed a delayed and persistent senescence response to injury in aged hearts. Therefore, we posit that the aged infarcted heals differently than the young. The aged scar contains more senescent myofibroblasts which may lead to a persistent inflammatory response. Together, these changes may be a mechanism capable of triggering arrhythmia that can be propagated and sustained by the aging heart.

5.4 Experimental and Systematic Challenges and Limitations

The studies that were performed and summarized in this dissertation presented several challenges and have limitations. All aged animals were retired female breeders. Females are retired after 3-3.5 years of age. Males are not kept to this age. Therefore, the availability of healthy, aged female animals was limited to 8 animals every 4 months. As such, in **Chapter 2**, most of the rabbits analysed to create the rubric were female.

In **Chapter 3**, single cell analysis of cardiac myocyte physiologic parameters from aged animals presented a challenge to culture. Cells tolerated culture conditions, however, after 36-48 hours in a petri dish the cells exhibited remodelling. However, we tested a variety of cell culture conditions and mediums to optimize the conditions which the cells were subjected to. Through empirical trials using commercially available

DMEM, DMEM-F12, and M-199 (Gibco) we decided to use DMEM cell culture medium. We tested a variety of concentrations of FBS as well, 0,5,7, and 10%. We found that 7% FBS allowed the cells to survive without affecting remodelling to the extent 10% FBS did. After optimization, aged cardiac myocytes tolerated adenovirus where MOI was empirically determined. Generally, MOI =1 was sufficient to detect and image the expression of the fluorescent tags. Based on the work we performed, the major limitation is the short 36-48 hour adenoviral incubation to allow for expression. Due to remodelling effect, we performed physiologic experiments studying calcium handling at 36 hours, then other measurements the following day. The next major limitation was the cell number after isolation and adenoviral treatment. After 36-48 hours relatively, few primary cells survived the treatments due to culture conditions. This phenomenon is well acknowledged in the field. Therefore, we were unable to attain enough cells to perform western blot experiments. We relied heavily on fluorescent reporters and physiologic assays and biosensors to confirm the expression of constructs.

A major challenge in detecting senescence cells is the specificity of the reagents we used. As the field recognizes, performing SA-βGal staining requires a pH specific enzymatic reaction that can lead to false-positive staining. For our work presented in **Chapter 4**, we optimized the conditions which we performed the staining reactions using a previously published protocol [11]. In addition, we performed gene expression analysis for senescence pathways as well as presence of a SASP. The limitation we faced in qPCR analysis was the poor availability of primer sets available and a poor annotation of the rabbit genome. Therefore, we designed primers carefully using NCBI

primer tool to maximize the specificity of primers while allowing for the detection of all splice variants.

5.5 Future Directions

5.5A Effect of Senescence on Cardiac Myocytes from Young and Aged Infarct Border Zones

As discussed in **Chapter 4**, senescent cells featured a drastically upregulated SASP in aged scar zones three-weeks post MI. Senescent cells through SASP can induce an inflammatory response and inflammation can result in arrhythmia [12-15]. Because no studies to date have studied the effect of SASP on arrhythmogenesis we posit that difference in the SASP response with age will mount a chronic immune response capable to modifying the excitability of cardiac myocytes immediately surrounding the scar in the infarct border zone through paracrine effects. To test this hypothesis, we can isolate cardiac myocytes from young and aged infarct border zone and remote zones using our previously established protocol [2] modified with additional dissection of injury zones. Single myocytes will be studied acutely following isolation using simultaneous patch clamp and calcium imaging methodologies to study the propensity for disturbances in pro-arrhythmic calcium or voltage disturbances.

5.5B Genetic Manipulation of Senescence in Cardiac Scar Formation

The induction of cellular senescence in the myocardium has been shown in a variety of reports [16, 17]. In **Chapter 4** we reported a dynamic and persistent senescence and SASP response in the aged infarcted hearts. However, due to the

limitation of using a large animal model such as rabbits, we plan to take advantage of mice to study the effects of manipulating senescence on arrhythmogenesis. To that end, we propose to use periostin promoter to induce fibroblast-specific expression of Cre [18, 19] which leads to deletion of p53 to suppress senescence, or to induce deletion of Mdm2 [20], a negative regulator of P53 to increase senescence post-MI.

Our initial studies (Fig 5.1) show the feasibility of inducing MI using LAD ligation in our mouse models. Fig 5.1A shows gross anatomy photos of mouse LV with large MI. Fig 5.1B shows a collagen enriched scar and infarct border zone using picrosirius red staining. Lastly, we detected senescent non-myocytes in the scar zone (Fig 5.1C). Mice will be monitored with *in vivo* telemetry to record spontaneous arrhythmia. *Ex vivo* optical mapping will be used to study these hearts for inducible arrhythmia. Finally, the different zones will be analyzed for SASP using biochemical and histochemical tools. Moving forward, we will continue to test the hypothesis that persistent senescence response post-MI promotes a chronic inflammatory response that underlies age-related arrhythmogenesis capable of being sustained by the aged heart.

5.6 Conclusion

This work presented in this dissertation describes new mechanisms of arrhythmogenesis in the aged heart. We demonstrate our novel experimental approaches to investigate SCD in an age-appropriate, physiologically relevant model of the aging heart. Leveraging the highly translational rabbit model we expanded mechanisms previously discovered in our lab such as increased mito-ROS generation in

the aging cardiomyocyte, as well as functional changes on the tissue level such as conduction disturbances that lead to aberrant excitability. We showed that mitochondria in aged cardiac myocytes produce increase mito-ROS that are pro-arrhythmogenic, and that autophagy is a regulator and therapeutic target for reducing mito-ROS production and pro-arrhythmic abnormal calcium release. Here we described for the first time that after acute injury (myocardial infarction) the aging heart accumulates senescent myofibroblasts in the infarct zone which likely contribute to the abnormal characteristics of APD in the IBZ of aged rabbits. Taken together, aging modifies the cellular as well as tissue level responses to injury and stress and promotes the formation of pro-arrhythmic disturbances that can be propagated and result in SCD. The Koren Lab will continue to use the aged rabbit cohort to uncover mechanisms of arrhythmia, as well as genetically tractable rodent systems to confirm our findings.

5.7 Figures and Tables

Figure 5.1: Cellular Senescence is Detectable in the Infarcted Mouse Heart

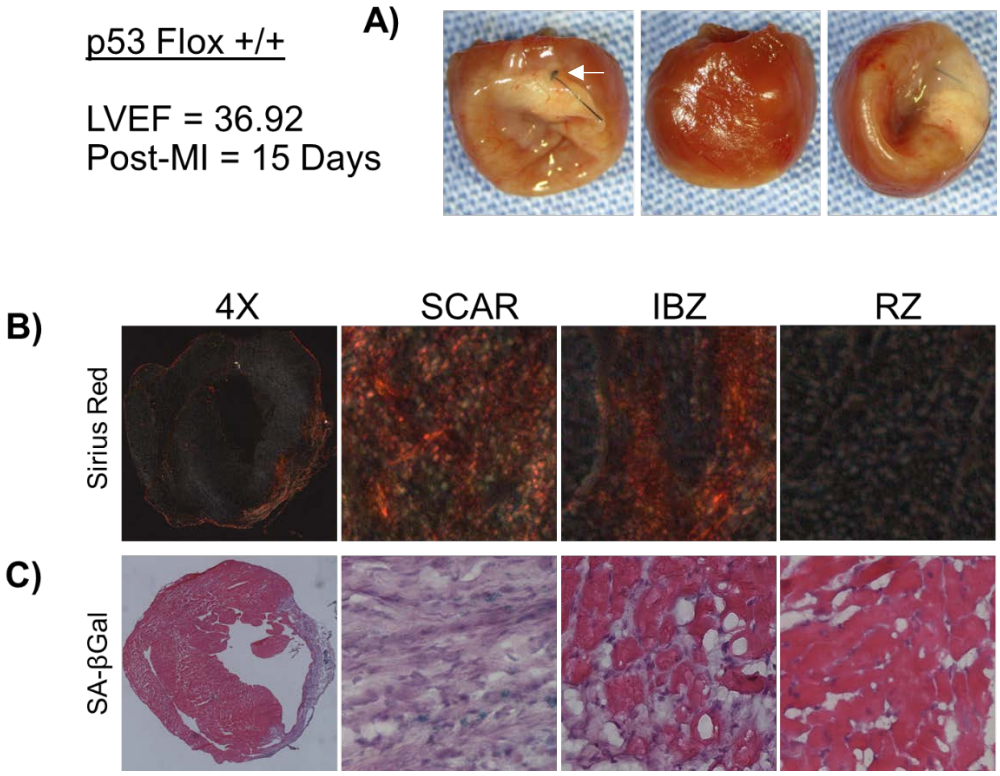

Representative myocardial infarction in a control, p53 floxed mouse. Two-weeks post-MI the ejection fraction is reduced (36%). (A) Gross anatomy reveals large apical, anterolateral infarction. From left to right: LV, RV, and apical photos. Arrow indicates location of LAD ligation. (B) The scar is detectable by picrosirius red staining imaged with plain polarized light. Large scan two-chamber view was imaged at 4x, where representative images from each injury zone was imaged at 40x. (C) SA-βGal staining was performed and imaged in an equivalent manner to panel B.

These experiments were performed in collaboration with Mr. Brett Baggett.

5.8 References

1. Ziv O, Schofield L, Lau E, Chaves L, Patel D, Jeng P, Peng X, Choi BR, Koren G: **A novel, minimally invasive, segmental myocardial infarction with a clear healed infarct borderzone in rabbits**. *Am J Physiol Heart Circ Physiol* 2012, **302**(11):H2321-2330.
2. Cooper LL, Li W, Lu Y, Centracchio J, Terentyeva R, Koren G, Terentyev D: **Redox modification of ryanodine receptors by mitochondria-derived reactive oxygen species contributes to aberrant Ca2+ handling in ageing rabbit hearts**. *J Physiol* 2013, **591**(23):5895-5911.
3. Zheng ZJ, Croft JB, Giles WH, Mensah GA: **Sudden cardiac death in the United States, 1989 to 1998**. *Circulation* 2001, **104**(18):2158-2163.
4. Podrid PJ, Myerburg RJ: **Epidemiology and stratification of risk for sudden cardiac death**. *Clin Cardiol* 2005, **28**(11 Suppl 1):I3-11.
5. Herbig U, Ferreira M, Condel L, Carey D, Sedivy JM: **Cellular senescence in aging primates**. *Science* 2006, **311**(5765):1257.
6. Krizhanovsky V, Yon M, Dickins RA, Hearn S, Simon J, Miething C, Yee H, Zender L, Lowe SW: **Senescence of activated stellate cells limits liver fibrosis**. *Cell* 2008, **134**(4):657-667.
7. Tchkonia T, Zhu Y, van Deursen J, Campisi J, Kirkland JL: **Cellular senescence and the senescent secretory phenotype: therapeutic opportunities**. *J Clin Invest* 2013, **123**(3):966-972.
8. Campisi J: **Senescent cells, tumor suppression, and organismal aging: good citizens, bad neighbors**. *Cell* 2005, **120**(4):513-522.

9. Coppe JP, Patil CK, Rodier F, Sun Y, Munoz DP, Goldstein J, Nelson PS, Desprez PY, Campisi J: **Senescence-associated secretory phenotypes reveal cell-nonautonomous functions of oncogenic RAS and the p53 tumor suppressor**. *PLoS Biol* 2008, **6**(12):2853-2868.

10. Coppe JP, Desprez PY, Krtolica A, Campisi J: **The senescence-associated secretory phenotype: the dark side of tumor suppression**. *Annu Rev Pathol* 2010, **5**:99-118.

11. Debacq-Chainiaux F, Erusalimsky JD, Campisi J, Toussaint O: **Protocols to detect senescence-associated beta-galactosidase (SA-betagal) activity, a biomarker of senescent cells in culture and in vivo**. *Nat Protoc* 2009, **4**(12):1798-1806.

12. Xu X, Pang J, Chen Y, Bucala R, Zhang Y, Ren J: **Macrophage Migration Inhibitory Factor (MIF) Deficiency Exacerbates Aging-Induced Cardiac Remodeling and Dysfunction Despite Improved Inflammation: Role of Autophagy Regulation**. *Sci Rep* 2016, **6**:22488.

13. Olivieri F, Rippo MR, Monsurro V, Salvioli S, Capri M, Procopio AD, Franceschi C: **MicroRNAs linking inflamm-aging, cellular senescence and cancer**. *Ageing Res Rev* 2013, **12**(4):1056-1068.

14. Menendez JA, Alarcon T: **Senescence-Inflammatory Regulation of Reparative Cellular Reprogramming in Aging and Cancer**. *Front Cell Dev Biol* 2017, **5**:49.

15. Lewek J, Kaczmarek K, Cygankiewicz I, Wranicz JK, Ptaszynski P: **Inflammation and arrhythmias: potential mechanisms and clinical implications**. *Expert Rev Cardiovasc Ther* 2014, **12**(9):1077-1085.

16. Zhu F, Li Y, Zhang J, Piao C, Liu T, Li HH, Du J: **Senescent cardiac fibroblast is critical for cardiac fibrosis after myocardial infarction**. *PLoS One* 2013, **8**(9):e74535.

17. Meyer K, Hodwin B, Ramanujam D, Engelhardt S, Sarikas A: **Essential Role for Premature Senescence of Myofibroblasts in Myocardial Fibrosis**. *J Am Coll Cardiol* 2016, **67**(17):2018-2028.

18. Takeda N, Manabe I, Uchino Y, Eguchi K, Matsumoto S, Nishimura S, Shindo T, Sano M, Otsu K, Snider P *et al*: **Cardiac fibroblasts are essential for the adaptive response of the murine heart to pressure overload**. *J Clin Invest* 2010, **120**(1):254-265.

19. Kaur H, Takefuji M, Ngai CY, Carvalho J, Bayer J, Wietelmann A, Poetsch A, Hoelper S, Conway SJ, Mollmann H *et al*: **Targeted Ablation of Periostin-Expressing Activated Fibroblasts Prevents Adverse Cardiac Remodeling in Mice**. *Circ Res* 2016, **118**(12):1906-1917.

20. Volk EL, Schuster K, Nemeth KM, Fan L, Harris LC: **MDM2-A, a common Mdm2 splice variant, causes perinatal lethality, reduced longevity and enhanced senescence**. *Dis Model Mech* 2009, **2**(1-2):47-55.